THE SPECTRUM OF CYCLOHEXANONE

THE SPECTRUM OF CYCLOHEXANONE

by

DANIELLE GRANGÉ,

LICENCIÉE ÈS-SCIENCES PHYSIQUES

A Thesis

Submitted to the School of Graduate Studies

in Partial Fulfilment of the Requirements

for the Degree

Master of Science

McMaster University

July 1971

MASTER OF SCIENCE (1971)
(Physics)

McMASTER UNIVERSITY
Hamilton, Ontario.

TITLE: The Spectrum of Cyclohexanone

AUTHOR: Danielle Grangé

Licenciée Ès-Sciences Physiques (University of Bordeaux-France)
Diplomée D'Études Superieures de Sciences - Physiques (University of Bordeaux-France)

SUPERVISOR: Dr. Gerald W. King

NUMBER OF PAGES: xii, 160

SCOPE AND CONTENTS:

The near ultraviolet absorption spectra of cyclohexanone, cyclohexanone $\alpha,\alpha,\alpha',\alpha' d_4$ and cyclohexanone d_{10} have been recorded and analysed under low and high resolution. The vibrational and rotational structure accompanying the electronic singlet-singlet $\underline{n}\rightarrow\pi^*$ transition have been analysed. Some complementary information has been obtained from the infrared vapour spectrum of cyclohexanones. The geometries of the ground and first excited state have been determined. In the excited state configuration, the oxygen atom is bent out of the plane of the three adjacent carbon atoms by about 30°, and the carbon oxygen bond increases by 0.08 Å between the ground state and the excited state. Some ring modes are strongly active in the electronic spectra of the three isomers. This may indicate some coupling between the carbonyl group and the ring. The results obtained by band contour analysis

are consistent with those obtained by calculation of a double minimum potential function, as well as those obtained in previous work on related molecules.

ACKNOWLEDGEMENTS

I wish to thank my supervisor, Dr. Gerald W. King, for providing me with the opportunity of working in his research group, and for his continuing advice and encouragement during this work.

I thank the following persons: my research colleagues, Mr. E. J. Finn, Mr. E. Farnworth, Mr. F. R. Greening, Mr. R. Maetherall, Mr. P. R. McLean, Dr. P. Pichat, Dr. S. P. So, Mr. C. R. Subramanian, Mr. A. A. van Putten, and particularly Mr. K. G. Kidd for friendly welcome into the group, stimulating discussions and experimental assistance; Dr. H. E. Howard-Lock, Dr. D. C. Moule, for many valuable suggestions; Mr. J. Bradford for valuable technical assistance and Dr. D. P. Santry for advice and helpful discussions.

Dr. R. N. Jones and Dr. H. H. Mantsh for communicating in advance of publication their results on the infrared and Raman liquid spectra of cyclohexanone.

I am grateful to Mrs. H. Kennelly for her skillful typing of this manuscript.

Finally, I wish to acknowledge generous financial assistance from the Physics Department (1969-1971).

TABLE OF CONTENTS

LIST OF TABLES

LIST OF ILLUSTRATIONS

CHAPTER 1

INTRODUCTION

In molecular spectroscopy the wave number and intensities of transitions between the various quantized rotational, vibrational, and electronic energy levels of a molecule are measured and analysed. This yields information on the geometrics, dynamics and electronic structures of the molecule in its different states. The basic theory is to be found in standard reference books (1,2,3). In this thesis, only those parts of the theory that are relevant to the cyclohexanone molecule are discussed.

Spectra are usually observed in absorption. In microwave spectroscopy, transitions between rotation levels associated with the ground electronic state are observed, and from these the rotational constants A, B and C, which are inversely proportional to the moment of inertia I_a, I_b, I_c about the principal axes of inertia, can be obtained. If the spectra of sufficient isotopic species are examined, then the molecular geometry can be determined from the values obtained for the principal moments of inertia.

In vibrational (infrared and Raman) spectroscopy, the normal frequencies of vibration in the ground electronic state

are determined, providing information about normal coordinates and force constants for vibration of the molecules.

In electronic absorption spectroscopy, the molecule is excited to higher electronic states, by absorption of light in the ultraviolet or visible regions of the spectrum.

Analysis of the vibrational band structure of an electronic absorption spectrum enables the vibrations of the molecule in the excited state to be determined.

Analysis of the rotational structure of bands provides information a) about the geometries of the molecule in the combining states b) about the polarisation of transitions.

In the present work, the absorption spectrum of the six membered ring compound Cyclohexanone ($C_6H_{10}O$) in the near ultraviolet has been examined. The spectra of two deuterated isomers, the $\alpha_1,\alpha_2,\alpha_1',\alpha_2'$ d_4 and the fully deuterated molecule were also comparatively analysed. For convenience, these three compounds will be referred to as CHh_{10}, CHd_4 and CHd_{10} respectively.

1.1 PREVIOUS SPECTROSCOPIC AND STRUCTURAL STUDIES OF CYCLOHEXANONE

The infrared and Raman spectra of cyclohexanone-h_{10} have been examined several times[4,5,6,7]. The spectra of the $\alpha_1\alpha_2\alpha_1'\alpha_2'd_4$ cyclohexanone and fully deuterated cyclohexanone have not been published previously. Neither a complete assignment of the fundamental frequencies of vibrations, nor a normal

coordinate analysis has been published to date.

The infrared and Raman spectra of cyclohexanone and various deuterated isomers are currently being studied in detail by Dr. R. N. Jones and his co-workers at the National Research Council in Ottawa, who kindly supplied us with their preliminary results. Consequently the vibrational spectra were not reinvestigated in detail, although a certain amount of infrared work complementary to that of Dr. Jones is reported below.

The microwave spectrum of cyclohexanone has not been measured, and no information on the ground state geometry is obtainable from this method. The structure of cyclohexanone has been investigated by electron diffraction[8].

Cyclohexanone (Fig. 1.1) can conceivably exist in either "boat" or "chair" forms (Fig. 1.2), the latter being more stable than the boat forms[9]. The energy difference between the boat and chair forms of cyclohexanone is estimated to be 5.3 kcal/mole[10], but a value has not been reported for cyclohexanone. The energy for the boat-boat interconversion is unknown. The energy of interconversion between chair-chair configurations (< 6.5 kcal/mole)[11] is smaller for cyclohexanone, and $\alpha_1\alpha_2\alpha_1'\alpha_2'd_4$ cyclohexanone (< 6.6 kcal/mole)[11], than for cyclohexane (11 kcal/mole)[9,12,13].

No vibrational analysis of the fluorescence and

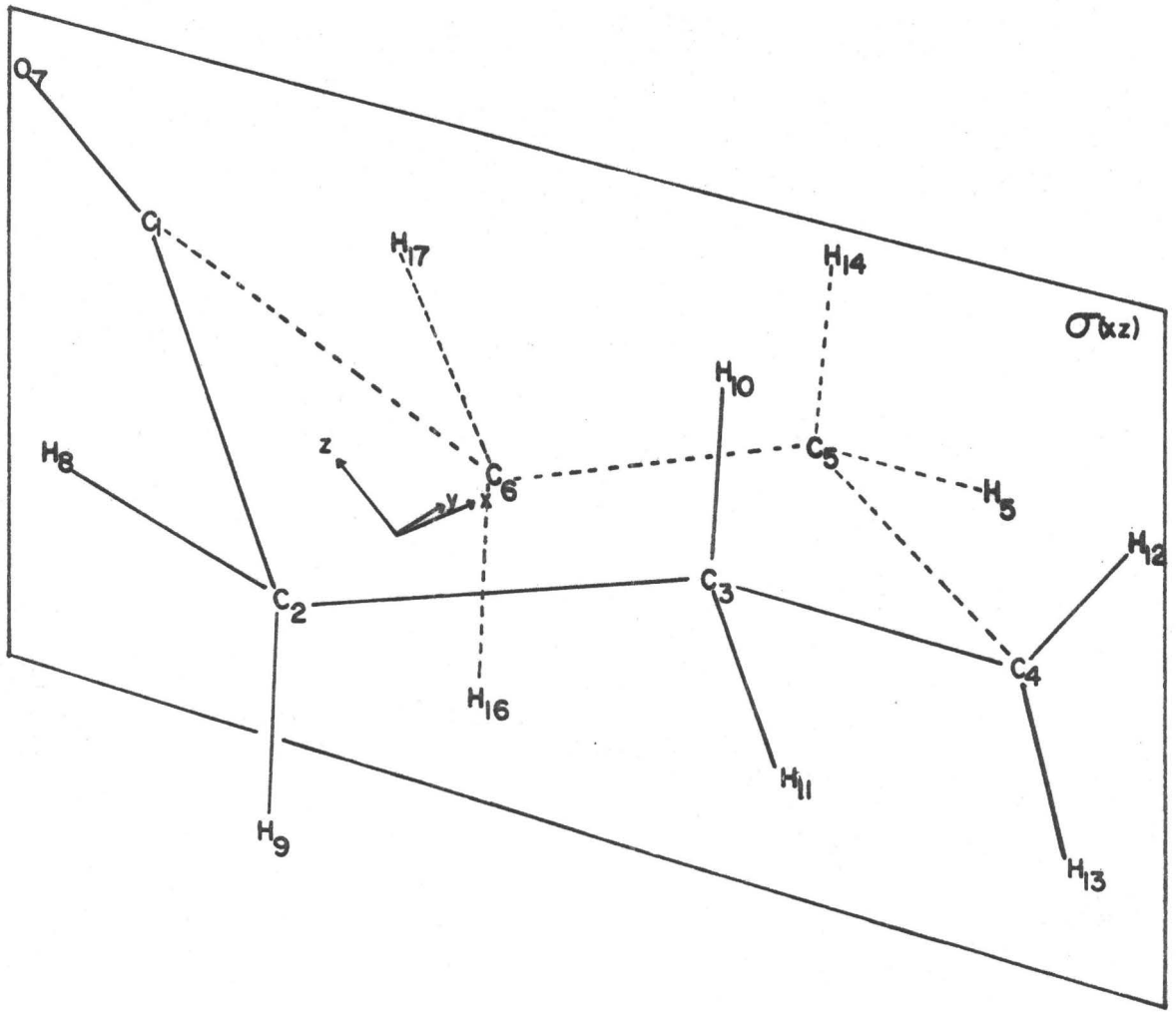

FIG(1·1) GROUND STATE GEOMETRY OF CYCLOHEXANONE

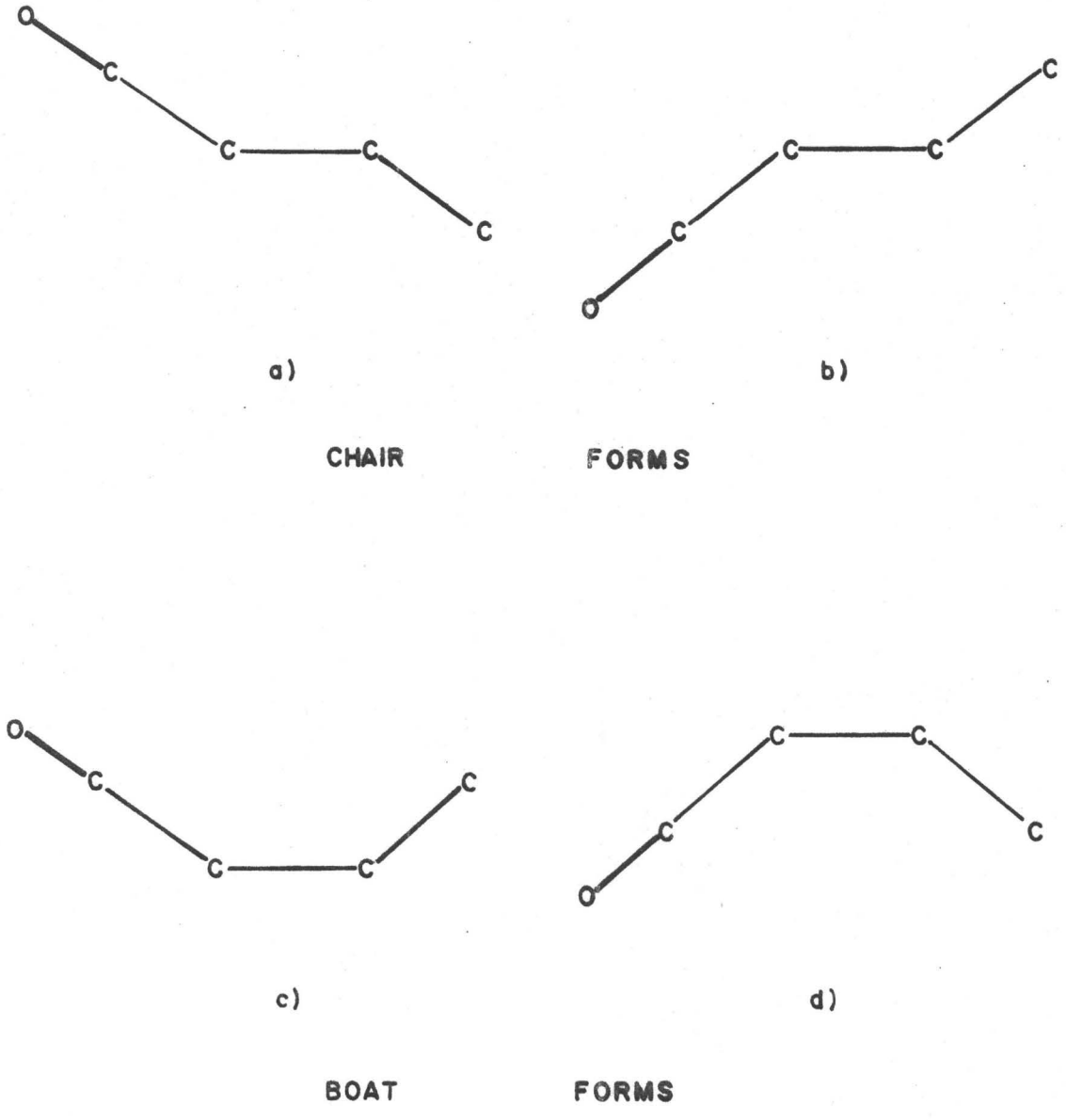

FIG (1·2) CHAIR AND BOAT CONFIGURATIONS IN THE GROUND STATE

phosphorescence electronic emission spectra is reported in the literature. Chandler and Goodman[14] have studied the emission spectra of some cycloalkanones in solvents, and observed that cyclic carbonyl compounds, like other aliphatic carbonyl compounds , and contrarily to aromatic carbonyls show i) weak emission, 2) the possibility of photo decomposition, 3) a diffuse emission spectra, 4) a diffuse excitation spectra, except for cyclopentanone, 5) a small singlet-triplet interval for the (π^*,n), configuration ($\sim$ 1500 cm^{-1}), leading to overlapping of the phosphorescence and fluorescence spectra[14].

From the polarized photoexcitation spectra (measured in EPA solvent at 77°K), of cycloheptanone, cyclohexanone, cyclopentanone, cyclobutanone, Chandler and Goodman[14] measured the oscillator strength of the singlet-singlet $n \rightarrow \pi^*$ transitions (see Table 1.1). In Table (1.1) are also listed the values of $\varepsilon_{max.}$ for these molecules. The values given represent the intensity of the $n \rightarrow \pi^*$ absorption transition measured in a solution of n-pentane at 20°C.

From the phosphorescence excitation spectra of cycloalkanones, the authors previously cited[14] conclude a) the $n \rightarrow \pi^*$ absorption transition (singlet-singlet) is polarized predominantly perpendicular to the plane of symmetry of the molecule, b) the $n \rightarrow \pi^*$ transition has considerable electronically allowed or vibronic type A character increasing in order of

TABLE 1.1

INTENSITIES OF $n \rightarrow \pi^*$ SINGLET-SINGLET ABSORPTION FOR SOME KETONES[14]

Molecule	Oscillator Strength $\times 10^4$	$\varepsilon_{Max.}$ [a]
Formaldehyde	2.4	
Cyclobutanone	5.4	15
Cyclopentanone	4.8	18
2,5 Dimethylcyclopentanone	4.7	20
Cyclohexanone	3.9	14
Cycloheptanone	4.2	16

a) $\varepsilon_{max.}$ is the intensity of the $n \rightarrow \pi^*$ absorption transition measured in solution of n pentane at 20°C.

distortion of the molecule from C_{2v} symmetry in the ground state (Cyclopentanone>cycloheptanone>cyclohexanone), c) the major path for non totally symmetric vibronic intensification of the $n \rightarrow \pi^*$ transition is through a b-type vibration.

Under low resolution the ultraviolet absorption spectrum of cyclohexanone vapor, like most of the simple ketones, shows four absorption regions between 3000-1500 Å[15]. These consist of a weak absorption at 3000 Å, two moderately intense regions at 1900 Å and 1750 Å and a very intense region at 1500 Å. Whereas the assignment of the first and last regions to the $n \rightarrow \pi^*$ and $\pi \rightarrow \pi^*$ transitions respectively is fairy certain[15,16], the second band can be assigned to either a $n \rightarrow \sigma^*$[17] or Rydberg[18] transition and the third band to a transition involving the c-c σ orbitals[19]. Barnes[20] reassigned the second transition as $n' \rightarrow \pi^*$ (n' is an oxygen orbital extending opposite to the Co axis) and the third to an $n \rightarrow \sigma^*$ transition.

1.2 THE STRUCTURE OF CYCLOHEXANONE IN THE GROUND STATE

-Geometry-

The electron diffraction study of cyclohexanone structure shows that ,at room temperature, in the vapour phase, cyclohexanone, like cyclohexane, exists predominantly in the chair form[8]. The result of this study shows that the angle $<c_2c_1c_6$ is not equal to angle $<oc_1c_2$ or $<oc_1c_6$ (see

Fig. 1.1). The first of these angles was found to be 117°±3° and the other two to be both 121°.5±1.5°.

It was assumed in the above work that the C=0 band is coplanar with the ring atoms $C_1C_2C_6$. The C=0 bond length was found to be 1.24±0.02 Å. The large error in the derived values of the angles obtained in this electron diffraction study will be discussed later in connection with the results of this work.

-Symmetry-

In a rigid chair form, cyclohexanone has just one symmetry plane and comes under the C_s point group, see Fig. (1.3). The same point group applies if the molecule is in a rigid boat configuration. There are two boat and two chair forms. If the potential barriers impeding interconversion of these forms are sufficiently low, then the molecule can, in effect, be regarded as having a planar carbon-oxygen framework, and comes under the C_{2v} point group as its delocalised domain. Granger and Claudon[21] on the basis of NMR studies, suggest that the actual physical interconversion of the two chair forms does occur via the planar form.

Character tables for the C_{2v} and C_s point groups are given in Table (1.2). These also show the symmetries of translation vectors (x,y,z), rotations (R_x, R_y and R_z) and the

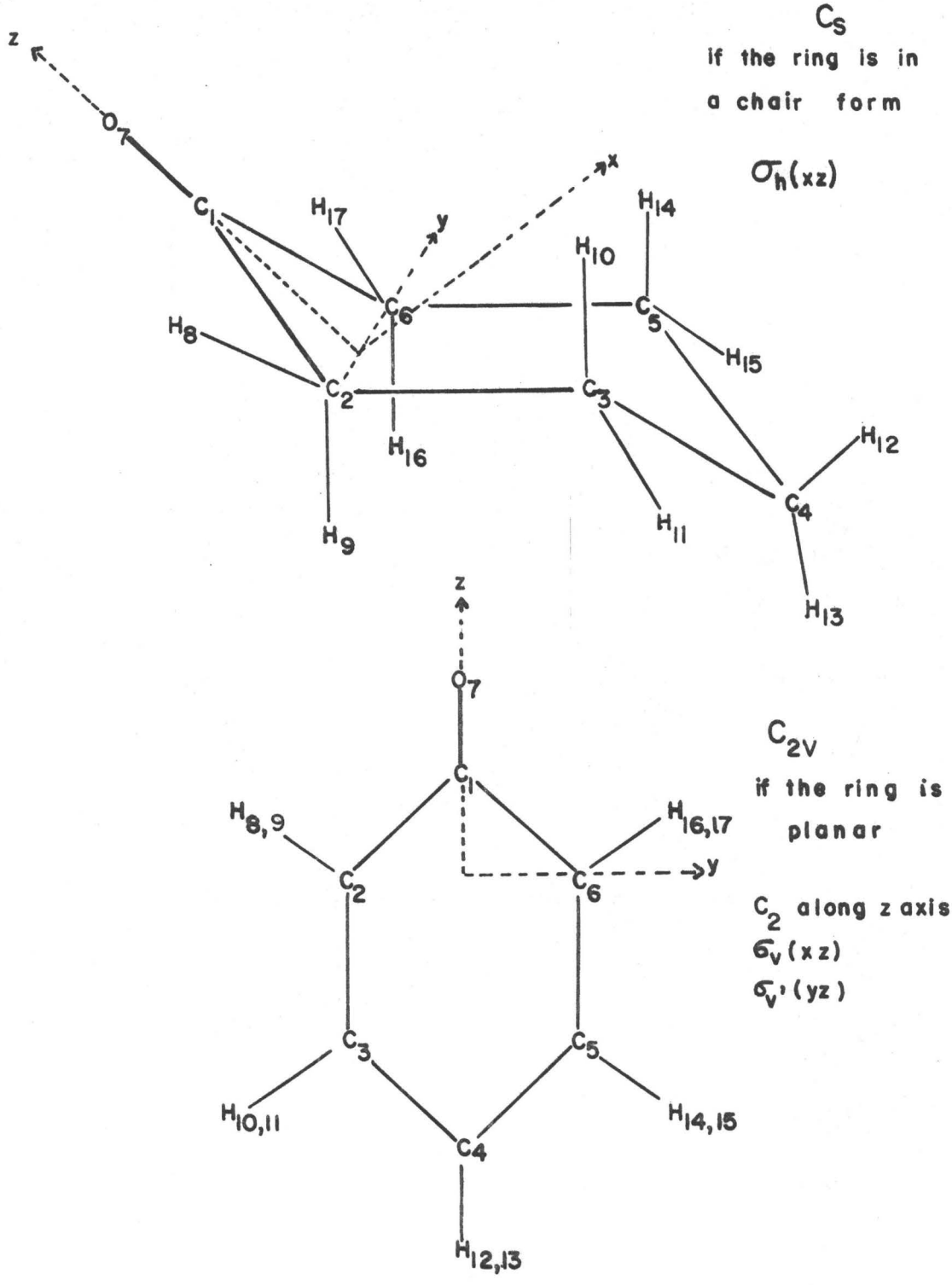

FIG (1·3) POSSIBLE SYMMETRIES OF CYCLOHEXANONE

TABLE 1.2

CHARACTER TABLES

C_{2v}	E	$C_2(z)$	$\sigma_v(xz)$	$\sigma_{v'}(yz)$		
A_1	1	1	1	1	z	$\alpha_{xx}, \alpha_{yy}, \alpha_{zz}$
A_2	1	1	-1	-1	R_z	α_{xy}
B_1	1	-1	1	-1	x, R_y	α_{xz}
B_2	1	-1	-1	1	y, R_x	α_{yz}

C_s	E	$\sigma_h(xz)$		
A'	1	1	x, z, R_y	$\alpha_{xx} \alpha_{yy} \alpha_{zz} \alpha_{xz}$
A''	1	-1	y, R_x, R_z	$\alpha_{xy} \alpha_{yz}$

components α of the polarisability tensor. Cyclohexanone has N=17 atoms, and therefore 3N-6 = 45 normal modes of vibration. The symmetries of these can be found by the method described in Herzberg[3] or King[1].

C_{2v} point group

The characters of the matrices corresponding to the coordinate transformations produced by the symmetry operators on a set of 3N vibrational displacement coordinates for the nuclei are

	E	$C_2(z)$	$\sigma_v(xz)$	$\sigma_v'(yz)$
$\chi(\Gamma_{3N})$	51	-3	5	7

These include the representations for the three translational and the three rotational motions, which must be subtracted out

$\chi(\Gamma_{T,R})$	6	-2	0	0

so the characters for the internal coordinates which represent vibrational motion are

$\chi(\Gamma_v)$	45	-1	5	7

Under the C_s point group, the same procedure gives

		E	$\sigma_h(x,z)$
	$\chi(\Gamma_{3N})$	51	5
minus	$\chi(\Gamma_{T,R})$	6	0
	$\chi(\Gamma_v)$	45	5

These representations decompose into irreducible representations, or symmetry species, as follows.

$$C_{2v} \text{ group } \Gamma_v = 14A_1 \oplus 8A_2 \oplus 11B_1 \oplus 12B_2$$

$$C_s \text{ group } \Gamma_v = 25A' \oplus 20\,A''.$$

In infrared spectroscopy, the intensity of a transition is proportional to the square of the transition moment R, where

$$R = \int \psi_v'^{*} P \psi_v'' d\tau \qquad (I.1)$$

where ψ_v' and ψ_v'' are the wavefunctions for the combining states, and P is the electric dipole moment operator, which has components, P_x, P_y and P_z that transform under group operations like the corresponding translations. For a transition to occur, one of the components of the transition moment

$$R_i = \int \psi_v'^{*} P_i \psi_v'' d\tau \qquad (i = x,y,z) \qquad (I.2)$$

must be non-zero; this requires that the direct product $\Gamma(\psi_v') \otimes \Gamma(P_i) \otimes \Gamma(\psi_v'')$ must be totally symmetric, i.e. $\Gamma(\psi_v') \otimes \Gamma(\psi_v'')$

must transform under the group operations as one of the $\Gamma(T_i)$. Hence the polarisation of a particular transition, along the x, y or z axes in the molecule, can be determined. The spectral band is called type A, B or C according to the direction of polarisation; $I_c \geq I_b \geq I_a$ are the principal moments of inertia of the molecule which coincide with the symmetry coordinates x, y and z in the manner shown in Fig.(1.3). Computed type A and C infrared bands are shown in Fig. (1.4). The type B is studied in the band contour section (Fig.(4.2).

Similar arguments show that a Raman transition can occur if the direct product $\Gamma(\psi_v')\otimes\Gamma(\psi_v'')$ transforms like one or more of the compoments of the polarisability tensor $\Gamma(\alpha_{ij})$. An important measurable property of bands in the Raman spectrum is the depolarisation ratio ρ:

$$\rho = I_{\perp}/I_{||} \qquad (I.3)$$

where $I_{\perp}$ and $I_{||}$ are the intensities of the light scattered perpendicular and parallel to the plane of polarisation of the electric component of the polarised exciting radiation. If the scattered light is observed at right angles to the latter, then a totally symmetric fundamental Raman band is expected to be polarised (ρ = 0 to 6/7) while any non totally symmetric vibration is depolarised (ρ = 6/7).

It follows from the above theoretical considerations that the 45 normal modes of vibration of cyclohexanone can

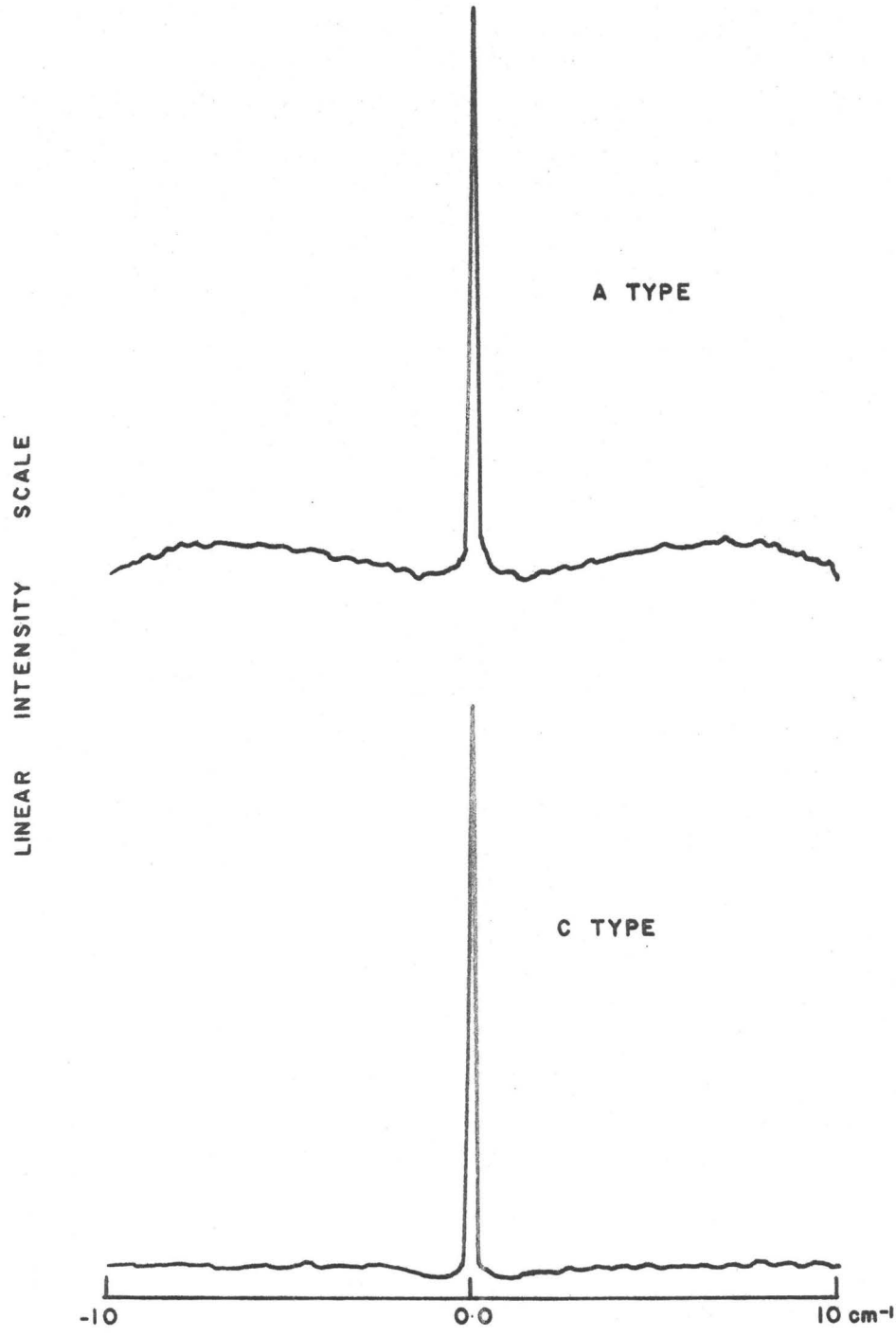

FIG(1·4) COMPUTED A AND C INFRARED TYPE BAND

be analysed as follows:

$$C_{2v} \text{ group; } 14a_1[\text{I.R.(A)},\text{Ram(p)}] + 8a_2[\text{Ram(dp)}] + 11b_1[\text{I.R.(c)}_1(\text{Ram(dp)}] + 12b_2[\text{I.R.(B)},\text{Ram(dp)}] \quad (I.4)$$

$$C_s \text{ group ; } 25a'[\text{I.R.(A+c)},\text{Ram(p)}] + 20a''[\text{I.R.(B)},\text{Ram(dp)}] \quad (I.5)$$

where the infrared and Raman activities, types of infrared band and depolarisations of Raman bands for the fundamentals are shown in parentheses.

The symmetries of combination and overtone levels are obtained by taking direct products for each vibrational quantum excited. Table (1.3) gives direct products for the C_{2v} and C_s point groups.

1.3 CYCLOHEXANONE AS A NON-RIGID MOLECULE

A non-rigid molecule is one which can pass easily from one configuration to another. The symmetry point group under which such a molecule must be classified is a subject requiring special attention. A simple example of a non-rigid molecule is ammonia NH_3. In each of its stable pyramidal forms, it is classified under the C_{3v} point group. But when its inversion motion via a planar form from one perpendicular shape to the other is considered, the vibrational states have to be classified under the D_{3h} point group, which is the "delocalised domain". The height of the barrier to the inversion is 2076

TABLE 1.3

DIRECT PRODUCTS FOR THE C_{2v} AND THE C_s POINT GROUPS

C_{2v}	A_1	A_2	B_1	B_2
A_1	A_1	A_2	B_1	B_2
A_2	A_2	A_1	B_2	B_1
B_1	B_1	B_2	A_1	A_2
B_2	B_2	B_1	A_2	A_1

C_s	A'	A''
A'	A'	A''
A''	A''	A'

cm^{-1}. Clearly, whether a molecule can be regarded as rigid or non-rigid depends upon the heights of the potential barriers between interconversion of different configurations.

Many molecules containing large rings have easily interconvertable different conformations. In the case of cyclohexane and cyclohexanone, the most important configurations are the chair and boat forms. The infrared spectrum of cyclohexane[22,23,24] is consistent with it being in a stable chair form. NMR studies[9,10,11] also confirm this, and indicate that the boat form is some 5.5 kcal/mol (1925 cm^{-1}) less stable. The barrier impeding chair-chair interconversion is about twice as large as this, being estimated as 11.1 kcal/mol (3885 cm^{-1})[9]. As is also shown by electron diffraction[8], cyclohexanone is also stable in the chair form. The relative energy of the boat form has not been calculated, but NMR work by Granger and Claudon[21] shows that the chair-chair interconversion barrier is smaller than in cyclohexane. Jensen and Beck[11] estimate the barrier to have a maximum value of 6.5 kcal/mol (2270 cm^{-1}).

Apart from boat and chair configurations for the ring, it has been postulated[4] that in cyclohexanone and some of its derivatives the oxygen atom is not coplanar with the adjacent C_2-C_1-C_6 ring atoms. The main evidence upon which this is based is an apparent doublet structure for the carbonyl stretching fundamental at 1710 cm^{-1} in the <u>liquid</u> phase infrared spectrum of CHh_{10}. Only a few investigators have

observed that this band has two components; Bauman and Thorsen[25] have shown that one of the components is identical in frequency to a water vapour absorption band, and disappears from the spectrum when the instrument is thoroughly flushed with dry nitrogen. We assume here, in common with most other investigators[5,18,26] that the C_2-C_1-C_6 and oxygen atoms are coplanar, or at least sufficiently close to coplanar that they do not give rise to separate absorbing species.

The questions to be decided are; firstly whether cyclohexanone has to be considered as a rigid or non-rigid molecule in its ground and lowest excited states, and secondly, what is the most appropriate point group to use in classifying its vibrational levels. To a certain extent, the first question is a matter of degree, since the non-rigid clarification depends upon the heights of potential barriers impeding the interconversion of different forms.

In the ground electronic state, the experimental evidence from analyses of the infrared and Raman spectra (see below) is that the vibrational levels can be classified under the C_s point group. Theoretically,this classification may not be strictly valid for vibrational modes of high frequency, of magnitude of the order of the barrier impeding chair-chair interconversion. However, because of their small Boltzmann population factor, transitions from such levels are not observed in the electronic spectrum, and so their symmetry

classification is not important for this.

In the electronic state produced by $n \rightarrow \pi^*$ electron promotion, we have no a priori knowledge of the barrier height between chair-chair interconversion. It might be expected to be slightly lower than in the ground state, since an $n \rightarrow \pi^*$ promotion has the effect of increasing the carbonyl bond length, and so decreasing non-bonded interactions between the oxygen and α-hydrogen atoms. On the other hand, there is the additional complication that $n \rightarrow \pi^*$ excitation in carbonyl compounds related to formaldehyde[27,28,29] and in cyclopentanone[30] produces a bending of the oxygen atom out of the plane of the adjacent carbon atoms. This leads to a further inversion doubling, at the carbonyl group. The molecule can now be non-rigid with respect to motion of the oxygen atom through the C_2-C_1-C_6 ring atom plane. In cyclopentanone, the barrier for this inversion is relatively low, 700 cm^{-1}[30], and the molecular vibrations in both the ground and (π^*,n) excited states can be classified under the C_{2v} point group.

Theoretically, it appears that the C_{2v} point group is the most appropriate for the (π^*,n) excited state of cyclohexanone, for two reasons. The first is that the $n \rightarrow \pi^*$ transition is highly localised in the carbonyl group, so that the vibrations associated with the group are primarily active in the electronic spectrum. The local symmetry at the carbonyl end of the molecule is C_{2v}, so, for selection rule purposes,

we can classify the vibrations under the C_{2v} point group. The same is true for the ground state vibrations localised in this region of the molecule, although the assignments of other authors for those under the C_s point groups will be used below. However the C_{2v} classification will not apply to other modes, such as ring vibrations for the above reason.

The second reason is that if the barrier to chair-chair inversion is low, the delocalised domain of the non-rigid molecule is now C_{2v}. This can be demonstrated as follows by the methods of Altmann[31,32,33] and Longuet-Higgins[34]. Recent theoretical work by Altmann[31] and Longuet-Higgins[34] use different approaches to the problem. Both of these theories will be applied here to cyclohexanone.

In both approaches the usefullness of this classification depends on the feasability of motion from one conformation to a different one of the <u>same energy</u>.

Longuet-Higgins[34] extended the concept of molecular symmetry to non rigid molecules by including nuclear permutations and permutation inversions as permissible group operations.

According to his notation E is the identity operation, P any permutation of position and spin of identical nuclei, or any product of such permutation, E^* is the inversion of all nuclear positions, and P^* the product $PE^* = E^*P = P^*$ is called the "permutation-inversion operation".

The molecular symmetry group is then the set of

1) all feasible P, including E

2) all feasible P^*, not necessarily including E^*.

Cyclohexanone has a plane of symmetry (see Fig. 1.1) $\sigma_v(xz)$. Then any reflection through this plane corresponds to a permutation of nuclei. Using the L.H. notation the permutation operation P is (26)(35) (ai)(bj)(cg)(dh) (see Fig. 1.5). E^* has no connection with the "inversion" belonging to the point group of a centrosymmetric molecule. L.H. says "E^* must be understood as being an operation which would not permute nuclei but reverse the sense of the molecular configuration"[34]. For cyclohexanone it is the operation which takes the molecule from one chair to the other chair form (see Fig. (1.5)).

for cyclohexanone

E	$\longleftrightarrow$	E
P(26)(35)(ai)(bj)(cg)(dh)	$\longleftrightarrow$	$\sigma_v(xz)$
E^*	$\longleftrightarrow$	$\sigma_{v'}(yz)$
P^*(26)(35)(ai)(bj)(cg)(dh)*	$\longleftrightarrow$	$C_2(z)$

For the L.H. notation the set of symmetry group for cyclohexanone is isormorphous to C_{2v}.

According to Atlmann[31,32,33] the symmetry group of a non rigid molecule possesses two subgroups: one is that of all symmetry operations of the Schrödinger groups of the molecule and the other is a group which is called an isodynamic group. The total group, called the Schrödinger super group (S),

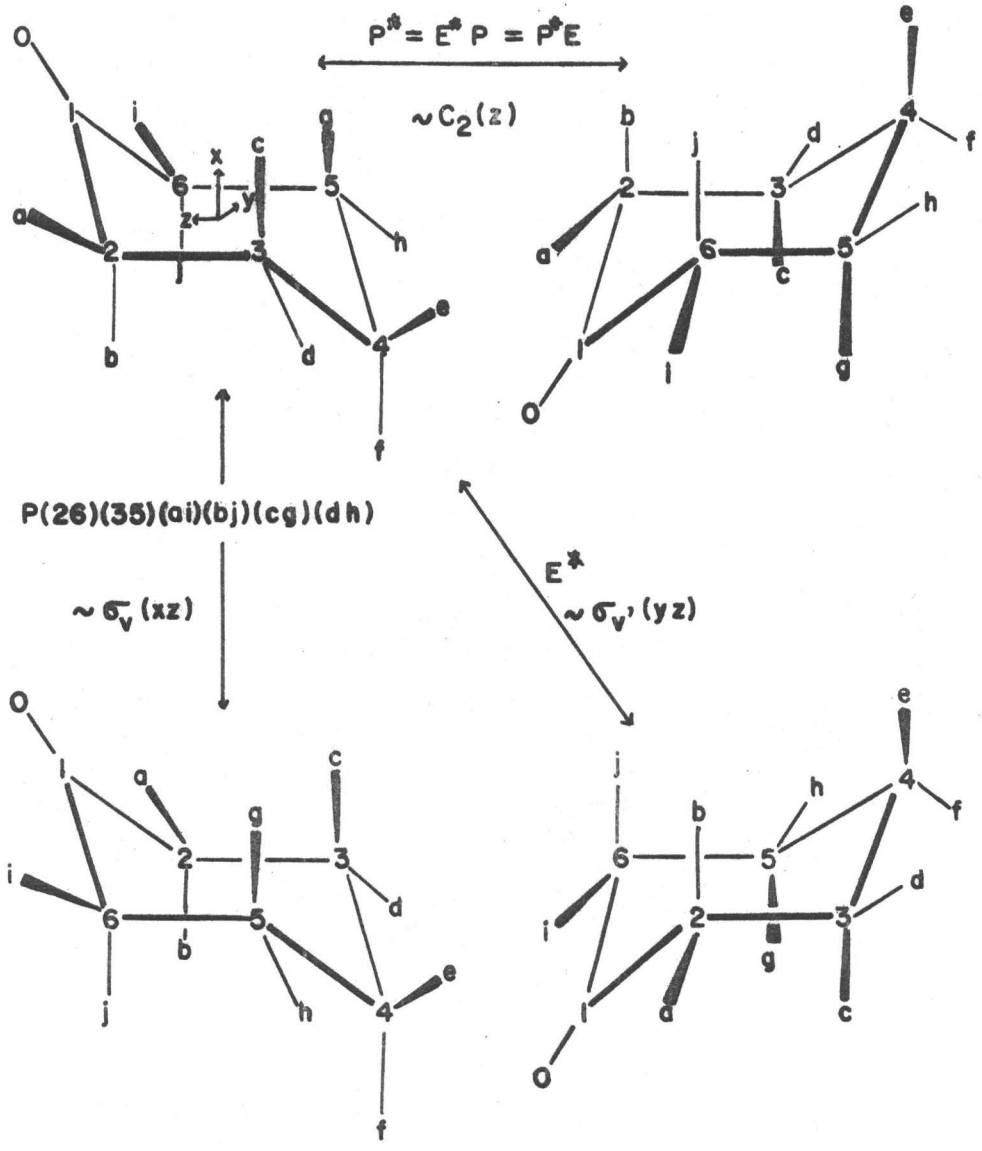

FIG(1·5) OPERATIONS OF THE NON-RIGID MOLECULE

is a semidirect product of the Schrödinger group (G) and the isodynamic group (I)

$$S = I_{\Lambda}G \qquad \text{(I-6)}$$

The Schrödinger group (G) is made of symmetry operations defined, exactly as for rigid molecule, in the usual manner.

for cyclohexanone

$$G \sim C_s \qquad \text{(I-7)}$$

The isodynamic group (I) is made of isodynamic operations, the latter involves isodynamic configurations.

Altmann means the following by Isodynamic Configurations. If a molecule posses two different configurations that cannot be transformed one into another by a Schrödinger group operation but have nevertheless identical eigenvalues, these configurations are called isodynamic. Thus cyclohexanone possesses two chair forms and two boat forms (Fig. 1.2). The two configurations (a,b) have the same eigenvalues. According to Altmann's definition they are isodynamic configurations. But (a) is not isodynamic to (c) or (d) because the energy of a chair form is different from the energy of a boat form. The two configurations (c,d) are also isodynamic configurations, but we said previously that we consider in this work only the chair forms which are the more probable forms.

Isodynamic operations are the operations which transform isodynamic configurations into one another. They are not symmetry operations but motions (translations or rotations) of

an atom or group of atoms with respect to the rest of the molecule.

For cyclohexanone the isodynamic operation is $\sigma_v'(yz)$ (Fig. 1.6). The isodynamic group contains elements $E, \sigma_v'(yz)$ (prime indicates the orientation of the symmetry plane).

$$I = E + \sigma_v'(yz) = (C_s')^I \qquad \text{(I-8)}$$

By the use of (I-6), (I-7)(I,8) formula

$$S = I \wedge G = (C_s')^I \wedge C_s = (C_s')^I \otimes C_s \sim C_{2v}$$

where $\sim$ means "is isomorphous to". The semidirect product can be replaced by the direct product since C_s' and C_s commute.

Thus the approaches of L.H. and Altmann give the same result.

Fig. (1.7) illustrates the effect of a double minimum potential on the ring flapping mode. For a barrier lower than zero point energy, the vibrational levels are only slightly perturbed from their values if the barrier were not present. For a medium energy barrier (of the order of one or two vibrational quanta), the components of the inversion doublets are well separated. For a high barrier (of the order of many vibrational quanta) the levels below the top of the barrier are coalesced into closely spaced inversion doublets; the doublets splittings near the potential minima may be too small to be observed. These splittings are additional to any

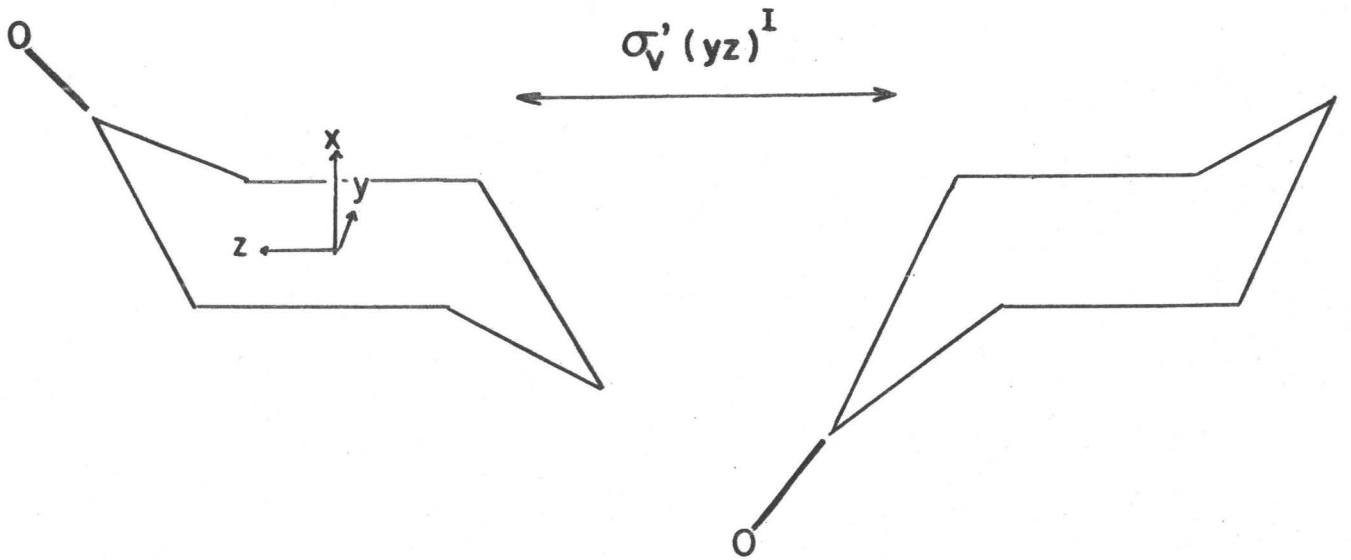

FIG(1·6) ISODYNAMIC OPERATION FOR TWO ISODYNAMIC CHAIR CONFIGURATIONS

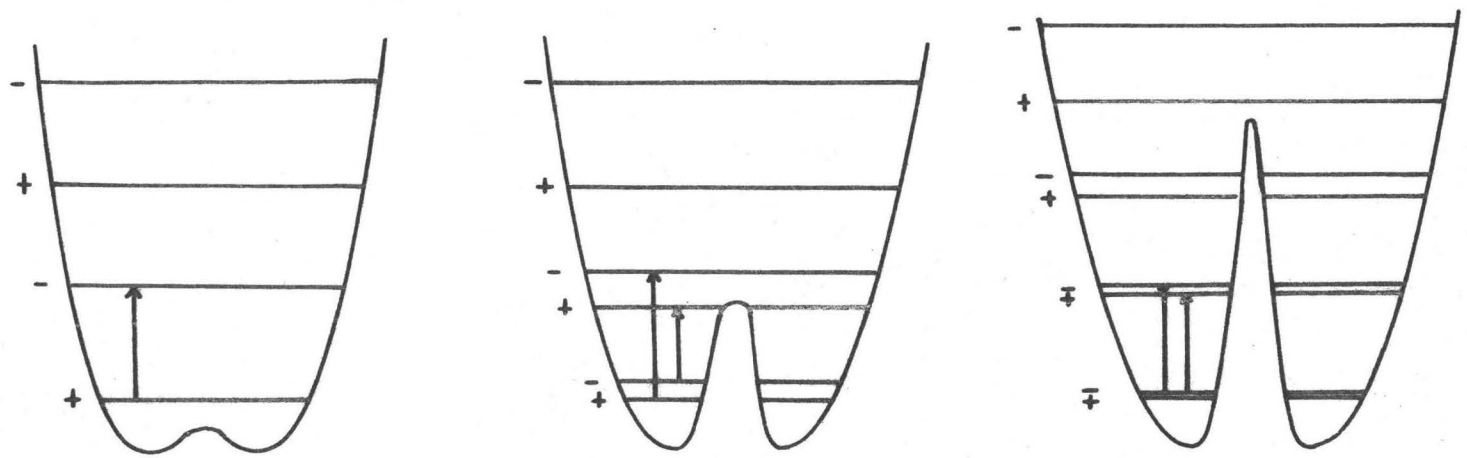

FIG(1·7) EFFECT OF BARRIER HEIGHT ON LEVEL SPACING

that may result from the inversion at the carbonyl group in the excited (π^*,n) state.

1.4 INFRARED AND RAMAN SPECTRA

Only points of particular relevance to the analysis of the electronic spectra will be mentioned in this section. As mentioned above the $n \rightarrow \pi^*$ transition involves promotion of an electron localised in the carbonyl bond. This, in general, causes vibrations of the carbonyl group and its neighbouring atoms to be active in the electronic spectrum.

For other cyclic ketones, some ring modes are also found to be active in their electronic spectra. In cyclopentanone, for example, Howard-Lock and King[30] found that the ring puckering mode of a_2 symmetry was active in the $n \rightarrow \pi^*$ system.

The infrared and Raman spectra of cyclohexanone (CHh10) have been examined several times, and many of the fundamentals have been assigned[4,7]. In particular, the C = 0 stretch fundamental frequency has been studied extensively[4,5,6,7,26,35,36] The absorption spectra of isotopes, cyclohexanone $\alpha\alpha\alpha'\alpha' d_4$ (CHd_4), and cyclohexanone fully deuterated CHd10) (see Fig. 1.8), have not been reported in the literature. Forel and Pétrissans[7] (their work will be referred to below as F.P.) analysed the liquid infrared spectra of CHh10 and assigned most of the bands by comparison with that of cyclohexane. Apart from the above

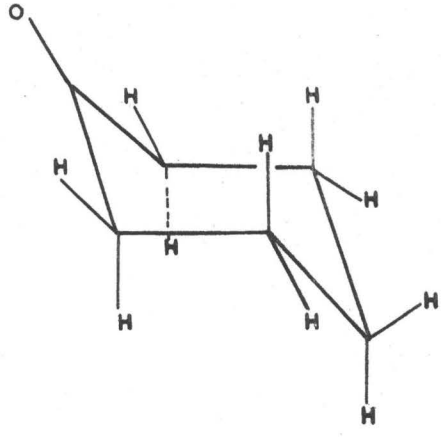

CHh10

CYCLOHEXANONE

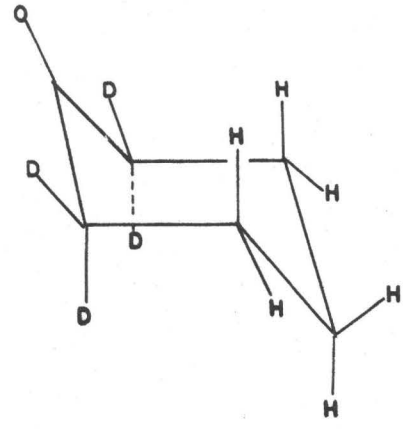

CHd4

CYCLOHEXANONE αα α'α' d4

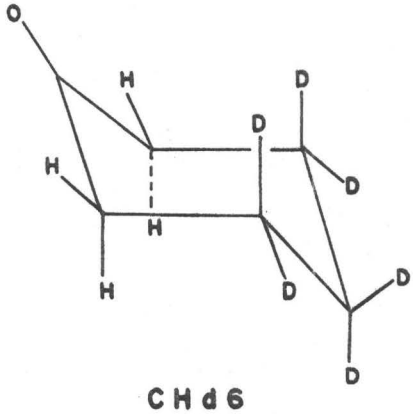

CHd6

CYCLOHEXANONE ββ β'β' γγ' d6

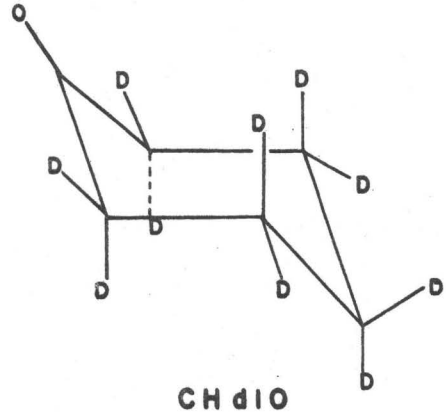

CHd10

CYCLOHEXANONE d10

FIG(1·8) CYCLOHEXANONE ISOMERS

little definite information about the vibrational ground state has been published.

Currently force constant calculations upon the cyclohexanone isomers CHh_{10}, CHd_4, CHd_6, CHd_{10} (see Fig. 1.8), using data from their infrared and Raman liquid spectra, are being carried out by Dr. R. N. Jones and his coworkers at the National Research Council of Canada in Ottawa. Dr. R. N. Jones kindly supplied us the latest results of their work[a], which will be referred to below as RNJM[26]. The results of RNJM[26] and F.P[7] are slightly different. Neither of them investigated the infrared spectrum of the vapour phase.

Although the vibrational spectra was not reanalysed here, some of the infrared bands were examined in detail, in the vapour phase, in order to obtain information relevant to the electronic band analysis.

The infrared liquid spectra and Raman liquid spectra examined by RNJM[26] shows that most of the vibrations are infrared and Raman active as fundamentals; only a few weak bands in the infrared liquid spectra did not appear in the

---

(a) We wish to thank Dr. R. N. JONES and Dr. H. H. MANTSH for communicating the liquid infrared and Raman data in advance of publication.

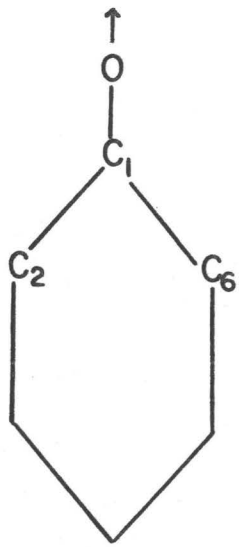

C=O STRECH

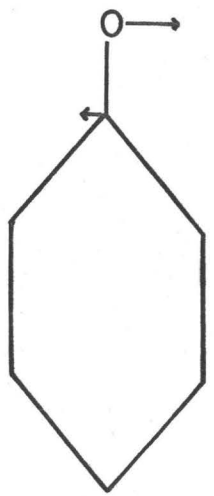

C=O BEND-IN-PLANE

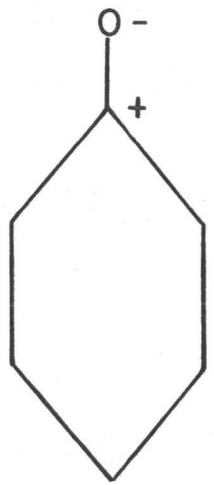

C=O OUT-OF-PLANE WAG

	ν_7	ν_{43}	ν_{21}
C_{2v}	a_1 (IR(A), R(p))	b_2 (IR(B), R(d))	b_1 (IR(C), R(d))
C_s	a' (IR(A,C), R(p))	a" (IR(B), R(d))	a' (IR(A,C), R(d))

FIG(1·9) VIBRATIONS OF THE CARBONYL GROUP

Raman spectra. If the molecule were classified under the C_{2v} point group, one would not expect this, since all the fundamentals of symmetry a_2 would be infrared inactive. If all the modes are active in both spectra, then the molecule must be classified under its "rigid" point group (C_s). The C_{2v} point group, will later be used for classification of the excited state vibrations.

VIBRATIONS OF THE CARBONYL GROUP

The three carbonyl vibrations are sketched in (Fig. 1.9). The carbonyl stretch numbering of the modes are those given by RNJM , and correspond largely to a stretching mode along the (C = 0) bond. The carbonyl "in-plane-bend" ν_{43} is a bending mode in the plane of the carbons C_1-C_2-C_6. The carbonyl "out of plane wag" ν_{21} refers to a motion approximately perpendicular to the C_1-C_2-C_6 plane.

In the present high resolution study of the vapour phase spectrum the fundamental ν_1 was found to be at 1735 cm^{-1}. Some authors have found a shoulder at slightly lower energy and have explained it as resulting from either a Fermi resonance or the possibility of two configurations arising from a small angle between the carbonyl group and the C_1-C_2-C_6 plane[4,5]. But these ideas have been criticized[7,25]. Baumann and Thomson[25] showed that the shoulder found in the liquid spectrum corresponds to an absorption band of

water vapour, which disappears when the spectrophotometer is flushed with dry nitrogen. It is also extremely difficult to remove traces of water from cyclohexanone. More detail on the infrared results will be given in Appendix I, but we note that the profile obtained in this work for the carbonyl stretch absorption band in the vapour has a maximum at 1735 cm^{-1} and does not show any shoulder due to cyclohexanone absorption. Two weak bands at 1717.5 cm^{-1} and 1700 cm^{-1} can definitely be identified as water vapour absorption bands. Consequently, in the rest of this thesis we will assume that the oxygen atom lies in the plane of three adjacent carbons. The band observed under high resolution definitively shows true P,Q and R branches, and can be identified as a hybrid of type A plus C, mainly type A.

The two other carbonyl frequencies Fig. (1.9) are expected to occur below 700 cm^{-1}. The values of the fundamental frequencies below 700 cm^{-1} obtained experimentally, from the infrared and Raman liquid spectra, are listed in Table 1.4. These values were measured by RNJM for the deuterated isomers. Table (1.4) also gives the results of potential energy distribution calculations done by RNJM[26] for CHh_{10}. The results obtained for the deuterated molecules are slightly different but these differences do not change the band assignment. The notations given in Table 1.4 for torsions, bending, and wagging are those used by RNJM. "ρ" represents the carbonyl

TABLE 1.4

FREQUENCIES OF CYCLOHEXANONES BELOW 700 cm^{-1} (GIVEN BY RNJM (26))

FREQUENCIES IN cm^{-1}												ASSIGNMENT		
CHh_{10}			CHd_4			CHd_6			CHd_{10}			RNJM(26)		FP(7)
I.R.	R[a)]	ρ[c)]	I.R.	R	ρ	I.R.	R	ρ	I.R.	R	ρ		P.E.D. for CHh_{10}	
	105_m[b)]			101			91			93		A'	$\omega_\alpha(32)\tau_{\beta\gamma}(13)\rho(13)\chi(12)$	not observe
	189_m	0.68		175			164			163		A"	$\tau_{\beta\gamma}(46)\omega_{\beta\gamma}(20)\omega_\alpha(16)$	not observe
	313_m	0.39		308_m			254	0.57		254_m	0.62	A'	$\omega_{\beta\gamma}(34)\tau_{\beta\gamma}(33)\omega_\alpha(10)$ $\gamma_\beta(10)\rho(6)$	
410_m	411_s	0.71	360_m	361_m		435_m	435_w	0.89	349	351_s		A'	$\chi(33)\omega_{\beta\gamma}(19)E(14)\rho(6)$	
460_{vw}			390_m	392_m	0.85	381_m	388_m	0.87	368_w	366_s	0.81	A"	$\omega_{\beta\gamma}(36)\omega_\alpha(28)\gamma_\alpha(15)$ $\gamma_\beta(12)$	
490_s	491_m	0.77	462*			483_{vs}	486_m	0.78	450_{vs}	452_s	0.70	A"	$E(70)\omega_\alpha(10)$	
491*	480[d)]		454_{vs}	455_s		379_m	379_m	0.77		381_m		A'	$\omega_{\beta\gamma}(36)\gamma_\alpha(21)\gamma_\beta(18)$ $\rho(16)\gamma_\gamma(14)$	
652_m	655_{vs}	0.06	616_m	614_{vs}	0.06	603_m	605_s	0.20	580_m	583_{vs}	0.25	A'	$\rho(33)R_\beta(14)R_\alpha(11)\gamma_\beta(11)$ $\gamma_\gamma(10)$	

a) Raman $\Delta\nu(cm^{-1})$ obtained with a laser source
b) Subscript gives the relative intensity of the band
c) ρ=polarisation ratio of Raman lines
d) Value given by F.P.(7) and observed by (4) in Raman

* Not observed in liquid IR or R spectra obtained by RNJM (26) by theoretical calculations

out-of-plane wag deformation, and "E", the carbonyl in plane bending motion. The assignments given by F.P[7] are also listed in Table 1.4 but do not correspond to those of RNJM.

A study of the infrared spectra of different cyclic ketones below 700 cm^{-1} has been performed by Katon and Bentley[6]. Five, six, seven member rings all show a very strong absorption band around 500 cm^{-1}. Cyclopentanone vapour[6,30] shows a strong band at 467 cm^{-1}, with a shoulder at 446 cm^{-1}. the first band has been assigned by Howard-Lock and King[30] to the carbonyl bending mode and the second to the carbonyl out of plane wag. These two bands are more clearly resolved in deuterated cyclopentanone[30] and in the 3-methyl cyclopentanone[6]. This strong absorption band around 500 cm^{-1} shows a well defined shoulder at lower frequency. In the case of acetone[59,60] the carbonyl in plane bending fundamental is assigned to the band at 530 cm^{-1} while 484 cm^{-1} is the value of the carbonyl out of plane wagging mode. In all these cases, as well as the other listed in Table 1.5, the carbonyl out of plane wagging mode appears at lower frequency than the carbonyl in plane bonding mode, and generally forms a rather weak satellite of the intense band attributed to the former. The liquid phase absorption spectra of the four isomers of cyclohexanone $CHh_{10}/CHd_4/CHd_6/CHd_{10}$, show a very strong band respectively at 490/454/484/450 cm^{-1}. This strong band is reported depolarized in the four respective Raman spectra by RNJM[26] with

a depolarisation ratio of ∿ 0.75. The irregular isotope shift is unusual if one assigns the strong band to a ring mode as suggested for CH10 by F.P[7]. The frequency of a ring mode is expected to decrease as the molecule becomes more ring deuterated.

On the other hand the molecules CHh_{10}/CHd_6 as well as CHd_4/CHd_{10} are identical in the region of the carbonyl group, CHh10/CHd_6 having only hydrogen atoms close to the carbonyl group (see Fig. 1.6) and CHd_4/CHd_{10} have only deuterated atoms here.

A similar "irregularity" in the isotope shift has been also observed for the carbonyl stretching mode, which is at 1715/1709/1715/1709 cm^{-1} respectively for $CHh_{10}/CHd_4/CHd_6/CHd_{10}$ in their liquid spectra.

The same effect had been observed for the carbonyl modes of other molecules related to cyclopentanone[30]. This variation presumably reflects differences in non bonded interactions between the oxygen atom and the α substituted hydrogen and deuterium atoms according to Howard-Lock and King[30]. Consequently in agreement with RNJM[26] we assign the strong band at ∿ 490 cm^{-1} to the carbonyl in-plane-bend. Our observation under high resolution in the vapour phase infrared spectrum of CHh10 and CHd10 show that the band at 490 cm^{-1} is broad and does not have a clear structure. According to RNJM's <u>theoretical</u> calculations a normal mode

involving the carbonyl wagging motion is active very close to the 490 cm^{-1} frequency (see Table 1.4). Moreover some workers report a very weak band in the Raman liquid spectrum of CHh_{10} at 480 cm^{-1} [4,7]. From our observations it is not possible to decide this point definitely, the band being too broad. There is a possible shoulder at 5 to 10 cm^{-1} lower frequency than the main band in the CHh_{10} spectrum.

According to RNJM's calculations no band can be definitely assigned to the carbonyl out of plane deformation motion. They write; "The C = 0 out of plane wag is distributed among several a' modes and couples strongly with C-C bend coordinates. The main contribution (circa 30%) see table (1.4) is to the band at 653/615/604/581 cm^{-1}. This is a highly delocalized mode. It is meaningless to attempt to characterize any band in the spectra as the C = 0 out of plane wag".

Such an interpretation is quite different for cyclohexanone than for other cyclic ketones for which, as Table (1.5) shows, the out-of-plane carbonyl wag gives a well characterized band at slightly lower frequency than the in plane bend. Furthermore, the out-of-plane wag is, by analogy with the $n \rightarrow \pi^*$ transitions in other carbonyl compounds, expected to be strongly active in the electronic spectrum, but the 653/615/581 cm^{-1} interval is not observed in the electronic spectra of the cyclohexanone isomers, whereas intervals of $\sim$ 490 cm^{-1}/454 cm^{-1}/460 cm^{-1} are.Of course, no fundamental can be

said to be entirely localized in a particular band in cyclohexanone. Nevertheless, calculations as to the degree of delocalization depend closely upon the type of free field used, and it is suggested here that cyclohexanone follow the other ketones rather more closely than RJNM suggest, having a weak band at $\sim 480\ cm^{-1}$ which is predominantly an out-of-plane wagging motion.

TABLE 1.5

(C=0) DEFORMATION FREQUENCIES

Molecule	δ(C=0) out-of-plane cm^{-1}	δ(C=0) in-plane cm^{-1}	Reference
Vinylene carbonate	532	565	61
β propiolactone	490	513	62
Cyclobutanone	395	454	63
Cycloheptanone	470	500	6
Acetone	484 sh	530 s	64
ααα acetone d_3	438 w	501 s	64
acetone d_6	405 w	475 s	64
Cyclopentanone h_8	446 sh	467 s	30
Cyclopentanone ααα'α'd_4	375	438	30
Cyclopentanone d_8	378	433	30

*notation

s = strong

sh = shoulder

w = weak

CHAPTER 2

EXPERIMENTAL WORK

2.1 ORIGIN, PROPERTIES AND PURITY OF SAMPLES

Cyclohexanone and two of its deuterated isotopes were studied. These are the $\alpha_1\alpha_2\alpha_1'\alpha_2'd_4$ cyclohexanone and fully deuterated cyclohexanone.

Cyclohexanone (CHh_{10}) was supplied by Matheson Coleman and Bell Co. It was stated to have 99% purity, and was used without further purification, except for a trap to trap distillation under vacuum immediately before spectral use. The sample was stored in a blown glass bottle and kept in a refrigerator.

Pure cyclohexanone is a clear, colourless liquid which boils at 155°C and has a vapour pressure of 3 mm at 25°C.[69] A plot of vapour pressure versus temperature is shown in Fig. 2.1.

Although cyclohexanone dissolves stopcock grease and attacks teflon tubing, this did not cause problems because most of the ultraviolet measurements were made using a metal multireflection cell.

The infrared, Raman, and vacuum ultraviolet spectra

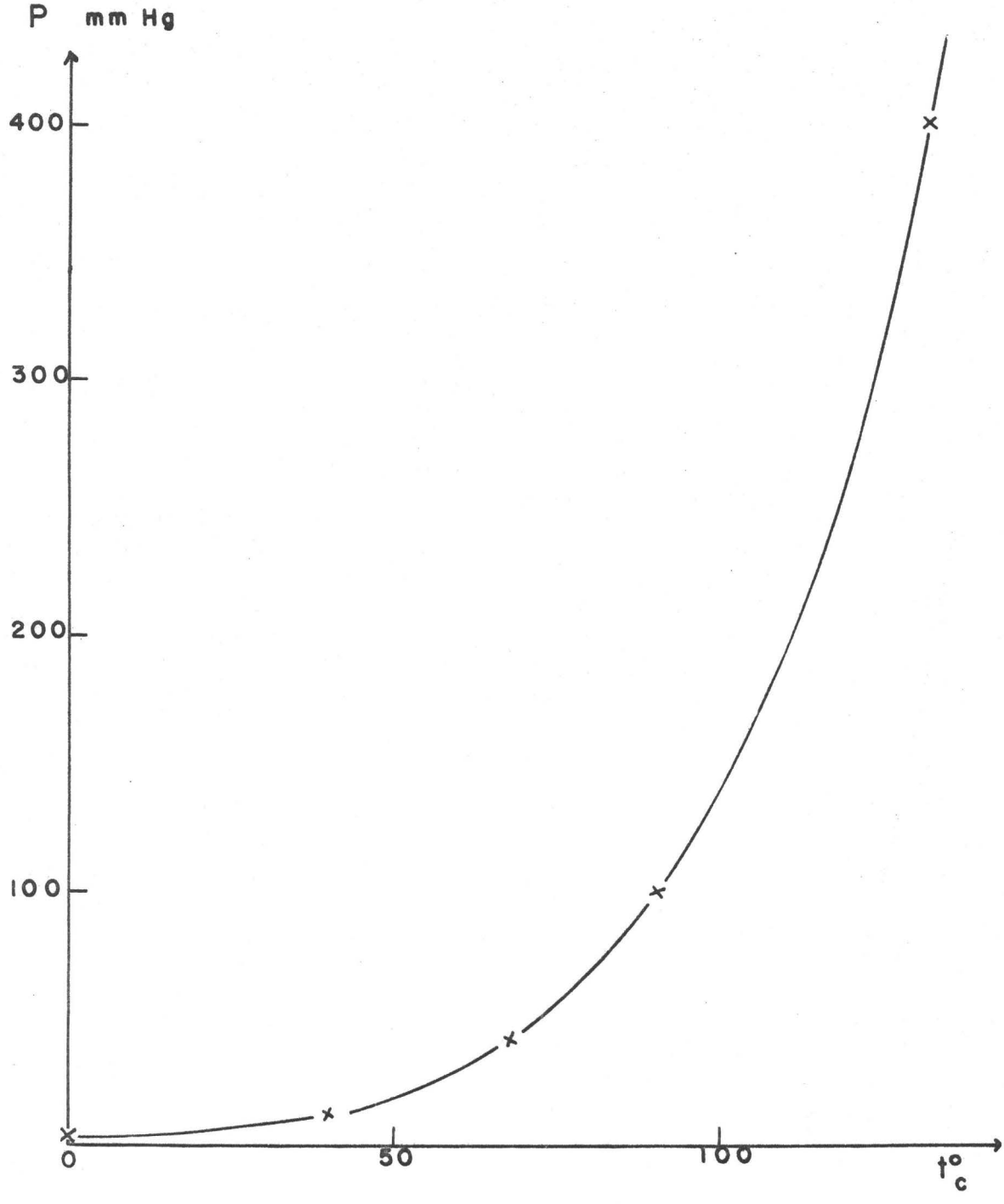

FIG(2·1) VAPOUR PRESURE OF CHhIO

of the samples of CHh_{10} used were very similar to such spectra of the molecule as have been previously reported[7,39] The NMR spectrum also agreed with the published[21,40] spectra and did not show that any impurities were present.

Fully deuterated cyclohexanone (CHd_{10}) was supplied by Diaprep Incorporated Co. The purity is given by the Company as being 99.9%.

This isotope was used without further purification other than a vacuum distillation, since only small quantities were available.

Cyclohexanone $\alpha_1\alpha_2\alpha_1'\alpha_2'd_4(CHd_4)$ was synthesised using the procedure described by Montgomery[40]. A solution consisting of 67.5 g (0.69 mole) of cyclohexanone, 15.0 g (7.5 moles) of deuterium oxide (99.8%), 8 ml of triethylamine and 475 ml of anhydrous diopane was refluxed for 22 hours. Deuterium oxide, water, triethylamine , and diopane were removed by distillation. The exchange procedure was repeated four more times using fresh 80 g portions of deuterium oxide in combination with 10 ml of triethylamine and 500 ml of diopane. The NMR and infrared spectra were recorded after each exchange. The compound was then dried over calcium chloride.

Proton NMR analysis of the deuterated ketone showed that the four α hydrogens had been deuterated to an extent greater than 99%. The boiling point of cyclohexanone $\alpha_1\alpha_2\alpha_1'\alpha_2'd_4(CHd_4)$ was 153-154°C.

2.2 INFRARED SPECTRA

Infrared spectra of cyclohexanone were recorded on a Perkin Elmer 521 double beam grating spectrophotometer in the 4000-250 cm^{-1} region.

For vapour phase work a 10 cm path length absorption cell fitted with cesium iodide windows and wrapped with a heating tape was used.

Most of the bands were strong enough to be observed with the sample at room temperature. A few required cell temperatures of 60°C.

An evacuated 10 cm cell with CsI windows was placed in the reference beam of the double beam spectrophotometer, in order to compensate for absorption bands of atmospheric water vapour and carbon dioxide.

The spectrophotometer was thoroughly flushed with dry nitrogen before use, but even so, traces of water vapour absorption remained in the spectra. These could come from residual water vapour in the instrument, from water adsorbed on the cell windows, or from traces of water in the samples. Even when the latter were thoroughly dried with a molecular sieve, the water bands remained. (The prototype molecule acetone, CH_3COCH_3 is notoriously difficult to obtain free of all water). In the ultraviolet work, the water presents no problem since it does not absorb in the near ultraviolet. In the infrared work, the water absorption only gave trouble when it was at the same frequency as a cyclohexanone band and distorted the profile of

the latter.

2.3 ULTRA VIOLET SPECTRA

-Low Resolution Spectra-

Preliminary work on the gas phase ultraviolet absorption spectrum of CHh_{10} was carried out on a Cary Model 14 recording Spectrophotometer. A 10 cm quartz cell, wound with nichrome wire which could be heated electrically to 150°C was used. The spectrum showed a strong continuous absorption with a maximum at 2900 Å (See Fig. 2.2). As the temperature was increased the continuum increased in intensity and some vibrational structure appeared in superposition.

Most of the spectra were obtained on a Bauch and Lomb 1.5 m grating spectrograph, model 11. The regions 3700-7000 Å in the first order and 1850-3700 Å in the second order could be photographed on single film strips. The discrete absorption of the cyclohexanones appears in the region of 2500 Å to 3500 Å and was photographed in the second order of the Baush and Lomb spectrograph. Separation of the first and second order spectra was accomplished by use of different combinations of optical filters and spectral emulsions for the film.

The instrument has a reciprocal dispersion at the film of 14.8 Å/mm and 7.4 Å/mm for these two orders and theoretical resolving powers of 35,000 and 70,000 respectively.

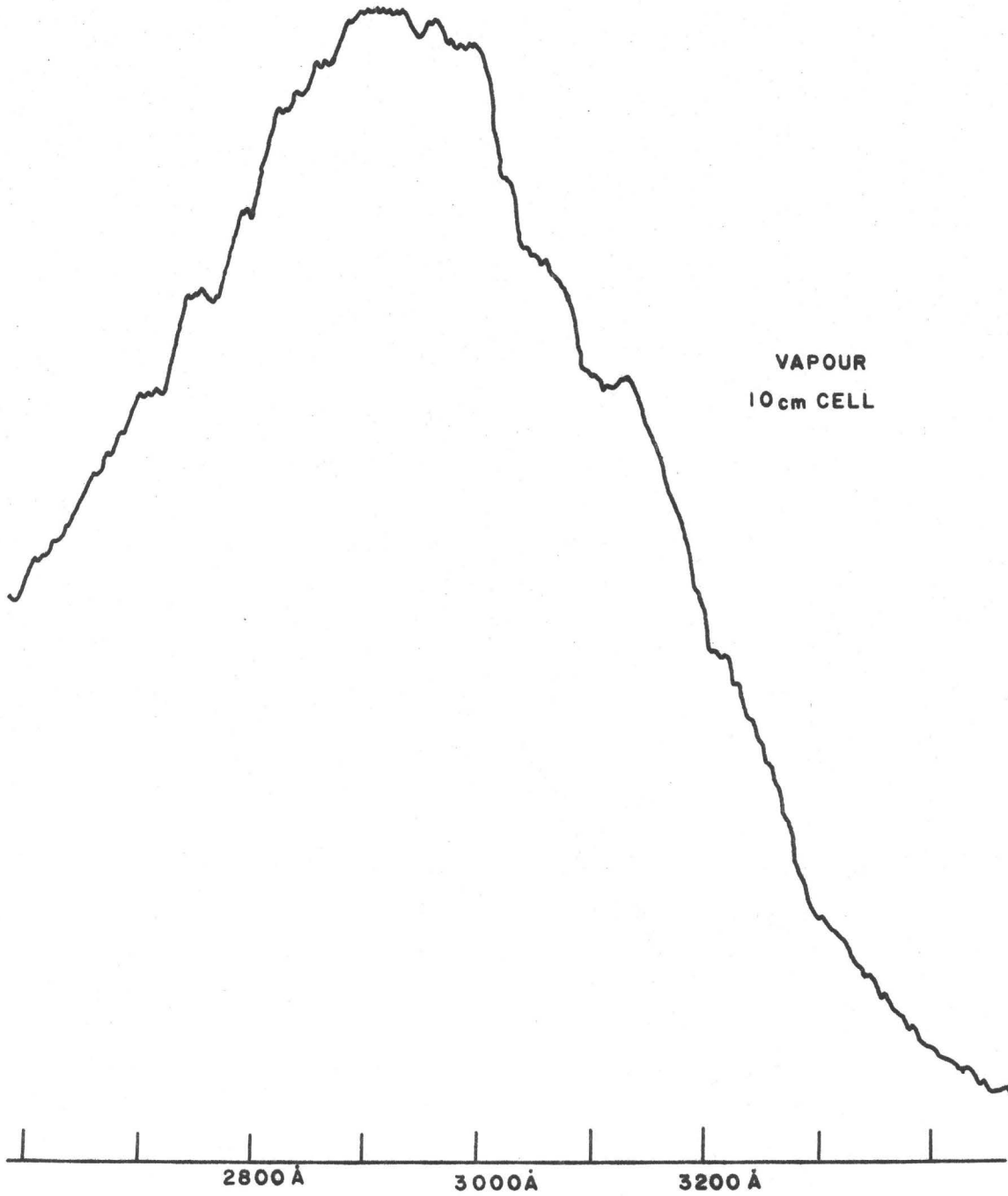

FIG(2·2) LOW RESOLUTION ABSORPTION SPECTRUM OF CHh10

A slit width of 10 microns was used.

The above spectrograph was used first in conjunction with a 1.8 m multireflection cell of the White type[41], which enabled absorption path lengths up to 36 m to be obtained.

Discrete bands first appear in the spectrum at a path length of 24 m, which correspond to a pressure path of 0.1 m. at. Much longer path lengths were required to observe the other discrete bands at the red end of the spectrum.

The 6 m multireflection cell which was also used, gives path length from 12 m up to 480 m. The cyclohexanone spectra were photographed using path lengths from 24 m up to 360 m. The corresponding pressure paths are respectively 0.1 m at to 1.4 m at. at room temperature.

The light source was a 450 watt, 115 volt d.c., high pressure OSRAM xe arc lamp, which was run at 25 amps. In order to minimize photo decomposition, a glass filter corning, o 54 was placed immediately in front of the light source. This cuts off light below 2600 Å.

Cyclohexanone does not attack the aluminised mirrors in the multireflection cell as does cyclopentanone[38]. Nevertheless the mirrors were cleaned and realuminized before each series of experiments. In the case of CHh_{10} and CHd_4 the sample was never left overnight inside the cell, but was kept frozen out in a liquid nitrogen trap. The cell was degassed by continuous pumping during the night. Fresh sample was then intro-

duced into the cell the next morning by vacuum distillation.

A certain amount of sample was lost during these numerous distillations, and so a slightly different procedure was used for CHd_{10}. The sample was kept in the 6m cell during the whole periods of experiments. After a week of photography with short path lengths and pressure path of 0.1 m at a very sharp spectrum was observed at 2500 Å, but this did not interfere with the cyclohexanone spectrum CHd_{10}. It appeared to be the benzene (C_6H_6) spectrum. Since CHd_{10} does not have any hydrogen atoms, the benzene could not have been produced by decomposition of CHd_{10}. It probably originated from degassing of the O rings of the cell which had been cleaned, several months before, with benzene.

-High Resolution Spectra-

High resolution ultraviolet spectra of the cyclohexanone isomers were taken on a 6 m Ebert plane grating spectrograph in the first order. The first order reciprocal dispersion at the plate at 3300 Å is 0.72 Å/mm. The resolving power is about 150,000 n where n is the order.

The discrete absorption bands always appear superimposed on top of the strong continuum. Exposure times of several hours were necessary to photograph these bands. Although the optimum slit setting is around 35 microns for the region of interest, a 50 micron slit was used to give reasonable exposure time.

The discrete spectrum could be photographed over the range 3500 Å to 3150 Å.

Only the 6 m multireflection cell was used for the high resolution work. The same experimental procedure as described above for low resultion work was used.

Because of the intensity of the strong continuum beneath the discrete spectrum increases at shorter wavelengths, the vibrational structure had to be photographed over a wide variety of absorption pressure paths. The spectrum was recorded between 3500 Å to 3350 Å, 3350 Å to 3250 Å, 3250 Å to 3150 Å at respective pressure paths of 1.4 m at, 0.9 m at, 0.7 m at. The discrete spectrum of CHh_{10} merged into broad, diffuse bands below 3200 Å.

For the isomers CHh_{10}, CHd_4, CHd_{10} in this order, under the same pressure path conditions. The relative intensity of the continuous absorption spectrum increases and the discrete spectrum becomes weaker with respect to the continuum.

Under high resolution only a few bands of CHd_4 showed up on the photographic plate, and none of the bands of CHd_{10} were observable under high resolution.

2.4 LOW TEMPERATURE WORK

Attempts to observe the absorption spectrum of CHh_{10} in the solid phase at liquid helium temperature were made with the aid of a Cary liquid helium dewar.

Two types of experiments were tried, one with pure crystals of CHh_{10}, the other with the substance dissolved in an SF_6 matrix at a concentration of 1%.

In both cases, the sample (plus any solvent) was sprayed on a quartz crystal window, the latter being cooled by conduction through a copper holder attached to the bottom of the liquid helium dewar.

The spectrum was observed on the Cary 14 Model spectrophotometer and pictures were also taken on a Hilger E-492 Littrow prism spectrograph over the range of 4000 Å-2600 Å. The spectrum in the SF_6 matrix is shown in Fig. 2.3. Very little information could be obtained, since the spectrum showed only few very broad bands. However the samples may have been above liquid helium temperatures; their temperature could not be determined with the apparatus available.

2.5 PHOTOGRAPHY AND MEASUREMENTS

Spectra were recorded on Kodak spectrum analysis film No. 1 and Kodak film type 1-0. The latter was found to be experimentally six times faster than spectrum analysis film No. 1. Kodak film type 1-0 was used for most of the high resolution work mainly because of its high speed but spectrum analysis No. 1 was preferred for low resolution work because of its fine grain and good resolution. Both types of film were developed by recommended procedures.

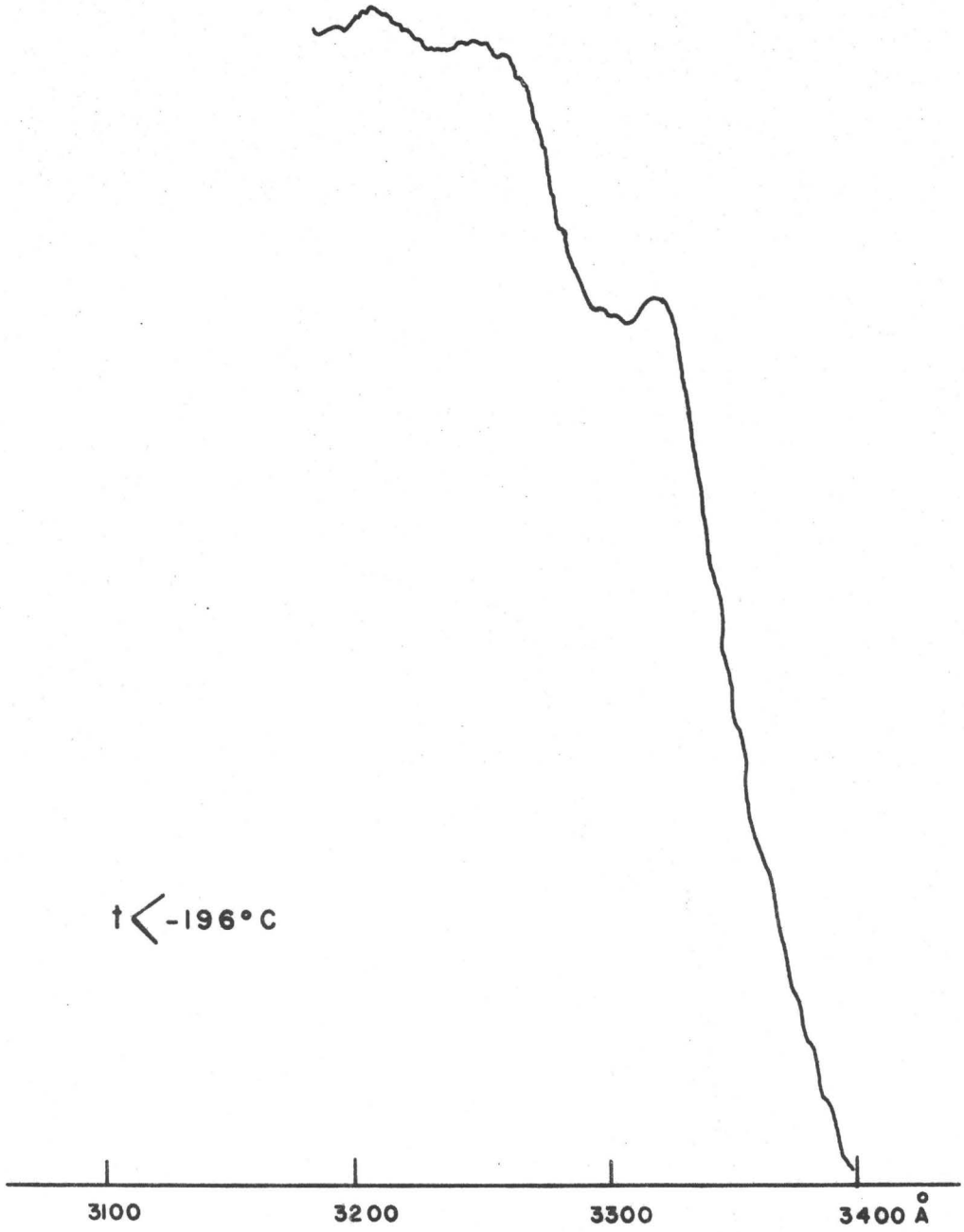

FIG(2·3) LOW TEMPERATURE ABSORPTION SPECTRUM OF CHhIO

Iron emission lines from a Pfund arc[48] were photographed adjacent to each absorption spectrum for calibration purposes. Accurate values for the wave length of the iron lines were obtained from Tables issued by the National Research Council[42].

The relative positions of band heads of cyclohexanone and iron emission lines were all measured by quadratic interpolation from traces made off the spectrograms on a Joyce-Loebl MKIII double beam microdensitometer.

The wavelength of the measured iron lines was fitted to a quadratic $y = a_o+a_1x+a_2x^2$ by means of a least squares fit, and the wavelength of the absorption bands obtained by interpolation. The calculated air wavelengths of the absorption bands were converted to vacuum wavelengths according to Edlen's formula[43], then converted to vacuum wave numbers.

The microdensitometer cannot record simultaneously traces of iron lines and absorption bands, and the small displacement of the pen in its holder necessary to record both spectra could introduce a very small shift between iron lines and absorption bands. To avoid this type of error, several traces (usually five) of each band were recorded and then measured in the way described previously. An average value for each band was then taken.

The accuracy is estimated to be $\pm 1\ cm^{-1}$ to $\pm 5\ cm^{-1}$ for most of the low resolution spectrum, depending upon the sharpness of the bands. Under high resolution from 1st order Ebert pictures, the accuracy of measurement of band heads is estimated to be less than $\pm\ 0.5\ cm^{-1}$.

CHAPTER 3

ANALYSIS

The prototype carbonyl-containing molecule is formaldehyde H_2CO. A qualitative diagram of the electronic energy levels obtained in simple molecular orbital (Mo) approximation is given in Fig. 3.1. The atomic orbitals (Ao) are represented on the left and the Mo's on the middle in order of increasing energy. The ordering of the orbitals in cyclohexanone follows that given for formaldehyde[44]. On the far right are indicated the symmetries of the Mo's under the C_s and the C_{2v} point groups.

In the electronic ground state, all the orbitals up to the (n) orbitals are filled with electrons, so that the ground state configuration is $(\sigma)^2(\pi)^2(n)^2$, which gives a singlet state only.

The lowest electronically excited state is obtained by promoting an oxygen lone pair electron from the n orbital into the antibonding π^* orbital. The configuration of this excited state is

$$(\sigma)^2(\pi)^2(n)(\pi^*)$$

and gives either a singlet or a triplet state. Formally, the $n \rightarrow \pi^*$ electronic transition can give rise to both a triplet$\leftarrow$singlet transition and a singlet$\leftarrow$singlet transition.

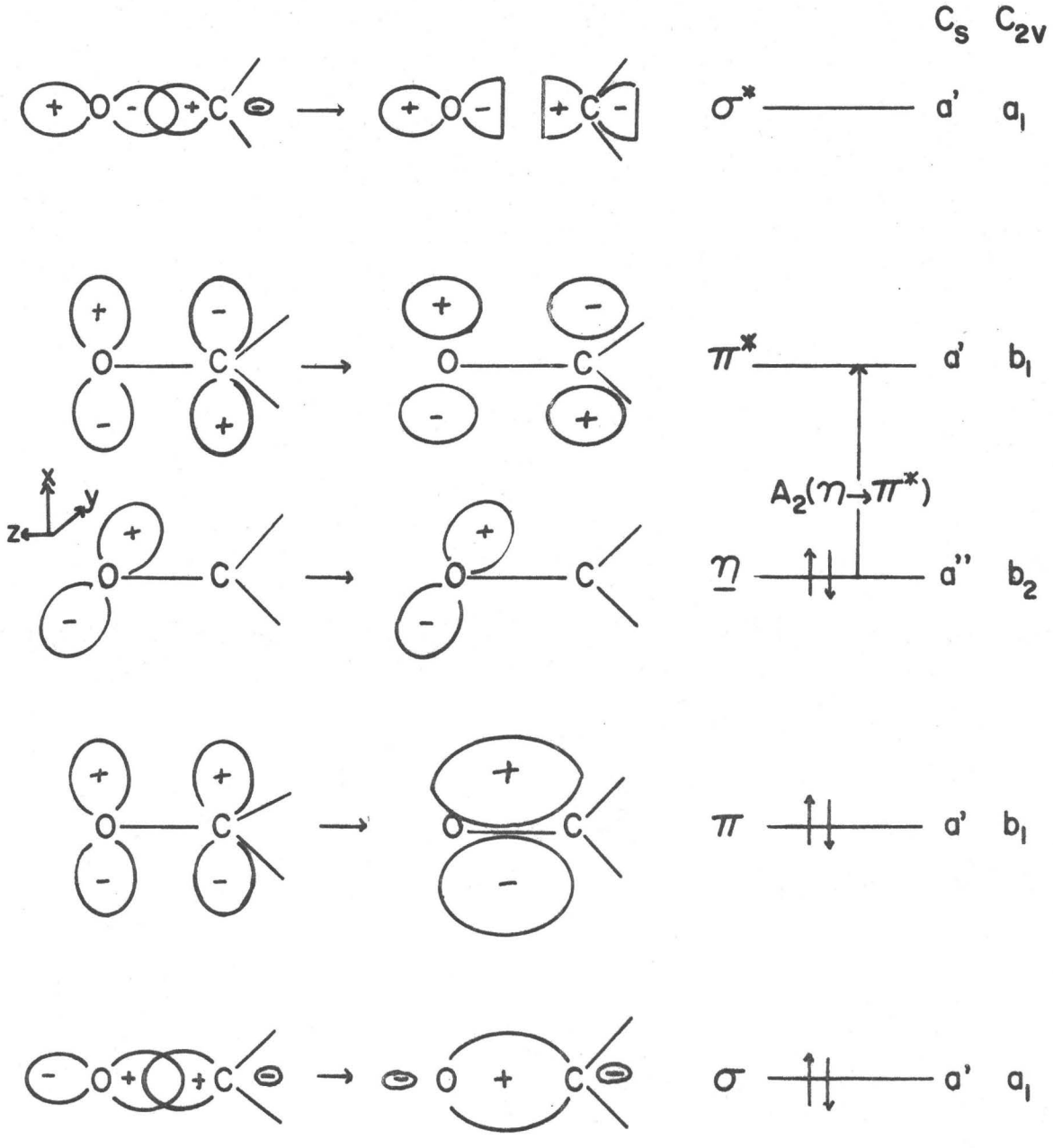

FIG (3·1) LOCALIZED MO'S AND $n \rightarrow \pi^*$ ELECTRONIC TRANSITION FOR THE CARBONYL GROUP

The triplet←singlet transition is always much weaker than the singlet←singlet one. Consequently it can only be observed in absorption at very long vapour path lengths, in a region of lower energy than the singlet←singlet transition. The triplet←singlet absorption transition is very weak in the formaldehyde spectrum, and has not been observed in the spectra of cyclopentanone[38], as in that of cyclohexanone.

The relatively strong absorption in the near ultra violet of formaldehyde and related molecules is due to the $\underline{n}\rightarrow\pi^*$, $^1A_2 \leftarrow {}^1A_1$ singlet←singlet transition, and it is the analogue of this transition in cyclohexanone which is studied here. The transition is of interest for two special reasons.

Firstly, in formaldehyde, the molecule is pyramidal in the $^1A_2(\pi^*,\underline{n})$ excited state, the potential function with respect to inversion of the molecule through the plane of symmetry through the nuclei in the ground state showing two minima. This leads to a doubling of out-of-plane vibrational energy levels below the central potential hump, Fig. 3.2, where θ is the out-of-plane angle. Similar out-of-plane equilibrium geometries are found for other related molecules, as summarized in Table 3.1. The question arises as to whether a similar bent geometry occurs in the excited state of cyclohexanone, and to what extent this is constrained by the presence of the carbon ring.

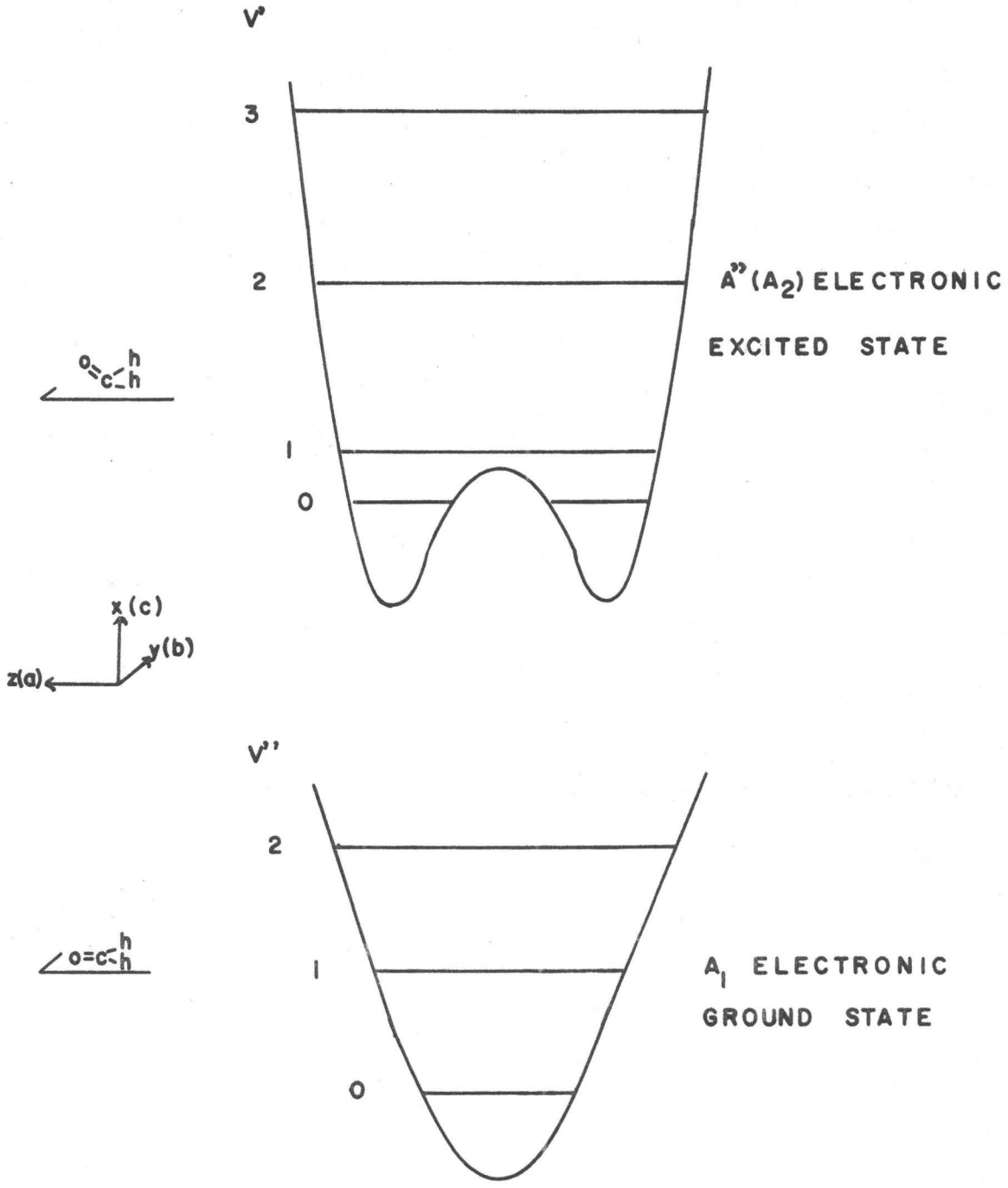

FIG(3·2) $A'' \longleftarrow A_1$ TRANSITION IN FORMALDEHYDE

TABLE 3.1

SINGLET-SINGLET $n \rightarrow \pi^*$ TRANSITIONS IN CARBONYL COMPOUNDS

Compound	Absorption	Transition	r"(CO)Å	r'(CO)Å	out of plane angle θ'	Remarks	Ref.
H_2CO (Formaldehyde)	3500-2300 Å	$^1A_2-^1A_1$	1.22	1.32	∿ 31°	Absorption bands become diffuse at about 2750 Å	27,28, 45
HFCO (Fluoroformaldehyde)	2700-2000 Å	A - A'	1.18	1.35-1.38	20°	Predissociation suggested for λ<2200 Å	46
CH_3CHO (acetaldehyde)	3500-2300 Å	$\tilde{A} - \tilde{X}$	1.22	(1.32)	?	Sharp bands followed by diffuse bands and continuum	2,47
$H_2C{=}CHCHO$ (Acrolein)	4100-3200 Å	A" - A'	1.22	(1.32)	?	Bands become diffuse and merge into a continuum below 3600 Å	48,49
$H{-}C{\equiv}CCHO$ (Propynal)	3800-3000 Å	A" - A'	1.22	(1.32)	?	Sharp bands	50
C_5H_8O (cyclopentanone)	3470-2760 Å	$^1A_2-^1A_1$	1.24	1.35	32°-35°	Sharp bands followed by diffuse bands and continuum	30
$C_6H_{10}O$ (Cyclohexanone)	3500-2500 Å	A" - A'	1.24	1.32	∿ 30°	This work	

Secondly, the $A_2 \leftarrow A_1$ transition in formaldehyde, as well as cyclopentanone, is an electronically forbidden transition and has to "borrow" intensity from another low-lying electronic transition. The other low lying excited states are $^1B_2(\sigma^*,\underline{n})$, $^1B_1(\pi^*,\sigma)$ and $^1A_1(\pi^*,\pi)$ and vibronic mixing with all three of these has been invoked[28] to explain the appearance of bands of different polarizations in the $^1A_2$ - $^1A_1$ formaldehyde spectrum. A, B, C types of band, respectively z, y, x polarized - Fig. 3.3 - arise in the formaledhyde spectrum. The electronic transition $^1B_2(\sigma^*,\underline{n}) \leftarrow {}^1A_1$ is an allowed transition polarized along the y axis . If the $B_2(\sigma^*,\underline{n})$ state is close to the $^1A_2$ state, then transition $^1A_2 \leftarrow {}^1A_1$ can "borrow" intensity from the $^1B_2(\sigma^*,\underline{n})$ state because of the mixing of the electronic wave functions of $^1A_2(\pi^*,\underline{n})$ and $^1B_2(\sigma^*,\underline{n})$ by vibrations of b_1 symmetry. This mixing depends on vibronic interaction, ie, mixing between the electronic and vibrational wavefunctions, so that only states ψ_{ev} of the same vibronic species interact. Fig. 3.3 gives the species of vibronic states for the $\tilde{X}$ A_1, $A_2(\pi^*,\underline{n})$, $B_2(\sigma^*,\underline{n})$, $B_1(\pi^*,\sigma)$ and $^1A_1(\pi^*,\pi)$ electronic states when a_1, a_2, b_1, b_2 vibrations are excited , and shows that the intensity of the Type B bands which appear in the spectrum of the $^1A_2 \leftarrow A_1$ forbidden transition is derived from the $^1B_2(\sigma^*,\underline{n})$ state via the b_1 vibration. The intensity of the type C bands

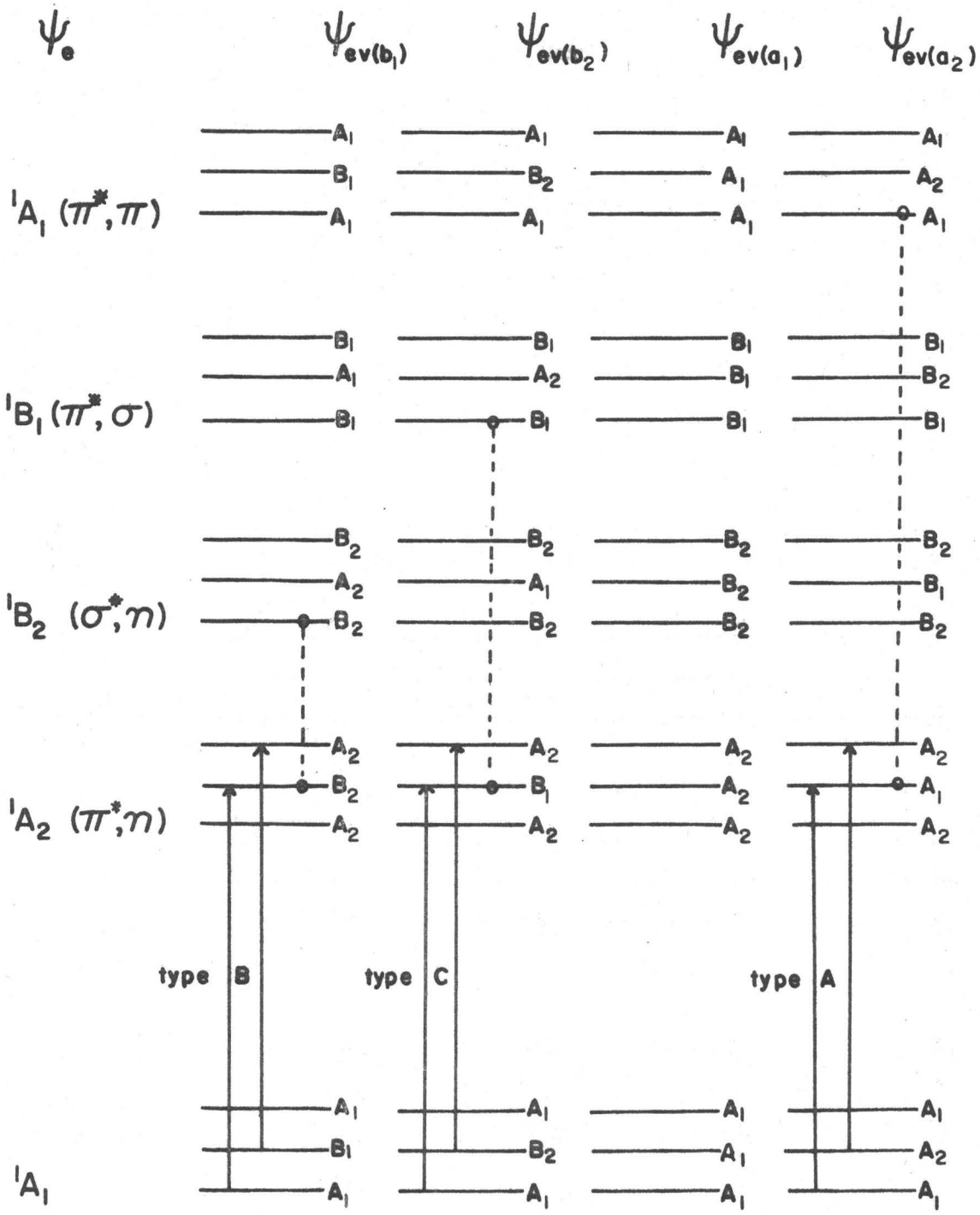

FIG(3·3) INTENSITY BORROWING IN ELECTRONIC TRANSITIONS

is probably borrowed from the $^1B_1(\pi^*,\sigma)$ state via a b_2 vibration. The intensity of A type bands in the $^1A_2$ - $^1A_1$ transition can be borrowed from the $^1A_1(\pi^*,\pi)$ state via an a_2 vibration. But formaldehyde has no vibration of a_2 species, and the only way in which A character can be introduced is by combination of b_1 and b_2 vibrations[28]. Cyclopentanone does possess vibrations of a_2 species, and King and Howard-Lock[30] showed that the strong c type bands in the cyclopentanone spectrum result from an admixture of $^1B_1(\pi^*,\sigma)$ state via a combination of a_2 and b_1 vibrations. The expected polarizations of the bands in the $^1A_2 \leftarrow {}^1A_1$ transitions for odd or even quanta change of the four species of normal modes are summarized in Table 3.2.

If the principal axis a does not coincide with the c = 0 bond, then hybrid bands of mixed polarization can occur in the spectrum. More important is the fact that vibrations may have components along the three principal axes, and in principle, these vibrations can mix electronic states of different symmetry species with the $^1A_2$ state. Does the $n \rightarrow \pi^*$ cyclohexanone spectrum result from a similar mechanism as the one of cyclopentanone? Or does it contain more allowed character as suggested by Goodman and Chandler's work[14]? These are questions whose answers will be sought in the following chapters.

TABLE 3.2

POLARIZATION OF THE BANDS (C_{2v}) IN THE $\underline{n}\rightarrow\pi^*$ transition

$V' - V''$				$\psi'_{ev}\psi''_{ev}$ species	Band Type
a_1	a_2	b_1	b_2		
unrestricted	even	even	even	A_2	A (magnetic dipole)
"	even	even	odd	B_1	C
"	even	odd	even	B_2	B
"	even	odd	odd	A_1	A
"	odd	even	even	A_1	A
"	odd	even	odd	B_2	B
"	odd	odd	even	B_1	C
"	odd	odd	odd	A_2	A (magnetic dipole)

POLARIZATION OF THE BANDS (C_s) IN THE $\underline{n}\rightarrow\pi^*$ transition

$V' - V''$		$\psi'_{ev}\psi''_{ev}$ Species	Band Type
a'	a''		
unrestricted	even	A''	B
"	odd	A'	A+C (hybrid)

NEAR ULTRAVIOLET SPECTRA

In the near ultra violet spectral region, the absorption spectrum of cyclohexanone extends from 2000 cm^{-1} to 3600 cm^{-1}. At long wavelengths, the absorption bands for the vapour phase are discrete and have very low intensity. The intensity and diffuseness of the bands rapidly increase as the wavelength decreases. Some band structure can be discerned in the spectrum at a pressure path of 0.1 m at, but pressure paths up to 1.4 m at are required to observe the discrete bands at the red end of the spectrum.

Detailed analyses of the vibrational structure of the singlet-singlet $\underline{n}\rightarrow\pi^*$ transitions of CHh_{10}, CHd_4 and CHd_{10} will be given in the following sections. The intense bands are assigned and some weak bands are explained. The labelling convention of Brand and Watson[51] is used for vibrational bands in the electronic spectrum: transitions are labelled $m_b^a n_d^c$ ... where m, n ... designate the normal modes of vibrations; the superscripts, a, c and the subscripts, b, d give the number of quanta of a vibration excited in the upper and the lower electronic states, respectively. For example, successive members of an excited state progression in ν_a are labelled $a_o^1, a_o^2, a_o^3 \ldots$.

The three spectra of CHh_{10}, CHd_4, CHd_{10} have been photographed under the same experimental conditions. In all

three spectra the first discrete absorption bands appear around 3450 Å at a pressure path of 1.4 m at. Under low resolution, at this pressure path of 1.4 m at, CHh_{10} shows bands without rotational structure, the main ones at the red end of the spectrum having a regular separation of $\sim 90\ cm^{-1}$. In the same region, the bands of CHd_4 are slightly weaker than those of CHh_{10}, the main ones being separated by about the same frequency, $\sim 90\ cm^{-1}$, but showing two apparent heads separated by $20\ cm^{-1}$. The spectrum of CHd_{10} is much weaker than the other two.

All three spectra appear as weak bands superimposed upon a continuum whose intensity increases very rapidly to shorter wavelengths. It was possible to get meaningful spectra at high resolution only for the CHh_{10} spectrum, which is relatively the strongest of the three. The spectra of the deuterated isomers showed no additional structure under high resolution than could be observed under low resolution. Consequently, most of the analysis was performed upon the low resolution spectra. However the high-resolution spectra of CHh_{10} was used for band contour analysis, see Chapter 4 .

3.1 LOW RESOLUTION SPECTRA

The low resolution spectra of $CHh_{10}/CHd_4/CHd_{10}$ show band structure from 28850-36000 cm^{-1}/29478-32537 cm^{-1}/ 29467-31321 cm^{-1}/ respectively (see Fig. 3.4.) About 110/85/34

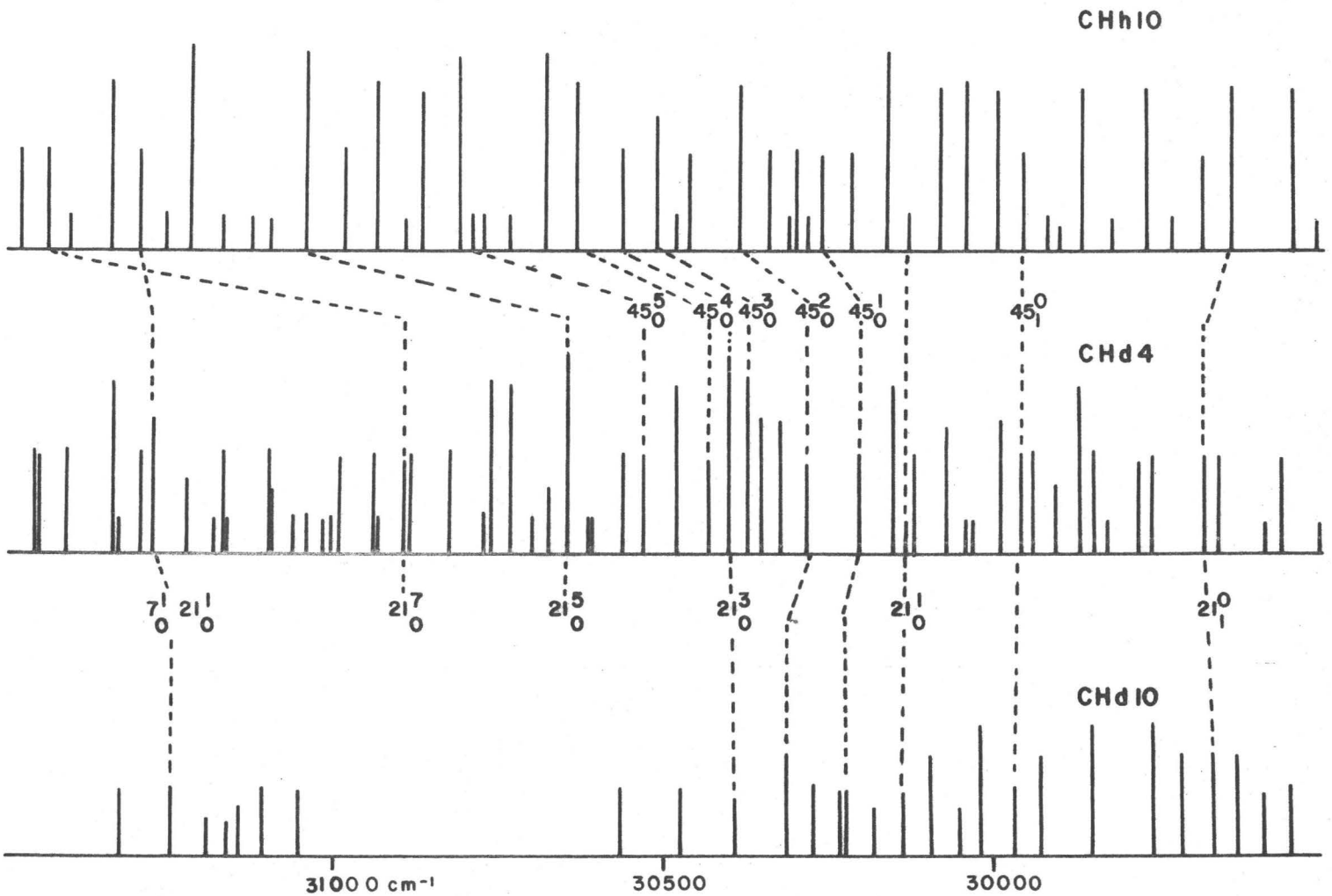

FIG(3·4) ABSORPTION FREQUENCIES OF CHh10, CHd4, CHd10 -

bands are observed for the respective species. The intensities of the bands measured with respect to the continuum are irregular, but none of the bands is very strong. The maximum ratio of observed band intensities is about seven to one.

We will see below that in the high resolution spectrum of CHh_{10}, some bands of strong intensity under low resolution are in fact two bands of medium intensity which are strongly overlapped. For this reason, some bands in the low resolution spectra of CHh_{10} have two different assignments.

In the spectra of the three isomers, it will be shown that two carbonyl group vibrations are active. These are the carbonyl stretching mode and the out-of-plane wagging mode, and will be referred to as $\nu_7(a')$ and $\nu_{21}(a')$. This numbering follows RNJM's[26] assignment for the ground state fundamentals*. Also observed is the $\nu_{45}(a'')$ mode, see Table 1.4, which is observed at 189/175/163 cm^{-1} in the infrared spectra. This is a low frequency ring mode, which is identified by RNJM[26] as

---

*The standard convention is to number the normal modes in order of decreasing frequency, starting with the 25 a' modes and continuing with the 20 a" modes. For a large molecule such as cyclohexanone, however, it is always possible that some of the fundamentals have been misassigned, and this will alter the numbering. As was discussed above, see Table 1.5 we believe that the band at 490/454/451 is not purely the in-plane-bend, but overlaps the out-of-plane wag which is at slightly lower frequencies in the vapour, however this does not affect its labelling as ν_{21}. RNJM's numbering will be used for the vibrations which are active in the UV spectrum.

an antisymmetric out-of-plane twist which tends to take the chair into the boat ring shape.

In common with the main features of $\underline{n}\rightarrow\pi^*$ transitions in other carbonyl compounds[27,28,29,30,37] the gross pattern of the spectra of the three isotopes consists of a progression in $\sim$ 1150 cm^{-1} to higher frequencies. The bands of this progression, which become increasingly diffuse, are at

CHh_{10}	CHd_4	CHd_{10}	Assignment
30127	30132	30135 cm^{-1}	0-0
31295	31272	31244	7^1_0
32464	n/o	n/o	7^2_0
33623	n/o	n/o	7^3_0

The first interval is 1168/1140/1109 cm^{-1}. This is believed to be the value for the excited state frequency of the CO stretch vibration. This assumption seems to be reasonable if one compares the value obtained for other ketones - Table 3.3. If $(\nu_1''-\nu_7')/\nu_7''$ represents the percentage drop between the ground state frequency and the excited state frequency, $\sim$ 32% for CHh_{10}, Table 3.3 shows that all the saturated molecules have a higher percentage drop ($\geq$ 30%) than the non saturated molecules (<30%). This could be due to a conjugation effect between the bonding electrons of the carbonyl group and the rest of the molecule, an effect which can occur for molecules like p-benzoquinone but not for saturated molecules like cyclohexanones.

TABLE 3.3

SINGLET SINGLET $n \rightarrow \pi^*$ TRANSITION IN CARBONYL COMPOUNDS. THE VIBRATIONAL WAVE NUMBERS ARE GIVEN FOR THE C=O STRETCHING MODE

Compounds	$\nu''cm^{-1}$	$\nu'cm^{-1}$	% Drop	References
H_2CO (Formaldehyde)	1738	1177	32.3	27-45
HFCO (Fluoroformaldehyde)	1837	1111	39.5	46
CH_3CHO (Acetaldehyde)	1743	1125	35.5	47
$H_2C{=}CHCHO$ (Acrolein)	1720	1270	26.1	48-49
$HC{\equiv}CCHO$ (Propynal)	1697	1304	23.1	50
$(CHO)_2$ (Glyoxal)	1740	1390	20.1	52-53
 (Benzoquinone)	1667	1220	26.8	54
C_5H_8O (Cyclopentanone)	1742	1225	29.6	30
$C_6H_{10}O$ (Cyclohexanone)	1714	1170	31.7	This work

Again as in other $\underline{n}\rightarrow\pi^*$ transitions, each band of the progression 7_0^n (except for the very weak band 7_0^1 for CHd_{10}) acts as an origin for a progression in the ground state frequency 490/454/460 cm^{-1}. This same interval is observed in the vibrational spectrum, and is assigned here to the carbonyl out-of-plane wag $\nu''_{21}(a')$. Up to four members of this progression are observed.

Other prominent bands can then be fitted into the typical pattern which would be expected for inversion doubling at the carbonyl group in the excited state. This is illustrated in Figs. 3.5, 3.6, 3.7) for the bands associated with the origin transition for each of the three isomers.

Each band whose frequency is given in Tables 3.5, 3.6, 3.7) acts as origin for a progression in $\nu_{45}(a'')$. This mode is active in both the ground and the excited state. Up to five quanta of the progression are observed. For $CHh_{10}/CHd_4/CHd_{10}$, the fundamental frequency of ν''_{45} is respectively 190/175/165 cm^{-1}, and ν'_{45} equals 130/75/82 cm^{-1}. A positive anharmonicity is apparent in the first overtone of the ground state frequency of ν''_{45}.

ν'_{45} shows a small irregular isotope shift; normally the most deuterated molecule has lowest frequency. We note that $\nu''_{21}(a')$ shows a similar anomaly in the ground state. This is probably due to slight changes in the normal coordinates. Similar small irregular shifts have been observed in

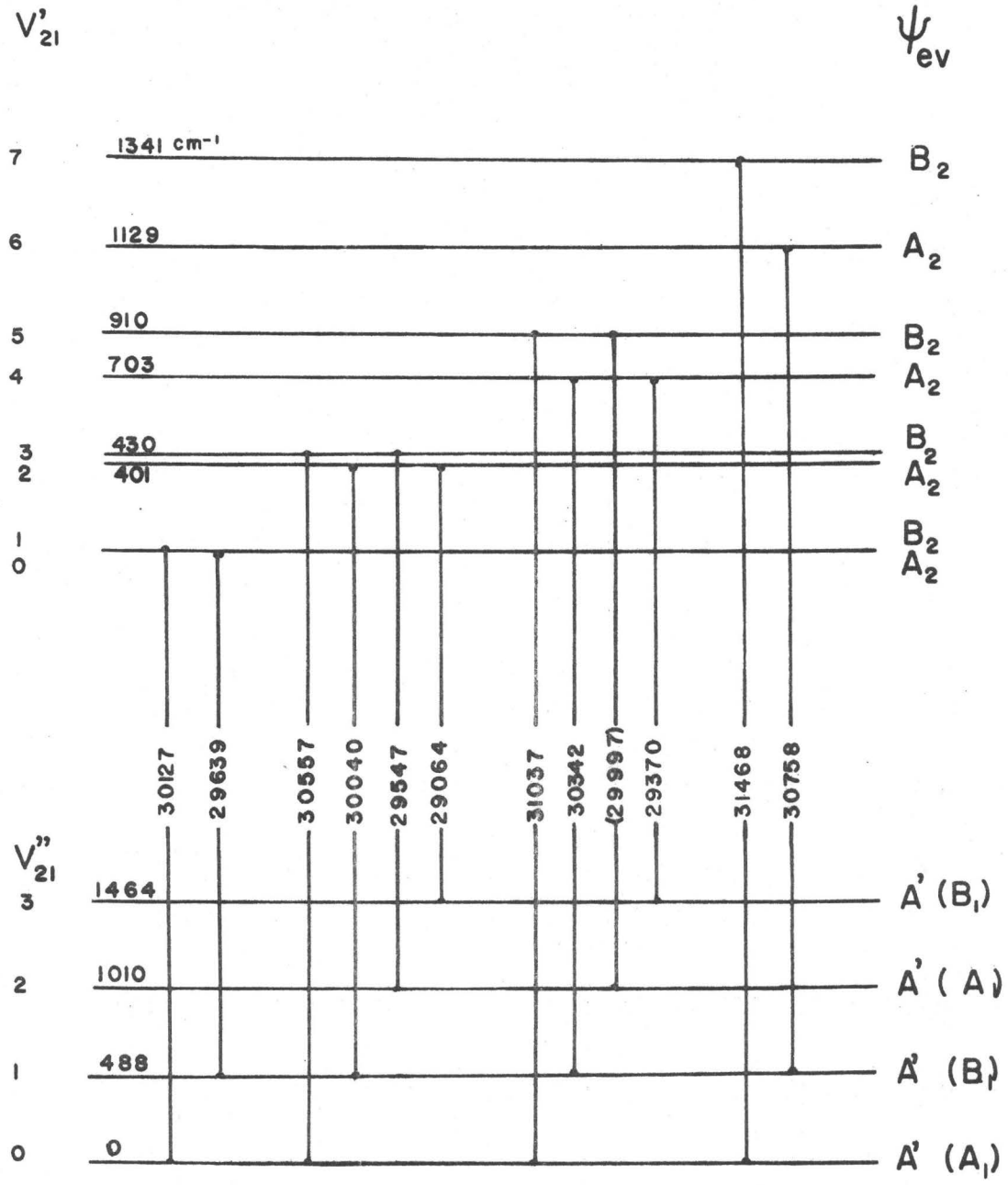

Fig(3.5) CHh_{10} - Low resolution spectrum - schematic energy level diagram and observed transitions for the ν_{21} vibration

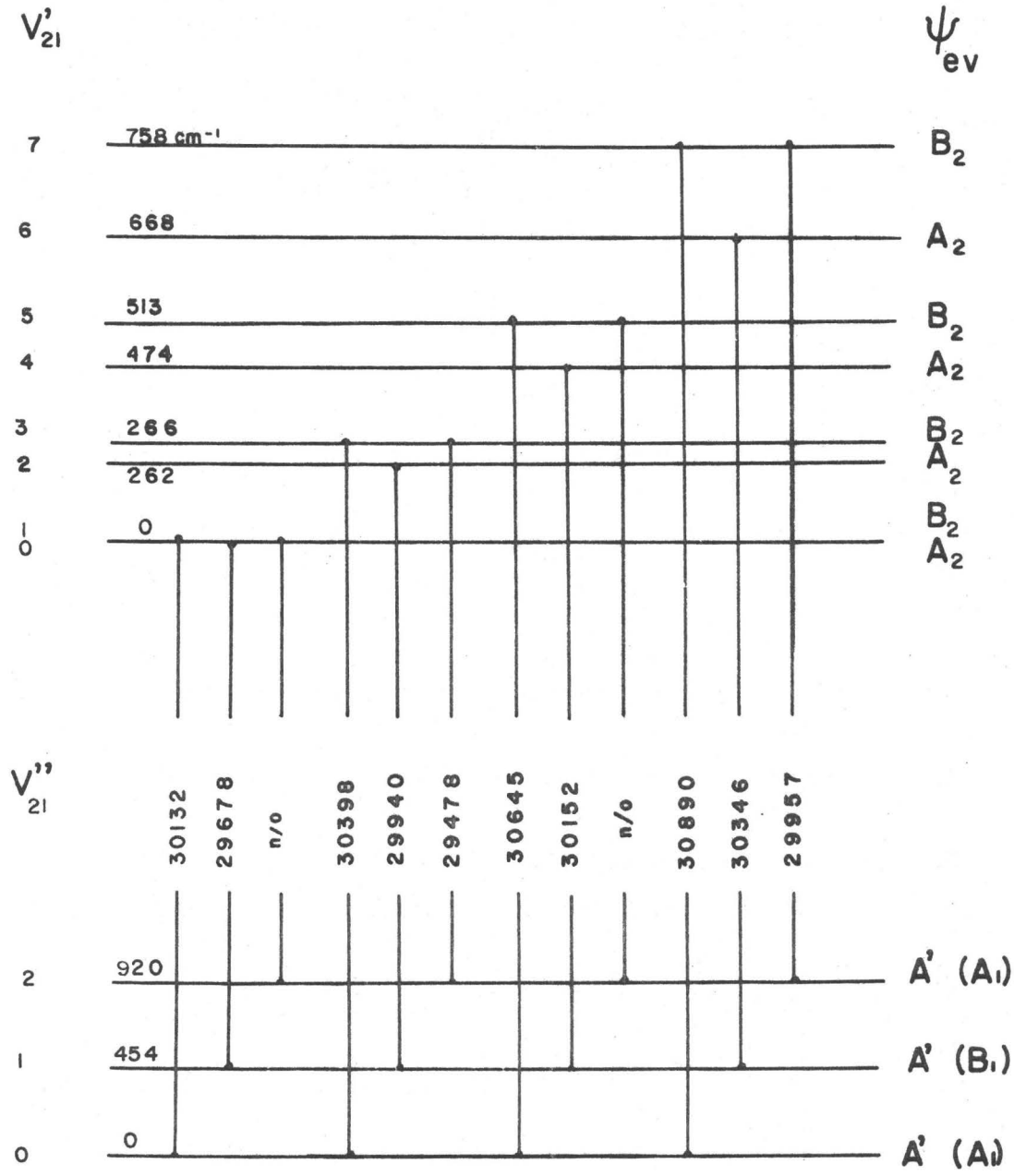

Fig(3.6) CHd_4 - Low resolution spectrum - schematic energy level diagram and observed transitions for the ν_{21} vibration

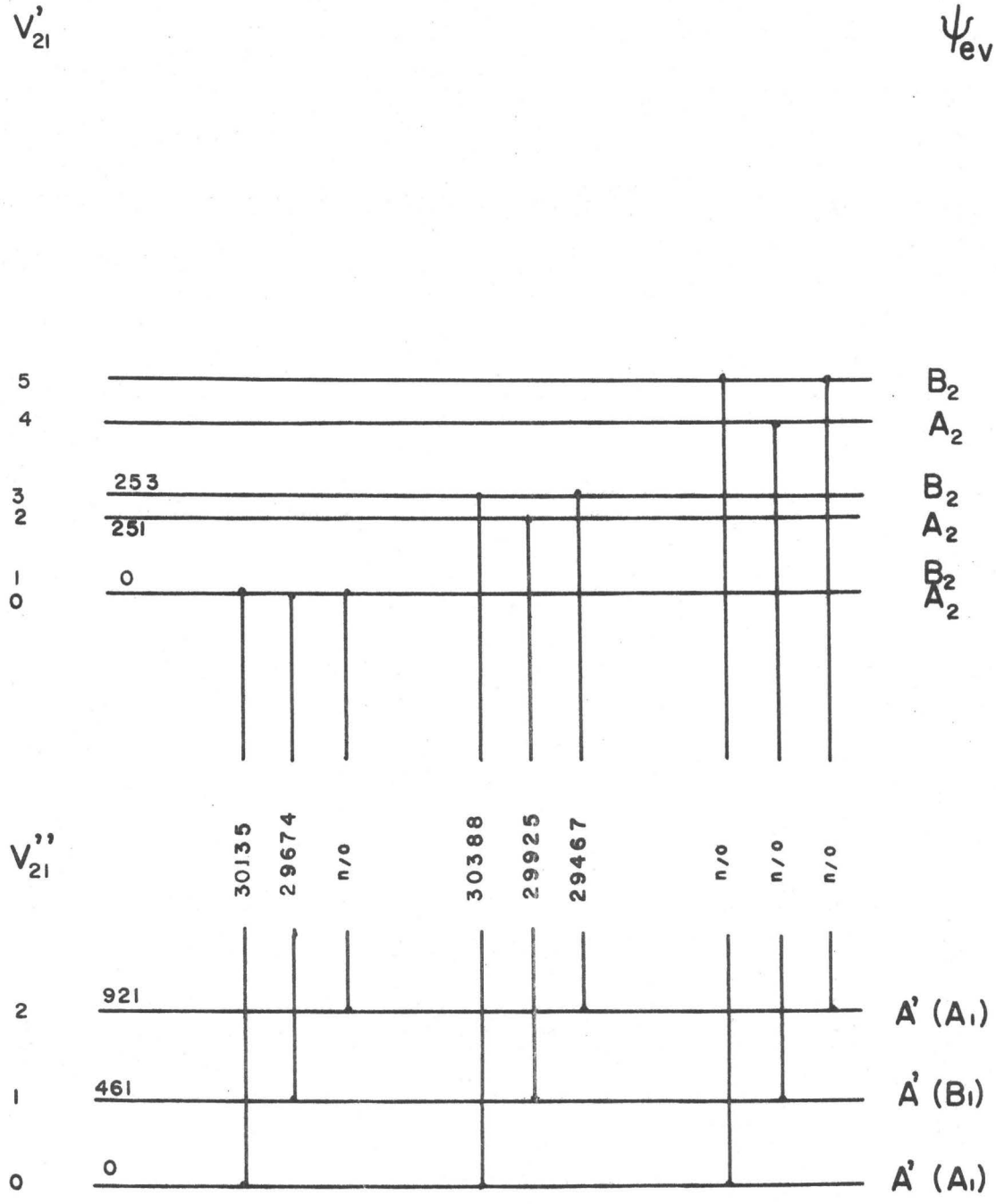

Fig(3.7) CHd_{10} - Low resolution spectrum - schematic energy level diagram and observed transitions for the ν_{21} vibration

the infrared spectra of cyclopentanone. Table 3.4 gives the values of the frequencies ν' and ν''derived from the ultraviolet spectrum. The results for ν'' from the infrared are also given.

In the column on the right are listed the percentage drop.

i.e. $$\frac{\nu'' - \nu'}{\nu''}$$

It can be seen that, for the two-carbonyl frequencies, the percentage drop increases on deuteration. But for ν_{45} the higher percentage drop is obtained for CHd_4; nevertheless, the percentage drop in the case of CHd_{10} is also very high, compared to that of CHh_{10}.

As was mentioned previously the ultraviolet spectrum of CHd_{10} is the weakest of the three, and only relatively few bands are observed above the continuum. These can be fitted into the assignments given above. But in the spectra of CHh_{10} and CHd_4, after the assignment of most of the bands to the ν_7, ν_{21}, ν_{45} normal modes, three strong bands are left unassigned in both spectra. The strongest is at +726 cm^{-1}/+629 cm^{-1} from the origin band at 30127/30132 cm^{-1}. The two bands are also origins for frequencies in ν'_{45}. The +726 cm^{-1} interval in the CHh_{10} spectrum can also be observed in conjunction with up to two quanta of the carbonyl stretching mode ν'_7.

TABLE 3.4

FREQUENCIES OF THE NORMAL MODES OBSERVED IN THE $n \rightarrow \pi^*$ SINGLET-SINGLET TRANSITION OF CYCLOHEXANONES

Description	Frequencies (cm^{-1})			% Drop
	ν'' From the Raman liquid spectrum (26)	ν'' From U.V. Vapour Phase	ν' From U.V Vapour Phase	
C=O stretch $\nu_7(a')$				
CHh_{10}	1710	n/o	1169	31.6
CHd_4	1708	n/o	1140	33.2
CHd_{10}	1709	n/o	1109	35.1
C=O out-of-plane Wag $\nu_{21}(a')$				
CHh_{10}	490	490	398	18.7
CHd_4	454	454	262	42.2
CHd_{10}	452	460	251	45.4
Ring mode $\nu_{45}(a'')$				
CHh_{10}	189	190	130	31.6
CHd_4	175	175	75	57.1
CHd_{10}	163	165	82	50.1
Mode ν_x				
CHh_{10}			726	
CHd_4			629	

It is not possible to assign this frequency to a normal mode. No corresponding ground state frequency is observed in the ultraviolet spectrum. From band contour analysis, some information can be obtained about the polarisation of the band. It is called ν_x in the assignment here. Table 3.5, 3.6, 3.7 gives the wavenumbers of the heads of bands for $CHh_{10}/CHd_4/CHd_{10}$ observed under low resolution. Assignments are given for most of the bands, apart from a few extremely weak ones.

Some bands are given two assignments in the low resolution spectrum of CHh_{10}. They can all be resolved in the high resolution spectrum. Moreover in the low resolution CHd_4 spectrum, the analogous bands are split by $\sim$ 20 cm^{-1}. They are in fact two different bands.

On the other hand, there are several bands to the blue of the origin in the low resolution spectrum of CHd_4 which apparently contain two components split by some 5-10 cm^{-1}. It is very unlikely that this appearance results from rotational structure, because the bands in the spectrum of CHh_{10} under the same conditions do not show any rotational structure and neither is such an appearance predicted by band contour calculations. A similar doubling may be present in the low resolution spectrum of CHd_{10}, but the bands are too weak for this to be certain. Most of the bands with two components are assigned to transitions in which one or more quanta of ν'_{45}

excited in conjunction with other excited states modes. It is suggested here that this particular doubling arises because the upper state vibrational levels involved are approaching the barrier to chair-boat interconversion of the ring. Close to the top of the barrier, and above, the motion of the carbonyl out-of-plane wagging could be strongly coupled to the ring modes. However a theoretical treatment of such coupling is not feasible on the basis of the limited amount of information available. The doubling is not observed for bands in the CHh_{10} spectrum; but the normal coordinates for the vibrations of CHh_{10} in the excited state can differ from those for the deuterated isomers.

3.2 LOW TEMPERATURE WORK

Very little information was available from these experiments. However the spectra taken of CHh_{10} at low temperature under the conditions described in the experimental section shows three broad absorption regions (see Fig. 2.3). The first one is between 29950-30160 cm^{-1}, the second one from 30600-3100 cm^{-1} and the third from 31000-31300 cm^{-1}, with maxima at $\sim$ 30050 cm^{-1}, 30800 cm^{-1}, 31200 cm^{-1}. The first maximum is in the region of the origin band (30132 cm^{-1} in the vapour phase), and provides support for this assignment. The second maximum corresponds to the $21_o^1 x_o^1$ vapour band, and the third to the $7_o^1 21_o^1$ band.

TABLE 3.5

BAND FREQUENCIES AND ASSIGNMENTS FOR THE LOW RESOLUTION SPECTRUM OF CHh_{10}

ν cm^{-1} vacuum	Relative Intensity[a)]	Assignment
29064	m	21_2^1
29369	m	21_3^4
29457	s	$21_1^0 45_1^0$
29510	w	$7_1^1 21_1^2$
29547	s	21_2^3
29597	w	$7_1^1 21_0^1$
29639	s	21_1^0
29684	m	$21_1^2 45_2^0 + 21_2^3 45_0^1$
29770	sb	$21_0^1 45_2^0 + 21_1^0 45_0^1$
29819	w	$21_1^2 45_2^1$
29864	s	$21_1^2 45_1^0$
29900	w	$21_1^0 45_0^2$
29921	w	$21_0^1 45_2^1$
29954	m	$21_0^1 45_1^0$
29997	s	$21_2^5 + 21_1^2 45_1^1$
30040	s	21_1^2
30081	s	$21_0^1 45_1^1$
30127	w	21_0^1
30162	vs	$21_1^2 45_0^1$
30214	m	$21_0^1 45_1^2$
30256	m	$21_0^1 45_0^1$

(continued next page)

ν cm^{-1} vacuum	Relative Intensity[a)]	Assignment
30268	w	$21_1^4 45_0^1$
30298	m	$21_1^2 45_0^2$
30310	w	$21_0^1 45_1^3$
30342	m	21_1^4
30385	s	$21_0^1 45_0^2$
30438	w	$21_1^2 45_0^3$
30462	m	$21_0^1 45_1^4$
30478	w	$21_1^4 45_0^1$
30508	ms	$21_0^1 45_0^3$
30557	m	21_0^3
30630	s	$21_0^1 45_0^4$
30676	vs	$21_0^3 45_0^1$
30731	w	$7_0^1 21_2^3$
30768	w	21_1^6
30784	w	$21_0^1 45_0^5$
30804	vsb	$7_0^1 21_1^0 + 21_0^3 45_0^2$
30857	s	$21_0^1 x_0^1$
30886	w	$21_0^1 45_0^6$
30930	s	$7_0^1 21_1^0 45_0^1 + 21_0^3 45_0^3$
30976	m	$21_0^1 x_0^1 45_0^1$
31037	vsb	21_0^5

(continued next page)

ν cm^{-1} vacuum	Relative Intensity[a)]	Assignment
31094	w	$21_0^1 x_0^1 45_0^2$
31122	w	$7_0^1 21_0^1 45_1^0$
31166	w	$21_0^5 45_0^1$
31212	vs	$7_0^1 21_1^2$
31253	w	$7_0^1 21_0^1 45_1^1$
31295	m	$7_0^1 21_0^1$
31329	s	$7_0^1 21_1^2 45_0^1$
31430	m	$7_0^1 21_0^1 45_0^1$
31468	m	21_0^7
31519	vw	$7_0^1 21_0^1 21_1^4$
31559	vw	$7_0^1 21_0^1 45_0^2$
31648	m	$7_0^1 21_1^4 45_0^1$
31690	m	$7_0^1 21_0^1 45_0^3$
31731	m	$7_0^1 21_0^1 21_0^3$
31768	w	21_1^6
31796	w	$7_0^1 21_0^1 45_0^4$
31856	m	$7_0^1 21_0^3 45_0^1$
31898	m	$7_0^2 21_2^3$
31945	w	$7_0^1 21_1^6$
31978	s	$7_0^2 21_1^0$
32025	s	$7_0^1 21_0^1 x_0^1$
32096	s	$7_0^2 21_1^0 45_0^1$

(continued next page)

ν cm^{-1} vacuum	Relative Intensity	Assignment
32138	vs	$7_0^1 21_0^1 X_0^1 45_0^1$
32210	s	$7_0^1 21_0^5$
32260	s	$7_0^1 21_0^1 X_0^1 45_0^1$
32300	w	$7_0^2 21_0^1 45_1^0$
32332	w	$7_0^2 21_2^5$
32377	s	$7_0^2 21_1^2$
32420	w	$7_0^2 21_0^1 45_1^1$
32464	w	$7_0^2 21_0^1$
32498	s	$7_0^2 21_1^2 45_0^1$
32581	w	$7_0^2 21_0^1 45_0^1$
32632	m	$7_0^1 21_0^7$
32679	vw	$7_0^2 21_1^4$
32735	ms	$7_0^2 21_0^1 45_0^2$
32818	m	$7_0^2 21_1^4 45_0^1$
32853	m	$7_0^2 21_0^1 45_0^3$
32899	vw	$7_0^2 21_0^3$
32980	m	$7_0^2 21_0^1 45_0^4$
33020	m	$7_0^2 21_0^3 45_0^1$
33065	w	$7_0^3 21_2^3$
33109	vw	$7_0^2 21_1^6$
33138	m	$7_0^3 21_1^0$

(continued next page)

ν vm^{-1} vacuum	Relative Intensity	Assignment
33183	ms	$7_0^2 21_0^1 x_0^1$
33254	w	$7_0^3 21_1^0 45_0^1$
33299	ms	$7_0^2 21_0^1 x_0^1 45_0^1$
33365	m	$7_0^2 21_0^5$
33413	ms	$7_0^2 21_0^1 x_0^1 45_0^2$
33455	w	$7_0^3 21_0^1 45_1^0$
33534	m	$7_0^3 21_1^2$
33577	w	$7_0^3 21_0^1 45_1^1$
33623	mw	$7_0^3 21_0^1$
33648	m	$7_0^3 21_1^2 45_0^1$

a) <u>Notation</u> I intensity measured with respect to the continuum

w = weak $1 < I < 2$

m = medium $2 < I \leq 4$

s = strong $4 < I \leq 6$

vs = very strong $6 < I < 8$

b = broad

d = diffuse

TABLE 3.6

BAND FREQUENCIES AND ASSIGNMENTS FOR THE LOW RESOLUTION SPECTRUM OF CHd_4

ν cm^{-1} vacuum	Relative Intensity	Assignment
29478	m	21_2^3
29505	w	$21_1^0 45_1^0$
29566	m	$21_2^3 45_0^1$
29589	w	$21_1^0 45_1^1$
29657	m	$21_2^3 45_0^2$
29678	mw	21_1^0
29765	m	$21_1^0 45_0^1$
29780	mb	$21_0^1 45_2^0$
29852	m	$21_1^0 45_0^2$
29870	s	$21_0^1 45_2^1$
29904	mw	$(21_1^2 45_1^2)$
29940	m	21_1^2
29957	ms	$21_2^7 + 21_0^1 45_1^0$
29991	ms	$21_1^2 45_0^1$
30031	w	$21_0^1 45_1^1$
30044	w	$21_0^3 45_2^0$
30068	ms	$21_1^2 45_0^2$
30115	m	$21_0^1 45_1^2$
30132	w	21_0^1
30152	s	21_1^4

(continued next page)

ν cm^{-1} vacuum	Relative Intensity	Assignment
30203	m	$21_0^1 45_0^1$
30288	mb	$21_0^1 45_0^2$
30320	ms	$21_0^3 45_1^1$
30346	ms	21_1^6
30367	s	$21_0^1 45_0^3$
30398	vs	21_0^3
30435	wb	$21_0^1 45_0^4$
30484	s	$21_0^3 45_0^1$
30533	m	$21_0^1 45_0^5$
30557	m	$21_0^3 45_0^2$
30604	w	$21_0^3 45_0^3$
30615	vw	$7_0^1 21_2^3$
30645	vs	21_0^5
30674	mw	$21_0^3 45_0^4$
30693	w	$7_0^1 21_2^3 45_0^1$
30729	s	$21_0^5 45_0^1$
30761	s	$21_0^1 x_0^1$
30813	m	$21_0^1 x_0^1 45_0^1$
30819	m	$7_0^1 21_1^0$
30880	m	$21_0^1 x_0^1 45_0^2$
30890	m	21_0^7
30929	w	$7_0^1 21_0^1 45_2^0$

(continued next page)

ν cm^{-1} vacuum	Relative Intensity	Assignment
30943	m	$21_0^1x_0^145_0^3$
30992	m	$7_0^121_1^045_0^2$
31008	w	$7_0^121_0^145_2^1$
31063	w	$7_0^121_1^2$
31097	mw	$7_0^121_0^145_1^0$ or $7_0^121_2^7$?
31167	m	$7_0^121_0^145_1^1$
31183	w	$7_0^121_0^345_2^0$
31223	mw	$7_0^121_1^245_0^2$
31272	ms	$7_0^121_0^1$
31293	m	$7_0^121_1^4$
31318	w	$7_0^121_0^345_2^1$
31332	s	$7_0^121_0^145_0^1$
31404	m	$7_0^121_0^145_0^2$
31436	m	$7_0^121_1^6$
31505	vwd	$7_0^121_0^145_0^3$
31524	vwd	$7_0^121_0^3$
31684	md	$7_0^121_0^345_0^2$
31974	mwd	$7_0^221_0^145_3^2$
32029	mwd	$7_0^221_0^145_2^0$
32094	md	$7_0^221_0^145_2^1$
32147	mwd	$7_0^221_0^145_2^2$

(continued next page)

ν cm^{-1} vacuum	Relative Intensity	Assignment
32216	mbd	$7_0^2 21_0^1 45_1^0$
32265	mbd	$7_0^2 21_0^1 45_1^1$
32368	mbd	$7_0^2 21_0^1 45_1^2$
32454	mbd	$7_0^2 21_0^1 45_0^1$
32537	wbd	$7_0^2 21_0^1 45_0^2$

TABLE 3.7

BAND FREQUENCIES AND ASSIGNMENT FOR THE LOW RESOLUTION SPECTRUM OF CHd_{10}

ν cm^{-1} vacuum	Relative Intensity	Assignment
29467	w	21_1^3
29508	m	$21_1^0 45_1^0$
29552	m	$21_2^3 45_0^1$
29590	m	$21_1^0 45_1^1$
29633	ms	$21_2^3 45_0^2$
29674	ms	21_1^0
29715	ms	$21_2^3 45_0^3$
29760	s	$21_1^0 45_0^1$
29847	s	$21_1^0 45_0^2$
29925	ms	21_1^2
29971	ms	$21_0^1 45_1^0$
30014	s	$21_1^2 45_0^1$
30050	mw	$21_0^1 45_1^1$
30098	ms	$21_1^2 45_0^2$
30135	m	21_0^1
30182	mw	$21_1^2 45_0^3$
30217	ms	$21_0^3 45_1^0$
30226	ms	$21_0^1 45_0^1$
30270	m	$21_1^2 45_0^4$
30307	ms	$21_0^1 45_0^2$

(continued next page)

ν cm^{-1} vacuum	Relative Intensity	Assignment
30388	mw	21_0^3
30473	m	$21_0^3 45_0^1$
30565	m	$21_0^3 45_0^2$
31051	mwd	$(7_0^1 21_1^2)$
31106	mwd	$(7_0^1 21_1^2 45_0^1)$
31139	mwd	$(7_0^1 21_0^1 45_1^1)$
31188	mwd	$(7_0^1 21_1^2 45_0^2)$
31244	mbd	$(7_0^1 21_0^1)$
31321	mbd	$(7_0^1 21_0^1 45_0^1)$

3.3 ISOTOPE SHIFTS

Brand et al.[55] have found that the chlorine isotope shift in progressions of the 5340 Å band system of thiophosgene is a linear function of quantum number. The same isotope effect has been found for oxalyl chloride[56] and cyclopentanone[30]. Deviation from linearity is found[38] when the energy levels involved correspond to a double minima potential function. In cyclohexanone the $21_0^{v'}$ progressions do not show a linear isotope shift because of the splitting of the energy levels due to the double potential minima (see Figs. 3.5, 3.6, 3.7). Calculations on the double potential minima energy levels of $CHh_{10}/CHd_4/CHd_{10}$ are given below. In the case of the carbonyl out-of-plane progressions of cyclohexanone the linearity cannot be checked for the ground state because only two members are observed.

The long progressions of the ring puckering mode which are observed both in the ground state and in the excited states do show a linear isotope shift between CHh_{10} and CHd_4 as well as CHh_{10}-CHd_{10}.

The observed isotope shift of the assigned origin bands are -5 cm^{-1}/-8 cm^{-1} respectively for (CHh_{10}-CHd_4)/ (CHh_{10}-CHd_{10})

Deuteration slightly shifts the origin to the blue in the case of cyclohexanone.

The isotope shift of the origin band of a system is given by the relation

$$\left(G'(o)-G''(o)\right) - \left(G'(o)-G''(o)\right)_{isotope}$$

where $G'(o)$ and $G''(o)$ are the zero point vibrational energies of the excited state and the ground state respectively. For cyclohexanone, there are 45 normal modes of vibration which all contribute to the zero point vibrational energy by the relation

$$G(o) = \sum_{n=1}^{45} \frac{1}{2} h\nu_n$$

Only a few ν_n' are observed experimentally for $CHh_{10}/CHd_4/CHd_{10}$ and there is not enough information to predict the shift of the origin band.

Each band of the carbonyl out-of-plane vibrational progression is an origin for a progression of the ring puckering mode in the excited state. The isotope shifts in these progressions are plotted in Figs. 3.8, 3.9 and 3.10. Fig. 3.8 shows the isotope effect in the $45_0^{v'}$ progressions based on the bands of the $21_0^{v'}$ progressions as origins. A very long progression, up to five quanta, is observed based upon the origin band of the system itself. Shorter progressions are observed originating from the 21_0^3 and 21_0^5 bands. The isotope effect is slightly greater for CHd_4 than for CHd_{10}. This implies that the ν_{45} normal mode involves slightly more motion of the α deuterated atoms in CHd_4 than in CHd_{10}. Fig. 3.9 shows the isotope shift of some progressions of $45_0^{v'}$

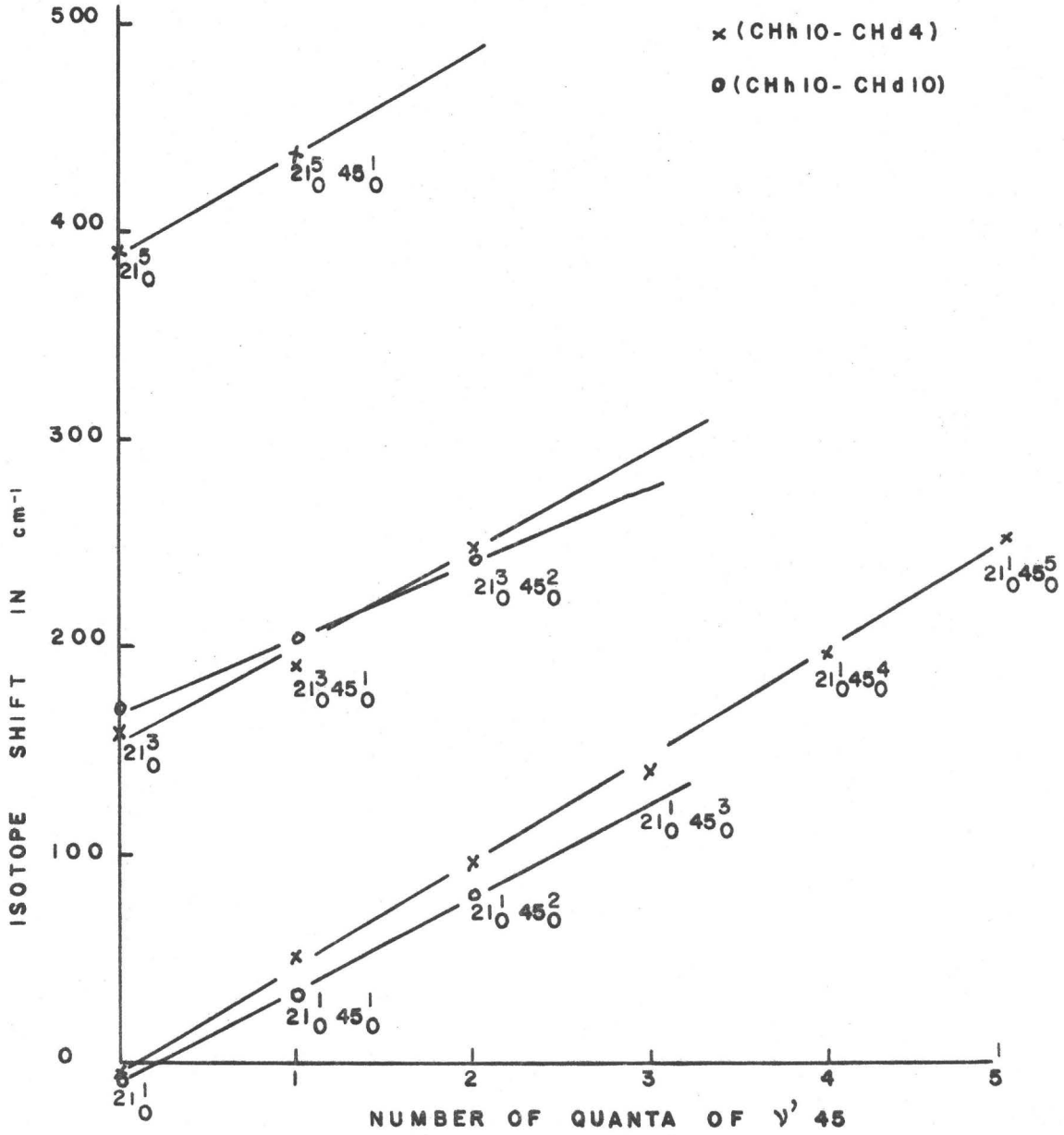

FIG(3·8) VIBRATIONAL ISOTOPE EFFECT IN THE $^1A_2 \leftarrow {}^1A_1$ TRANSITION OF CYCLOHEXANONES - SOME $21_0^{v'}\ 45_0^{v'}$ PROGRESSIONS -

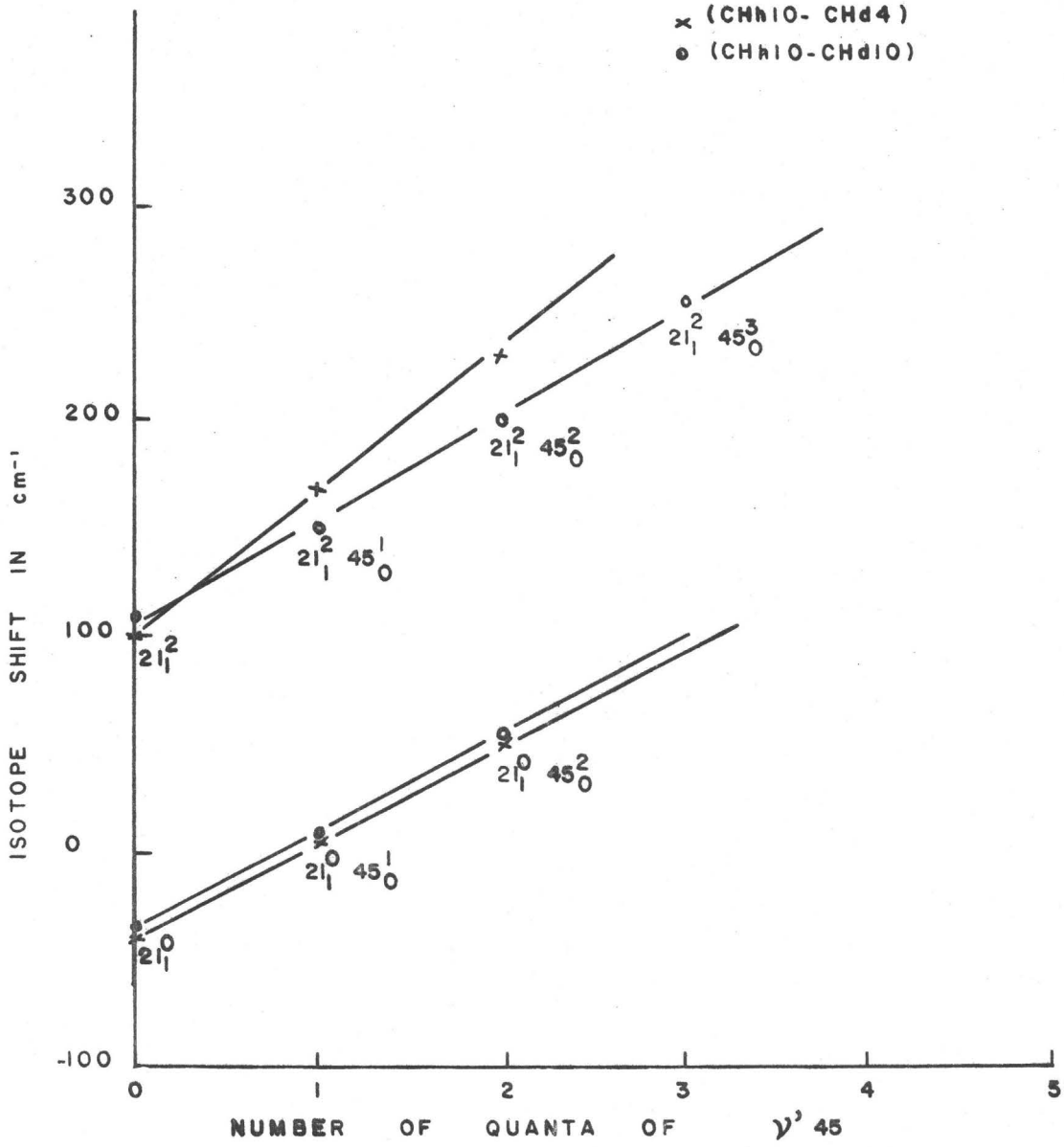

FIG(3·9) VIBRATIONAL ISOTOPE EFFECT IN THE $^1A_2 \leftarrow {}^1A_1$ TRANSITION OF CYCLOHEXANONES - SOME $21_1^{v'}\ 45_0^{v'}$ PROGRESSIONS-

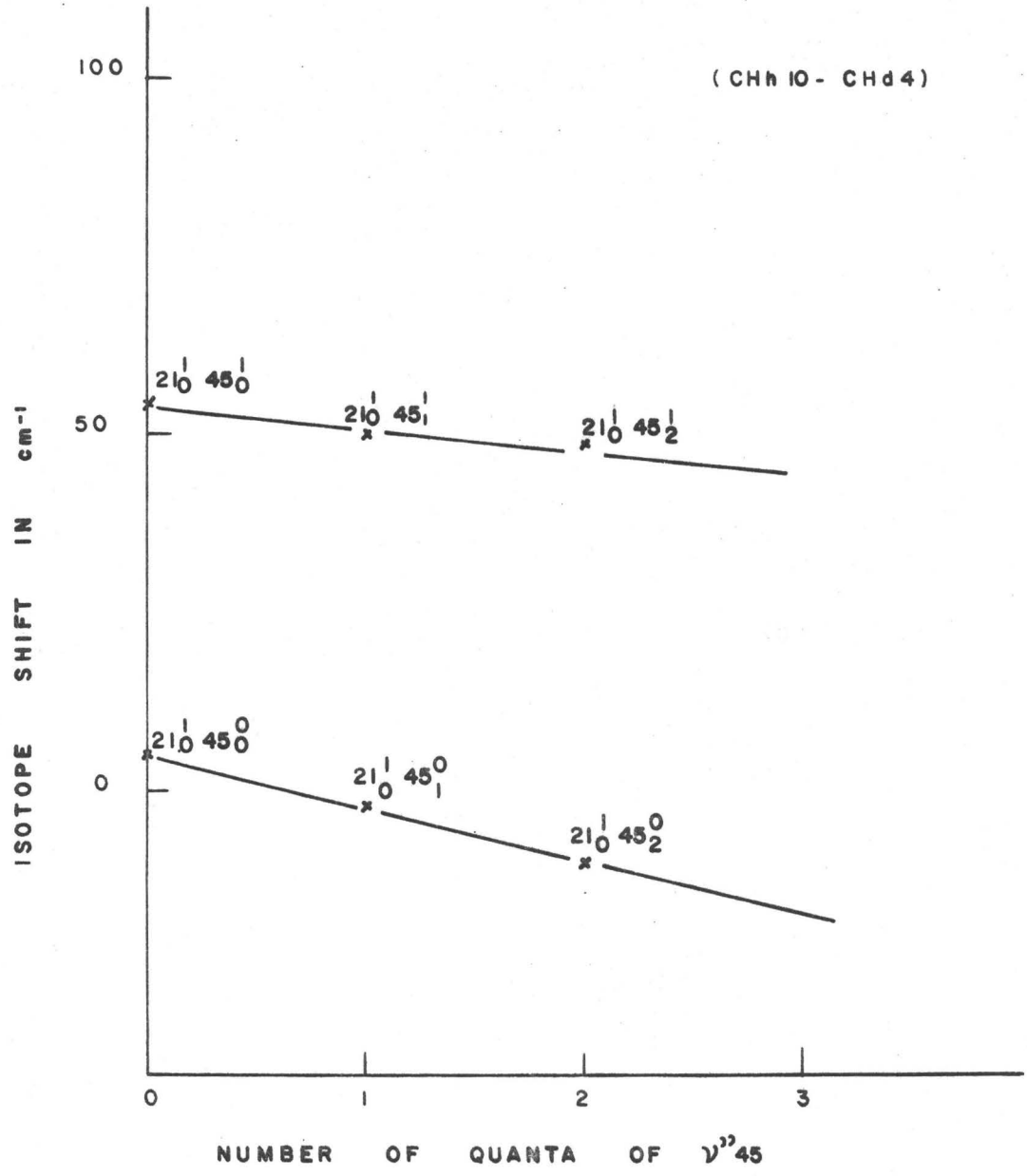

FIG(3·10) VIBRATIONAL ISOTOPE EFFECT IN THE $^1A_2 \leftarrow {}^1A_1$ TRANSITION OF CYCLOHEXANONES - SOME $21_0^1\,45_{v''}^{v'}$ PROGRESSIONS -

based on bands in the $21_1^{v'}$ ground state progression. Fig. 3.10 represents the isotope shift for the $45_{v''}$ progressions for CHh_{10}-CHd_4 (the isotope effect is not shown for CHd_{10} because only one member of the $45_{v''}$ progression is observed.

3.4 THE HIGH RESOLUTION SPECTRUM OF CHh_{10}

Because of its higher intensity relative to the background continuum, the spectrum of CHh_{10} could be photographed under high resolution, revealing a large number of additional peaks and band heads. The results of the high resolution work for this species can therefore be used to refine and improve upon the analysis of the low resolution spectrum given above. It should be emphasized, however, that the basic interpretation of the high and low resolution spectra remains the same.

The high resolution spectrum of CHh_{10} shows discrete bands from $\sim$ 29300 cm^{-1} to 31500 cm^{-1}. Bands at higher energy than 31200 cm^{-1} become increasingly broad and diffuse.

So most of the additional information is obtained from bands associated with the origin band at 30132 cm^{-1}, and not from those associated with members of the excited state carbonyl stretching progression which extends to higher frequencies, and which cannot be measured very accurately. In the $n \rightarrow \pi^*$ spectrum of related ketones[27,28,30,37], the more prominent features are progressions in the carbonyl wagging

frequency and the carbonyl stretching mode.

In the low resolution spectrum of CHh_{10} long progressions in the carbonyl stretching mode ν_7' do appear. In the region measured under high resolution, only two members of the progression in ν_7' as well as combination bands with 7_0^1 occurred.

The most obvious frequency interval in the spectrum is 490 cm^{-1}. This frequency is assigned here to the carbonyl out-of-plane wag, or at least to a normal mode which contains a large component of this motion.

As discussed in the previous chapter RNJM[26] on the basis of force constant calculations for the electronic ground state found about 30% of carbonyl wagging motion in the infrared band at 653 cm^{-1}. Their theoretical work suggested that several fundamentals involved the carbonyl out-of-plane motion. One of the frequencies is at 490 cm^{-1}. In the ultraviolet spectrum attempts to find progressions in 653 cm^{-1} were unsuccessful. This frequency does not seem to be active in the spectrum. Only the 490 cm^{-1} interval, which drops to 454 cm^{-1} in CHd_4 and 460 cm^{-1} in CHd_{10}, is clearly observed.

As has been discussed in the section on low resolution work, the corresponding progression in the excited state is about 398 cm^{-1} and shows a measurable splitting of the $\nu_{21}' = 2$ and 3 levels. The first member of the progression in the corresponding ground state vibration gives a weak band at $\sim$ 30132 cm^{-1}. To the red of this band appear two other bands at 29642 cm^{-1} and 29152 cm^{-1} which could be members of the

ground state progression in ν_{21}. This interval of 490 cm^{-1} is not repeated in other ground state progressions based on 21_0^3, 21_0^5 and 21_0^7. It appears instead that the difference in energy between the v"(21)= 1 and v"(21) = 2 levels at 540 cm^{-1}, which is somewhat larger than the fundamental frequency, see Fig. 3.11. One possible reason for this is that the 29102 band, at an interval of 1030 cm^{-1} to the red of the origin, arises from excitation of another fundamental instead of from 2 quanta of ν''_{21}. There are several observed bands in the infrared spectrum of the liquid[26] which could correspond to this fundamental, but according to RNHM[26], none of these has an out-of-plane wag component. From the low resolution spectra of the isotopic species, see Fig. 3.6 and 3.7, the corresponding intervals in the CHd_4 spectrum give only a small positive anharmonicity for ν''_{21} and no anharmonicity at all for CHd_{10}. Two possible explanations for the apparent large anharmonicity of the first overtone of ν''_{21} in CHh_{10} are a) that it is caused by a Fermi resonance with some other mode, which disappears upon deuteration, or b) that the 1030 cm^{-1} interval is approaching most closely to the barrier to chair-boat ring interconversion, and some coupling is occurring between ν''_{21} and a ring flapping mode. Whatever the reason, the ease with which the 1030 cm^{-1} = 490 + 540 cm^{-1} interval fits into the analysis, Fig. 3.11, indicates on Franck Condon grounds that it results from a vibration containing carbonyl wagging motion.

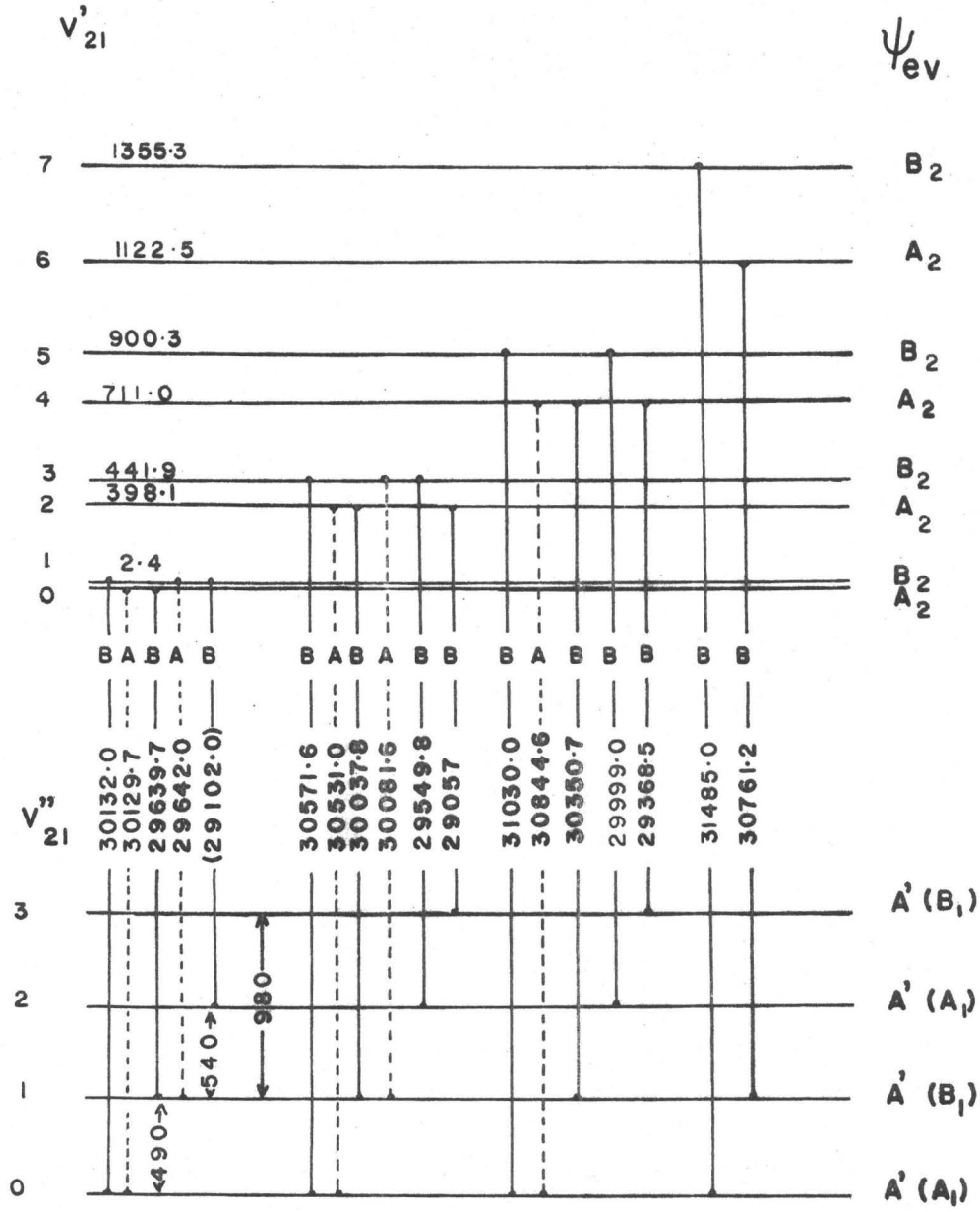

FIG(3·11) CH$_3$I - HIGH RESOLUTION SPECTRUM - SCHEMATIC ENERGY LEVEL DIAGRAM AND OBSERVED TRANSITIONS OF THE ν_{21} VIBRATION -

On the other hand three bands can be assigned to the 21_3^0, 21_3^2, 21_3^4 transitions, see Fig. 3.11. All these transitions are very weak and the polarization of the bands cannot be determined. Nevertheless they are observed under both high and low resolution. This gives the v"21 = 3 level at ∿ 980 cm^{-1} = 2×490 from the v"21 = 1 level. This tends to rule out two of the possible explanations given above and favours the explanation that a Fermi resonance occurs between the v"21 = 2 level and another mode.

In Fig. 3.11 the dashed lines show the transitions Δv_{21} = 0,2,4 which are forbidden by electric dipole selection rules. These transitions are weaker than those with $\Delta v = \pm 1,3,5$ but do appear in the spectrum , especially those of lower energy. The same transitions are found in the $\underline{n}\rightarrow\pi^*$ transition in formaldehyde, where the origin 0_0^0 band has been shown to be due to a magnetic dipole transition.

The expected polarization of the bands is given in Fig. 3.11. More details are given in the band contour section.

The progressions of Fig. 3.11 are repeated at 1170 cm^{-1} to the blue. The band at 1170 cm^{-1} to the blue of the origin band shows the same contour. It is composed of overlapping B+A type bands. More details are given in the band contour section.

Each allowed transition (B type) shown in Fig.3.11

is an origin for a progression in the ν'_{45} ring mode of a" symmetry. About 190 cm^{-1} to the red of these bands is the first member of the corresponding ν''_{45} progression.

To the blue of the band at 30132 cm^{-1} it is a long progression of about 130 cm^{-1}, the wavenumbers of the bands being

Wavenumber (cm^{-1})	Δ (cm^{-1})	Assignment
30132.0		21^1_0
	130.0	
30262.0		$21^1_0 45^1_0$
	127.6	
30389.6		$21^1_0 45^2_0$
	126.3	
30515.9		$21^1_0 45^3_0$
	125.1	
30641.3		$21^1_0 45^4_0$

To the blue of the band at 30571.6 assigned as 21^3_0 , is another progression in ν'_{45}

Wavenumber (cm^{-1})	Δ (cm^{-1})	Assignment
30571.6		21^3_0
	119.0	
30690.6		$21^3_0 45^1_0$
	123.3	
30813.9		$21^3_0 45^2_0$
	120.3	

30934.2		$21_0^3 45_0^3$
	121.0	
31055.2		$21_0^3 45_0^4$
	119.4	
31174.6		$21_0^3 45_0^5$

The ν_{45}' progression to the blue of the 21_1^2 transition is

Wavenumber (cm^{-1})	$\Delta(cm^{-1})$	Assignment
30037.8		21_1^2
	130.2	
30168.0		$21_1^2 45_0^1$
	129.9	
30297.9		$21_1^2 45_0^2$
	126.2	
30424.2		$21_1^2 45_0^3$

A schematic level diagram and the observed transitions based on the 21_0^1 origin are given in Fig. 3.12. The ground state frequency ν_{45}'' is 190 cm^{-1} and the first overtone is 186 cm^{-1}. These intervals are observed for transitions terminating on the levels with $v_{45}' = 0$, 1 and 2. The energy differences between the bands $21_0^1 45_0^3 - 21_0^1 45_1^3$ and the $21_0^1 45_0^4 - 21_0^1 45_1^4$ are $\sim$ 200 cm^{-1} instead of 190 cm^{-1} observed for other bands. This suggests a splitting of the $v_{45}' = 3$ and 4 levels. It must be realized that none of the normal modes corresponds exactly to a one dimensional out-of-plane oscillation of the oxygen, but in principle many of the normal modes contain

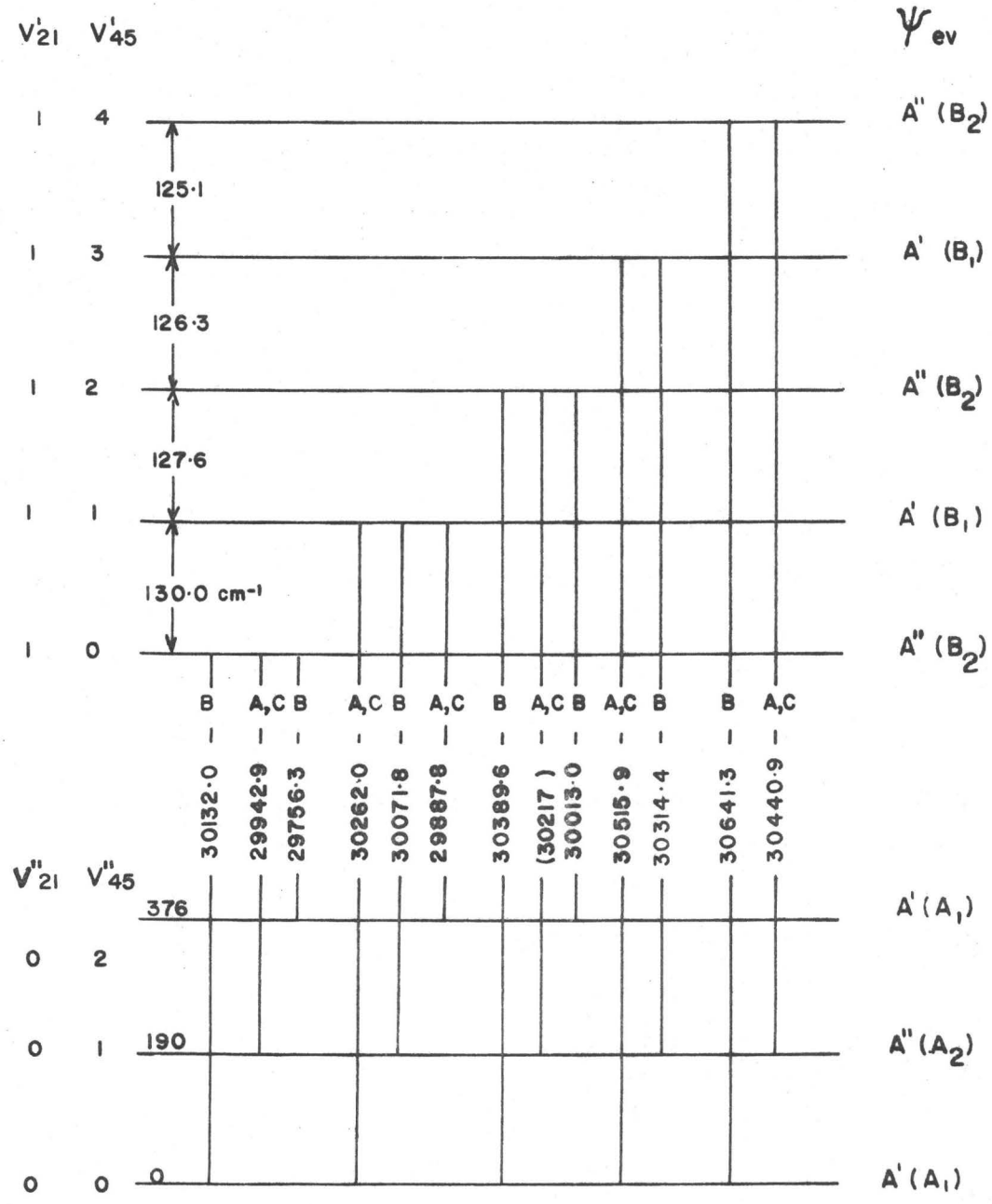

FIG(3·12) - CHh 10 - HIGH RESOLUTION SPECTRUM - SCHEMATIC ENERGY LEVEL DIAGRAM AND OBSERVED $21^{1}_{0}\,45^{v'}_{v''}$ TRANSITIONS

a component of out-of-plane deformation.

At 731 cm^{-1} from 21_0^1 is a strong band which does not fit in any of the previous pattern but is itself a new pseudo origin for a progression of two quanta of ν'_{45} . The assignment of this frequency is rather more difficult, no value for the ground state frequency can be obtained from the ultraviolet spectrum. It is possible that this frequency corresponds to the ring mode ν''_{12} at 861 cm^{-1} in the infrared spectrum which according to R.N.J.M.[26] calculations involves some carbonyl out-of-plane motion. Another possibility is that this mode increases from its ground state frequency and corresponds to the $\nu''_8(a') = 652\ cm^{-1}$, which also involve a high percentage (33%) of carbonyl out of plane motion. An increase in an excited state frequency is not unusual and has been observed in the cyclopentanone spectrum[30].

We shall call this band $21_0^1X_0^1$. The $21_0^1X_0^1$ band is an origin for two quanta of ν'_{45} frequency.

Wave number (cm^{-1})	Δ(cm^{-1})	Assignment
30863.0		$21_0^1X_0^1$
	119.0	
30982.0		$21_0^1X_0^1 45_0^1$
	119.7	
31101.7		$21_0^1X_0^1 45_0^2$

Under low resolution these bands are repeated strongly at a 1170 cm^{-1} interval to the blue. This mode is also active in

the low resolution spectra of CHd_4 at 629 cm^{-1} to the blue of the origin band.

The assignment of the high resolution spectra oc cyclohexanone is given in Table 3.8. The frequencies given are those calculated for the band origins. In Appendix 5 are listed the frequencies for the band heads.

3.5 THE DOUBLE MINIMUM POTENTIAL

The method used in this section for calculating the double minimum potential function has been described by Coon and All[29,57]. The double minimum potential function used was

$$V(Q) = \frac{1}{2} \lambda Q^2 + A \exp(-a^2 Q^2) \qquad (3.1)$$

where Q is a mass adjusted coordinate defined by

$$2T = \dot{Q}^2 \qquad (3.2)$$

The minima of this three parameter function are located at $\pm Q_m$, given by

$$Q_m = (1/a^2) \ln(2a^2 A/\lambda) \qquad (3.3)$$

A parameter ρ is defined by

$$a^2 = e^{\rho} \lambda/2A \qquad (3.4)$$

The parameter ν_o (cm^{-1}) is introduced through the relation

$$\lambda = (2\pi c \nu_0)^2 \qquad (3.5)$$

and a dimensionless parameter B is defined so that the barrier height is $Bhc\nu_o$.

TABLE 3.8

BAND FREQUENCIES AND ASSIGNMENT FOR THE HIGH RESOLUTION SPECTRUM OF CHh_{10}

ν cm^{-1} vacuum	Relative Intensity	Type of Band	Assignment
29057	vw		21_3^2
29102	w		21_2^1
29152.4	w		$7_1^1 26_0^1 X_0^1$
29241.4	w		$7_1^1 21_0^1 X_0^1 45_0^1$
29368.5	w		21_3^4
29458.5	m	(A,C)	$21_1^0 45_1^0$
29549.8	m		21_2^3
29582	vw		$7_1^1 26_0^1$
29639.7	m	B	21_1^0
29642.0	m	A	21_1^1
29684.6	mw		$21_1^2 45_2^0$
29756.3	vw		$21_0^1 45_2^0$
29771.0	m		$21_1^0 45_0^1$
29820.0	w		$21_1^2 45_2^1$
29859.4	m		$21_1^2 45_1^0$
29905.7	w		$21_1^0 45_0^2$
29913	w		$21_0^1 45_2^1$
29942.9	m	A,C	$21_0^1 45_1^0$
29951.6	m		$21_1^4 45_2^0$

(continued next page)

ν cm^{-1} vacuum	Relative Intensity	Type of Band	Assignment
29993.9	ms	B	$21_1^2 45_1^1$
29999.9		(B)	21_2^5
30037.8	s	(B)	21_1^2
30071.8	s		$21_0^1 45_1^1$
30081.6		A	21_1^3
30129.7	mw	A	21_0^0
30132.0		B	21_0^1
30154.4	vw		$21_1^4 45_1^0$
30168.0	m	A,C	$21_0^1 45_0^1$
30217.0	w		$21_0^1 45_1^2$
30262.0	m	A,C	$21_0^1 45_0^1$
30272.0	vw		$21_1^4 45_0^1$
30297.9	mw		$21_1^2 45_0^2$
30314.4	w		$21_0^1 45_1^3$
30350.7	ms	B	21_1^4
30389.6	ms	(B)	$21_0^1 45_0^2$
30424.2	w		$21_1^2 45_0^3$
30440.9	m		$21_0^1 45_1^4$
30471.9	mw		$21_1^4 45_0^1$
30515.9	m	A,C	$21_0^1 45_0^3$
30531.5	vw	(A)	21_0^2
30571.6	m	B	21_0^3

(continued on next page)

ν cm^{-1} vacuum	Relative Intensity	Type of Band	Assignment
30641.3	m		$21_0^1 45_0^4$
30690.6	vs		$21_0^3 45_0^1$
30731.1	vw		$7_0^1 21_2^3$
30761.2	vw		21_1^6
30773.1	vw		45_0^5
30809.5	vs		$7_0^1 21_1^0$
30816.9			$21_0^3 45_0^2$
30844.6	w	A	21_0^4
30863.0	s		$21_0^1 X_0^1$
30889.8	vw		$21_0^1 45_0^6$
30934.2	s		$21_0^3 45_0^3$
30940.9	m		$7_0^1 21_0^1 45_0^1$
30982.0	sb		$21_0^1 X_0^1 45_0^1$
31030.0	w		21_0^5
31055.2	m		$21_0^3 45_0^4$
31101.7	mw		$21_0^1 X_0^1 45_0^2$
31123.1	w		$7_0^1 21_0^1 45_1^0$
31169.1	w		$21_0^5 45_0^1$
31174.6	w		$21_0^3 45_0^5$
31215.9	vs		$7_0^1 21_1^2$
31229.5	w	A	$7_0^1 21_0^0$
31301.5		B	$7_0^1 21_0^1$

(continued next page)

ν cm^{-1} vacuum	Relative Intensity	Type of Band	Assignment
31335.9	vs		$7_0^1 21_1^2 45_0^1$
31429.9	m		$7_0^1 21_0^1 45_0^1$
31474.1	m		$7_0^1 21_1^2 45_0^2$
31485.0	mw		21_0^7
31516.0	w		$7_0^1 21_1^4$

NOTATION

w = weak, vw = very weak, m = medium, ms = medium strong

mw = medium weak, vs = very strong.

Bracket between two frequencies means that the two bands are strongly overlapped.

From equations (3.1), (3.3), (3.4)

$$Bhc\nu_o = V(o) - V(Q_m) = A(e^{\rho}-\rho-1)/e^{\rho} \tag{3.6}$$

The barrier height b in cm^{-1} is

$$b = B\nu_o \tag{3.7}$$

and the positions of the minima are given by

$$Q_m^2 = \frac{2\rho}{e^{\rho}-\rho-1} \cdot \frac{h}{4\pi^2 c} \cdot \frac{B}{\nu_o} \tag{3.8}$$

where $h/4\pi^2 c = 55.9810\times10^{-40}$ g.cm.

We may determine the parameters λ, A, a^2 of equation (3.1) if the parameters ν_o, B and ρ are known.

If the potential function along an asymmetrical coordinate Q has a double minimum, the function may be approximated by making an appropriate choice of ν_o, B and ρ. The barrier height is then given by equation (3.7) and the position of the minima by equation (3.8). The shape of the potential is shown in Fig. 3.13. For the potentials plotted, the two quantities Q_m and b are held fixed while ρ is varied. For low values of ρ the outer walls of the function rise more steeply than the walls of the barrier. For $\rho = 1.5$. The minima are parabolic, $(\partial^3 v/\partial Q^3) = 0$ at Q_m. For larger values of ρ the walls of the barrier rise more steeply than the outer walls of the potential function.

If three energy levels for a double minimum potential function can be determined spectroscopically, a potential function with the same levels and the form of equation (3.1)

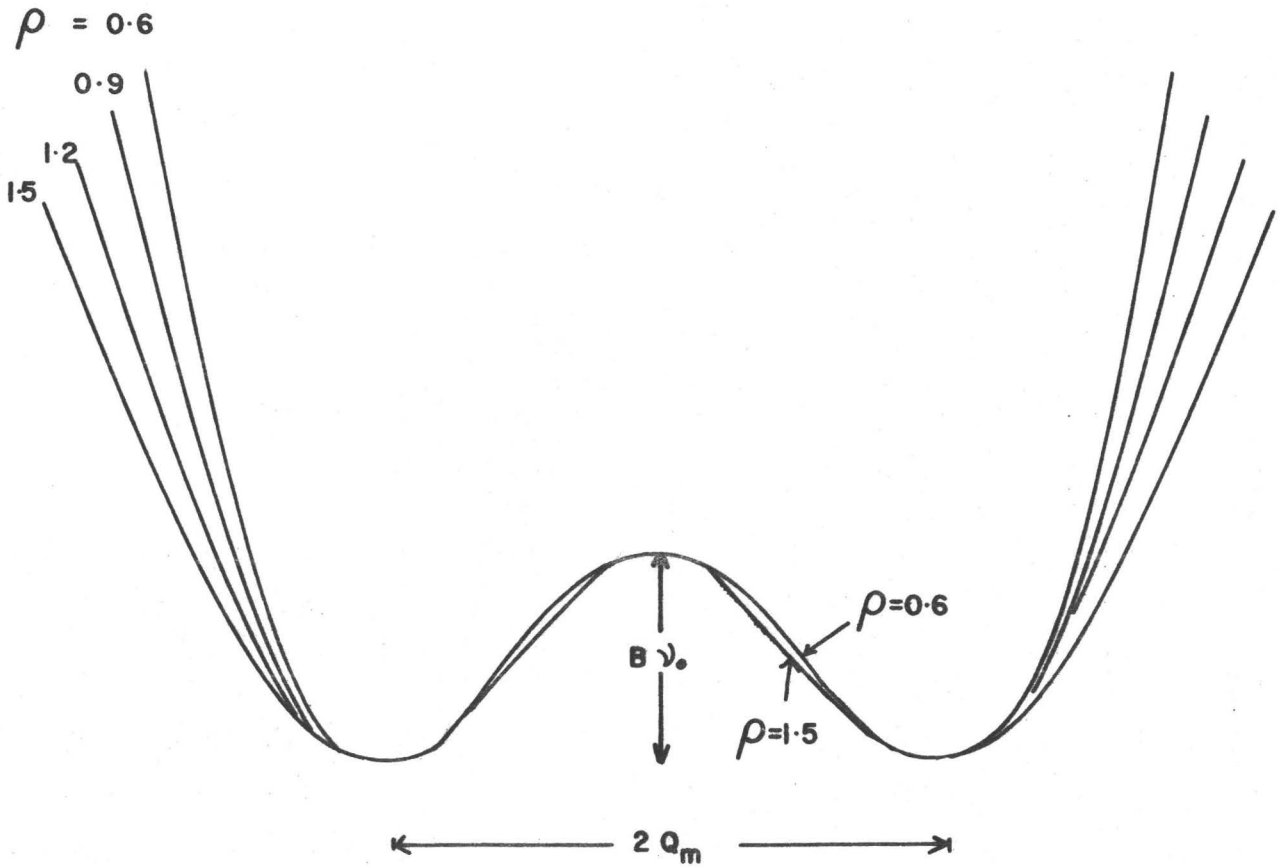

FIG (3·13) THE EFFECT OF ρ ON THE SHAPE OF THE DOUBLE MINIMUM POTENTIAL FUNCTION. (AFTER COON AND AL.[57])

may be found. For a given value of ρ the other two parameters may be determined from two known levels by use of tables of eigenvalues for the function[57]. The same tables give the ten lowest eigenvalues for the double minimum potential. If the calculation is then repeated for different ρ values, the final choice of ρ is the one which leads to best agreement between observed and calculated levels.

Coon's tables 1(a) and 1(b)[57], give energy levels G/ν_o as a function of B for $\rho = 0.6$. In order to conform with the notation in this paper, we label the successive inversion levels v'21 = 0,1,2,3,... as 0^+, 0^-, 1^+, 1^-, ... etc. respectively. The vibrational energy in cm^{-1} may be written as

$$G(v_i) = G(0^+) + G_o(v_i) \qquad (3.9)$$

For CHh_{10}, the level separations $1^+-1^- = 43.8\ cm^{-1}$ and $0^+-1^+ = 398.1\ cm^{-1}$ were used in the calculation of the potential. (The interval 0^+-0^- was not used because it is too small to be measured accurately from the spectra.) For an assumed value of ρ, the theoretical value of the ratio $[G(1^+)-G(0^+)]/[G(1^-)-G(1^+)]$ was calculated from tables 1(a) and 1(b)[57] and plotted as a function of B. The experimental value of this ratio is 9.09 for CHh_{10}. Graphical interpolation shows that this figure corresponds to a B value of 1.740 for $\rho = 0.6$. Table 3.9 gives the B values deduced by interpolation using different values of ρ. All the calculations are based on the

TABLE 3.9

PARAMETERS OF THE DOUBLE MINIMUM POTENTIAL FUNCTION

ρ	$B^{(b)}$	$\nu_o^{(b)}$ cm^{-1}	$B\nu_o = b$ cm^{-1}	$G^{(b)}(0^+)$
.60	1.740	445.3	774.8	231.9
.90	2.172	359.9	781.9	229.1
1.2	2.572	309.6	796.3	226.8
1.5	2.92	274.9	802.8	223.9

$$\frac{G(1^+)-G(0^+)}{G(1^-)-G(1^+)} = 9.09^{(a)}$$

(a) observed experimentally for CHh_{10}

(b) deduced by graphical interpolation.

experimental value of $[G(1^+)-G(0^+)]/[G(1^-)-G(1^+)] = 9.09$. The value of ν_o was obtained from the identity

$$\nu_o = [G(1^+)-G(0^+)]/[G(1^+)/\nu_o - G(0^+)/\nu_o] \qquad (3.10)$$

The numerator is obtained as the experimental frequency 398.1 cm^{-1} for CHh_{10} and the denominator by graphical interpolation, which gives 0.894 for B = 1.74 and $\rho = 0.60$.

The results for ν_o at different ρ values are listed in Table 3.9.

$G(0^+)$ was calculated by the same method.

$G(0^+)/\nu_o = 0.52085$ was deduced by graphical interpolation using Coon's tables 1(a), 1(b)[57] at B = 1.74 and ν_o was calculated previously using equation (3.10) $G(0^+) = 231.93$ for B = 1.74.

The barrier height was then calculated using relation (3.7).

The lowest 8 levels were calculated from equations (3.9)

$$G_o(v_i) = [G(v_i)/\nu_o]\nu_o - G(0^+) \qquad (3.11)$$

Calculations similar to the above were carried out for $\rho = 0.6$, $\rho = 0.9$, $\rho = 1.2$ and $\rho = 1.5$. For these ρ values the average deviations of the observed from the calculated levels were $\sim$ 11 cm^{-1}, 7 cm^{-1}, 4 cm^{-1}, 9 cm^{-1} respectively for CHh_{10}. The value $\rho = 1.2$ gave the best fit.

Similar calculations were carried out for CHd_4 and

CHd_{10} for $\rho = 0.6$ and $\rho = 1.2$ but the accuracy is less for these isomers, as bands could only be measured from the low resolution spectra. The average deviation of the observed from the calculated levels were 3 cm^{-1} for $\rho = 1.2$, and 6 cm^{-1} for $\rho = 0.60$ for CHd_4. Insufficient experimental data were available to calculate the best value of ρ for CHd_{10}.

The resultant calculated levels are compared with the observed levels in Table 3.10 for the three isomers.

The best values for the parameter ρ, B, ν_o are listed on Table 3.11 as well as the zero point energy $G(0^+)$, and the barrier height b. Q_m was calculated for CHh_{10} using the relation (3.8)

$$Q_m^2 = 0.99638\times10^{-40} \text{ g. cm}^2$$

$$Q_m = \pm0.998188\times10^{-20} \text{ g}^{1/2} \text{ cm.}$$

Q_m was only calculated for CHh_{10} because the observed frequencies for this molecule could be determined from the high resolution spectra, and are the most accurate. The potential function is shown in Fig. 3.14.

Let θ measure the displacement of a molecule along the normal coordinate corresponding to the bending mode which has a double minimum potential. The kinetic energy T is expressed in terms of the reduced mass μ by

$$2T = \dot{Q}^2 = \mu r^2\dot{\theta}^2 \qquad (3.12)$$

where r is a bond length and Q is the mass adjusted coordinate.

TABLE 3.10

OBSERVED AND CALCULATED VALUES OF THE INVERSION LEVELS $G_o(v_i)$ FOR THE $^1A_2$ STATE

	CHh_{10}		CHd_4		CHd_{10}	
v_i	obs.	calc.	obs.	calc.	obs.	calc.
0^+	0.0	0.0	0.0	0.0	0.0	0.0
0^-	2.4	2.3		0.12		0.05
1^+	398.1[a]	398.6	262[a]	262	251[a]	250
1^-	441.9[a]	443.1	266[a]	266	253[a]	253
2^+	711.0	709.9	474	472		462
2^-	900.3	882.2	513	515		488
3^+	1122.5[b]	1120.6	668[b]	657		630
3^-	1348.7[b]	1360.8	758[b]	770		722

a Values on which calculations are based

b Data from band assigned after calculations.

TABLE 3.11

THE DOUBLE-MINIMUM POTENTIALS

	CHh_{10}	CHd_4	CHd_{10}
ρ	1.2	1.2	(1.2)
B	2.572	3.562	3.867
ν_o	310 cm^{-1}	185 cm^{-1}	175 cm^{-1}
b^*	796 cm^{-1}	660 cm^{-1}	678 cm^{-1}
$G(0^+)$	226.8	138.5	131.5
Q_m		$.9982 \times 10^{-20}\ g^{1/2}\ cm$	
θ_m		30°	

$G(0^+)$ = zero point energy

b = barrier height

θ_m = oxygen out of plane angle at minimum.

*The difference in barrier height between CHh_{10}, CHd_4, CHd_{10}, probably reflect the fact that what is being measured is the barrier of inversion along the normal coordinates ν_{21}. This can change between the isotopic species.
In any case the accuracy of frequency measurement for the deuterated species is far less than for CHh_{10}.

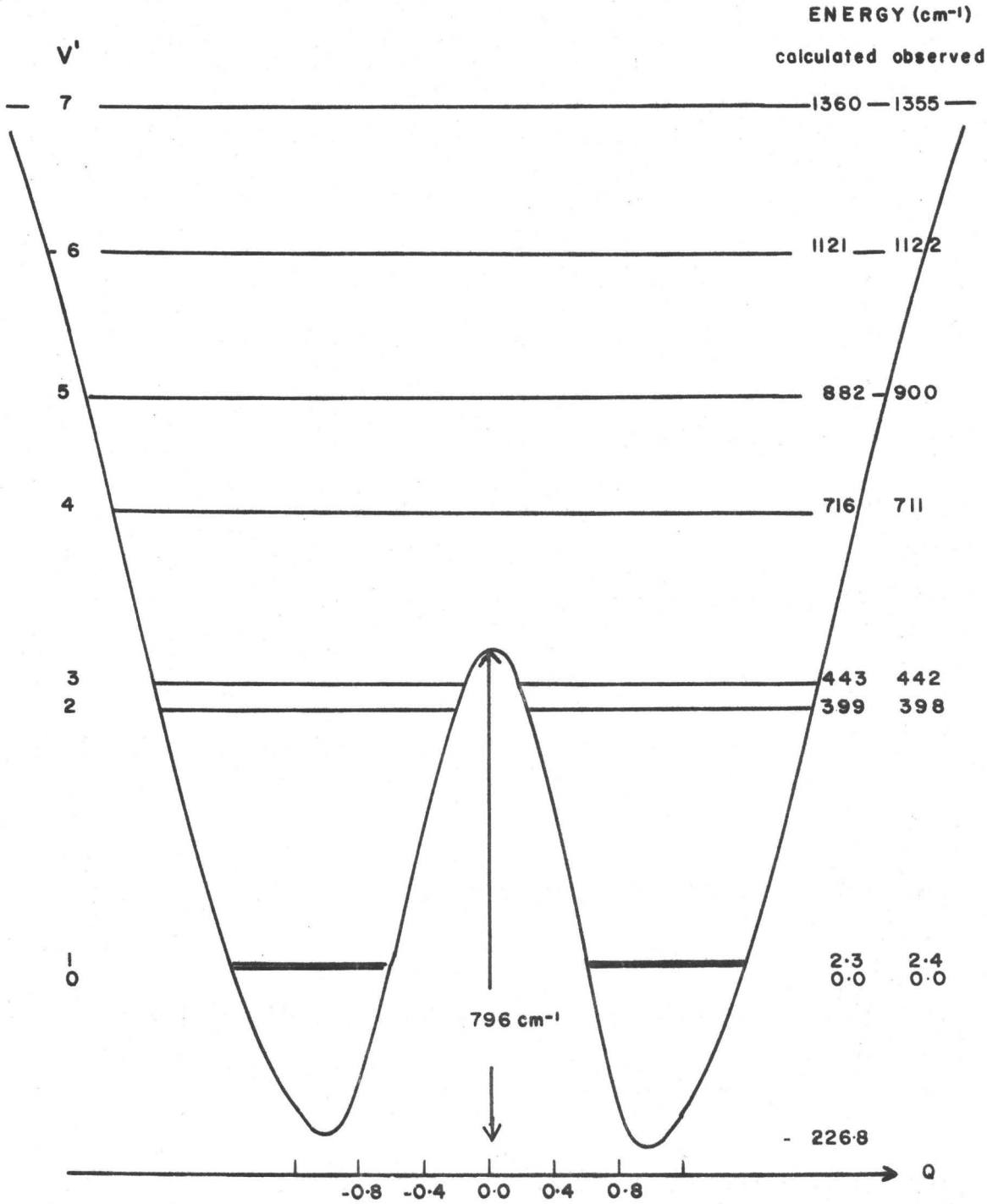

FIG(3·14) THE DOUBLE MINIMUM POTENTIAL FUNCTION OF - CHhIO -

$$Q = \mu^{1/2}\, r\, \theta \tag{3.13}$$

This relation, together with equation (3.8), permits a calculation of the angle θ_m, the position of the potential minimum

$$\theta_m = \frac{Q_m}{\mu^{1/2} r} \tag{3.14}$$

In the case of a large molecule like cyclohexanone the reduced mass cannot be calculated in a simple way. But the kinetic energy can be expressed in terms of internal coordinates[58] p 62

$$2T = \sum_{tt'} (G^{-1})_{tt'}\, \dot{S}_t \dot{S}_{t'} \tag{3.15}$$

where S_t and $S_{t'}$ are internal coordinates.

For each atom, α, each internal coordinate has a displacement vector $\vec{s}_{t\alpha}$ associated with it. The quantity $G_{tt'}$ is given in terms of $\vec{s}_{t\alpha}$ by

$$G_{tt'} = \sum_{\alpha=1}^{N} m_\alpha^{-1}\, \vec{s}_{t\alpha} \cdot \vec{s}_{t'\alpha} \tag{3.16}$$

where m_α is the mass of the atom α. There will be one element, $G_{tt'}$, for each pair of internal coordinates, $S_t, S_{t'}$. If the internal coordinate S_t is assumed to be a normal coordinate then S_t is orthogonal to $S_{t'}$ and $G_{tt'} = 0$. The G matrix only possesses diagonal elements and the $(G^{-1})_{tt}$ matrix element is equal to the reciprocal of the G_{tt} matrix element.

If we assume that the carbonyl bending motion is a normal mode, that is, there is no coupling between this motion and other displacements then one need consider only that part

of the molecule adjacent to the carbonyl bond, that is

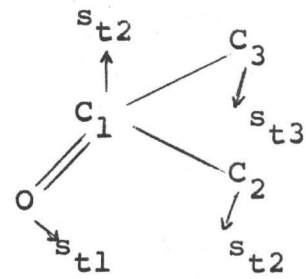

for such displacements, Wilson, Delcius and Cross have expressed the $\vec{s}_{t\alpha}$ vectors in terms of unit vectors $\bar{e}$ along the interatomic connecting lines, see ref. (58) p. 60 for this displacement $S_t = \Delta\theta$. The kinetic energy expressed in equation (3.15) becomes for this particular mode t

$$2T = (G^{-1})_{tt}\,\dot{\theta}^2 = \dot{Q}^2 \tag{3.17}$$

so

$$\theta_m = \frac{Q_m}{\sqrt{G^{-1}_{tt}}} \tag{3.18}$$

or

$$\theta_m = Q_m \cdot \sqrt{G_{tt}} \tag{3.19}$$

The G_{tt} matrix element was calculated using formula (3.16) and $\vec{s}_{t\alpha}$ vectors given in ref. (58) p. 60 or in (38) p. 201. The matrix element G_{tt} is a function of θ. An iterative procedure was used to calculate the final value of θ_m. Q_m was the value calculated previously in Table 3.11.

The angle θ_m was calculated for different values of the geometrical parameters around the carbonyl group. The C=0 bond length was varied between 1.31 Å up to 1.34 Å by steps of 0.01 Å. The C-C from 1.52 to 1.53 Å. The C.C.C. angle from 117° to 120° by step of 1°. For geometries within the ranges, the out-of-plane angle θ_m was found to be 30°±2°.

CHAPTER 4

BAND CONTOUR ANALYSIS

4.1 GEOMETRY OF CYCLOHEXANONE IN THE GROUND STATE

The electron diffraction study by Romers[8] gives for the geometry of the ground state the parameters listed in Table 4.1. Using these parameters, one can calculate the coordinates of the nuclei with respect to a coordinate system of axes u,v, w see Fig. 4.1 and then calculate the moment of inertia I_A, I_B, I_C of the molecule with respect to the principal axes of the molecule. The rotational constants $A = h/8\pi^2 I_A$, etc. for the ground state can then be calculated also.

A set of relative nuclear coordinates for the nuclei in cyclohexanone have been calculated by Yoh.Han.Pao and D. P. Santry[16]. These authors used an idealized model in which it was assumed that all bond angles were tetrahedral, save those between the carbon carbon bonds joining the carbonyl group, for which angle a value of 120° was assumed. The carbon carbon bonds adjacent to the carbonyl group were assumed to be 1.52 Å, all other carbon carbon bonds being 1.54 Å. The carbon hydrogen bonds were assumed to be 1.09 Å and the

TABLE 4.1

GEOMETRICAL PARAMETERS OF CYCLOHEXANONE IN ITS GROUND ELECTRONIC STATE BY ROMERS (8)

Distance		Angle	
C-H	1.09±0.02 Å	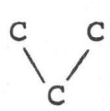	109.5°±2.5°
C-O	1.24±0.02		
C-C	1.54±0.01		
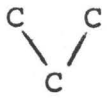	2.51±0.02		α = 117° ± 3° β = 121.5° ± 1.5°

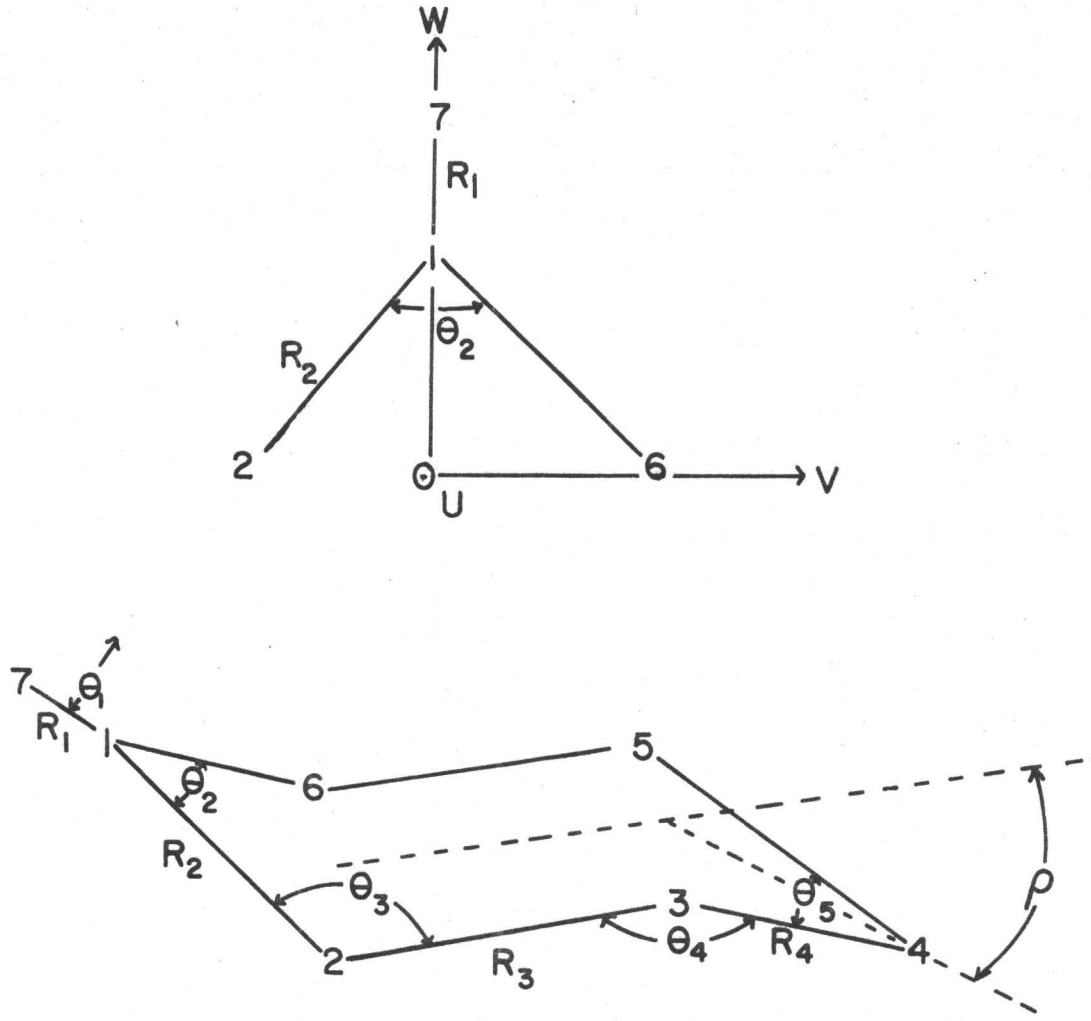

FIG (4·1) SYSTEM OF AXES USED FOR COORDINATE CALCULATIONS

carbonyl oxygen 1.23 Å.

The coordinates of cyclohexanone were recalculated in this work using a vector analysis method. First, the coordinates were calculated using the geometry of Pao and Santry, and found to be in good agreement with their results[16]. The coordinates, moments of inertia, and rotational constants were thencalculated using Romers'[8] geometry. The rotational constants obtained in this case are

$$A'' = 0.138 \text{ cm}^{-1}$$

$$B'' = 0.084 \text{ cm}^{-1}$$

$$C'' = 0.058 \text{ cm}^{-1}$$

The degree of asymmetry is measured by the dimensionless parameter

$$\kappa = \frac{2B-A-C}{A-C} \qquad (4.1)$$

The κ value in this case is -0.35941.

The molecue is thus an asymmetric top molecule. This κ value is closer to the limiting prolate top case (κ =-1.0) than the oblate top case (κ = +1.0). Using those values of the ground state rotational constants one can calculate the contours of A,B, C types of band of the molecule in its ground electronic state.

For the ground state, a check on the rotational constants can be made by using them to calculate an infrared band profile (assuming the same values for the constants in both combining vibrational levels), and then comparing this with

an experimental profile. If good agreement is not obtained, then the A", B", C" values used in the calculation do not correspond to the true values. When this was carried out using the rotational constants derived above from Romers' geometry, the observed and calculated contours matched rather poorly. This is not surprising, in view of the magnitude of the limits of error in the electron diffraction work, see Table 4.1 and the fact that band contours are often very sensitive to small changes in the rotational constants. Consequently, improved values of the ground state rotational constants were obtained by systematically varying their assumed values until the experimental and calculated infrared profiles agreed. The procedure is described in the following section.

-Band Contour Analysis-

The computer program used to calculate band contours for asymmetric top molecules is based upon one described by Parkin[65], and successively improved by Balfour[66] and Kidd[67]. The program calculates the frequencies and intensities of all rotational lines up to J = 70, K = 30, in asymmetric top approximation, and then up to J = 70, K = 60 in symmetric top approximation. It then divides the whole band interval into boxes 0.2 cm^{-1} wide, distributes the intensity of each line into adjacent boxes in accordance with a gaussian function of half width 0.1 cm^{-1}, and prints

out the sum of the intensities in each box against its wave number. Each contour takes some 65 seconds to compute on a CDC6400 computer.

-Rotational Constants Deduced from Band Contour Analysis -

The theory of asymmetric rotor levels and selection rules for transitions is to be found in (1) and (2). Here we shall simply identify the quantum numbers used to label the rotational levels.

The rotational term values (in cm^{-1}) for a prolate symmetric top in a vibronic state, v, are given by

$$F_v(J,K) = B_v\, J(J+1) + (A_v - B_v)K^2 \qquad (4.2)$$

where J is the total angular momentum quantum number and K is the quantum number for the component of the total angular momentum along the a axis. K has the value 0, 1, 2 --- $|J|$; all levels with K values greater than zero are doubly degenerate.

The rotational term values for a vibronic state, v, of a molecule which is an asymmetric top are given by

$$F_v(J,\tau) = \frac{1}{2}(A_v + C_v)J(J+1) + \frac{1}{2}(A_v - C_v)E_v(\kappa) \qquad (4.3)$$

where τ is a running number which labels different levels and $E(\kappa)$ is a function which depends on k, J, τ.

The rotational term values for a vibronic state, v, of

a molecule which is nearly a prolate symmetric top are given approximately by

$$F_v(J,K) = \bar{B}_v\, J(J+1) + (A_v-\bar{B}_v)K^2 \qquad (4.4)$$

where

$$\bar{B}_v = \frac{1}{2}(B_v+C_v)$$

In asymmetric top molecules, K is not a valid quantum number, although for small asymmetry it is still approximately defined. The double degeneracy of $K \neq 0$ levels is removed when the top is asymmetric. The deviations from the symmetric top approximation decrease as the quantum number K increases.

From the high resolution infrared spectrum of CHh_{10} in its vapour phase, two bands at 1120 cm^{-1} and 1222 cm^{-1} which appeared to be pure type B bands were selected. A grid search, which consisted in varying each of A", B", C" in successive incremental steps and calculating the resultant type B profile, was carried out until good agreement between the calculated and the observed infrared band profile was obtained. It was found that the calculated contour is very sensitive to small changes in the rotational constants.

A comparison between the observed and the best calculated band profile is given in Fig. 4.2. Because of the very low intensity of the infrared bands recorded in a 10 cm cell at room temperature vapour pressure, the height of the recorded infrared bands had to be expanded five times. In

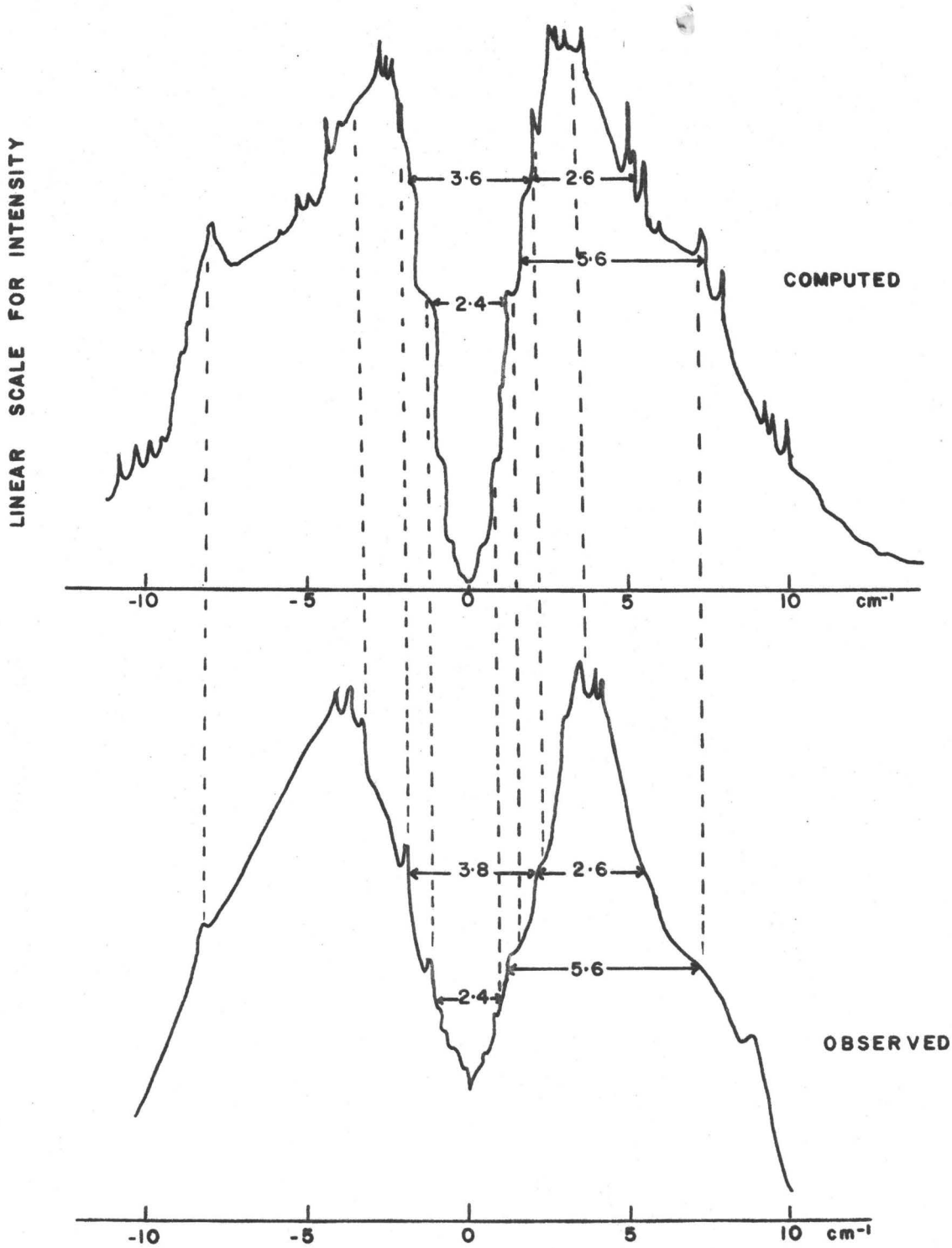

FIG (4·2) CONTOUR OF AN INFRARED CHh10 TYPE B BAND

order to increase the resolution, the slit of the spectrophotometer was kept fixed at 80 μ and the amplifier gain was increased to compensate for the decrease in radiation falling on the detector. Because of the low power level, the average noise level on a high resolution spectrum was of the order of 2 to 3%. The scanning time was kept very long; it took about 4 hours to run one band. Because of the high noise level it was not possible to get an exact match between the observed and calculated spikes. The fitting was considered to be good when the general features of the observed and calculated bands matched, particularly the width of the heads and of the inside hump of the band.

The values of the rotational constants obtained by this method are

$$A'' = 0.140 \pm 1 \text{ cm}^{-1}$$

$$B'' = 0.082 \pm 1 \text{ cm}^{-1}$$

$$C'' = 0.057 \pm 1 \text{ cm}^{-1}$$

-Geometry of the Ground State-

The geometrical parameters $\theta_2, \theta_3, \theta_4, \theta_5$, R_2, R_3, R_4, (see Fig. 4.1) were then varied over the experimental error limits given by Romers[8] (see Table 4.1), and the values of the rotational constants calculated for these different cases. The possible geometries which give A", B", C" (within the limits of accuracy obtained by band contour analysis)

that correspond to the values of the parameters are listed in Table 4.2 and are shown in this table with those of Romers[8].

Our results are in good agreement with those of Romers but show that the carbon-carbon bond to the carbonyl group is probably shorter than the other carbon-carbon bonds of the ring. Our results also suggest that the θ_2, θ_3 and θ_4 angles (see Fig. 4.1) are very slightly greater than those predicted by Romers. This implies a more planar ring than the one predicted by the electron diffraction results.

The rotational constants obtained by the method described above were then used for the band contour analysis of the electronic spectrum. Fig. 4.3 shows the directions of the principal moments of inertia of the molecule in the ground state. The center of mass of the molecule is in the (u,w) plane. Its coordinates with respect to the u,v,w system of axis are

$$\begin{cases} 0.342\ \text{Å} \\ 0.000 \\ -0.251 \end{cases}$$

The principal axes a and c are in the symmetry plane of the molecule (u,w); the b axis is parallel to the v axis. The a axis is at an angle of 14° to the C-O bond in the ground state.

4.2 GEOMETRY OF CYCLOHEXANONE IN THE EXCITED STATE

-The Electronic Band Structure-

Comparison of the observed and calculated rotational band profiles in the electronic spectrum should give information

TABLE 4.2

GEOMETRICAL PARAMETERS OF CYCLOHEXANONE IN ITS GROUND ELECTRONIC STATE

PARAMETERS (Notation of Fig.(4.1)	Calculated from IR band contour analysis	Romers (8)
C=O = R_1	1.24 ± 0.02 Å	1.24 ± 0.02 Å
C-C = R_2	1.53 ± 0.01 Å	1.54 ± 0.01 Å
C-C = R_3 = R_4	1.54 ± 0.01 Å	
C-H = R_6=R_7=R_8	1.09 ± 0.02 Å	1.09 ± 0.02 Å
θ_1 (out of plane angle)	0.00°	0.00°
θ_2	119° ± 3°	117° ± 3°
θ_3	111.5° ± 1.0°	109.5° ± 2.5°
θ_4	111° ± 2°	
θ_5=θ_6=θ_7=θ_8	109.5°± 1.0°	
ρ*	53.5 ± 2.5°	58° (a)
γ*	18° ± 2°	12.5° (a)

(a) calculated by us using Romers' geometry

* ρ angle between planes (C_2,C_3,C_5,C_6) and (C_3,C_4,C_5)

* γ angle between planes (C_1,C_2,C_6) and (C_3,C_4,C_5)

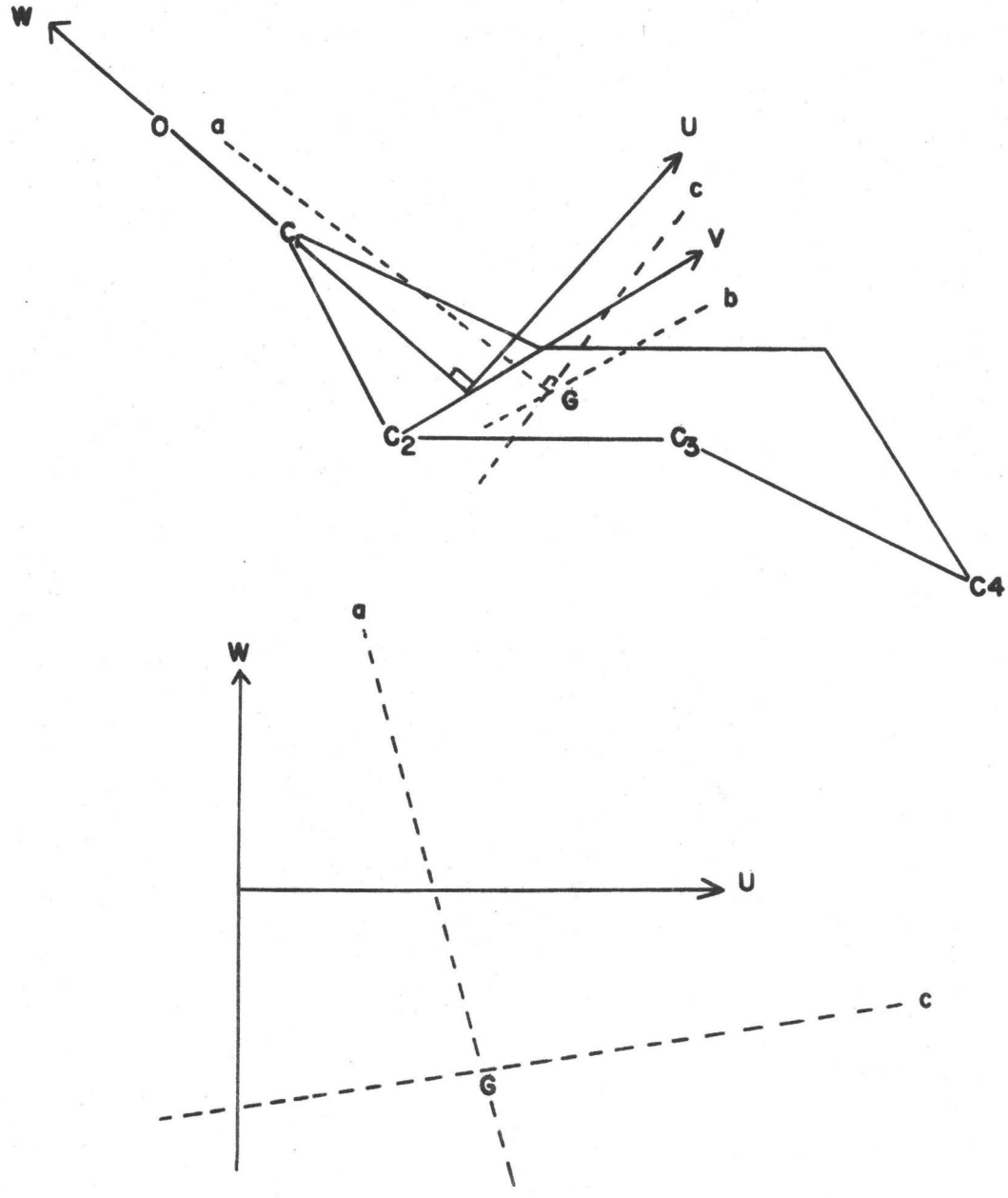

FIG(4·3) PRINCIPAL AXES OF INERTIA OF CHhIO IN ITS GROUND STATE

about the polarisation of the bands, and, from the calculated best values of the excited state rotational constants, about the excited state geometry. If the $\underline{n} \rightarrow \pi^*$ system is similar to that in formaldehyde, the strongest bands involving the ν_{21} progressions and based on the true electronic origin should be B type bands, i.e., A_1-B_2 and A_2-B_1 (see Fig. 3.11). On the other hand, in cyclopenatone, the strongest progressions are based on a hot pseudo origin and are vibronically A_2-B_2 with C type profiles.

It has been shown for formaldehyde[28,29] that the effective carbonyl out-of-plane angle in the $^1A_2(\pi^*,\underline{n})$ state, as well as the C=O bond length, both vary considerably according to the number of quanta of the out-of-plane mode which are excited. The profiles of bands corresponding to transitions to levels above the barrier to carbonyl inversion in the excited state can be drastically altered from those of bands close to the origin.

Theoretical band contours were obtained using the computer program described above. Lines up to J = 70 and K = 30 were calculated in asymmetric top approximation, and the remainder up to J = 70, K = 60 in symmetric top approximation. The frequency interval was 0.2 cm^{-1} and the line width was 0.3 cm^{-1}. For the ground state, the rotational constants obtained from the infrared band contour analysis, A" = 0.140, B" = 0.082, C" = 0.057 cm^{-1}, were assumed. In order to obtain a first approximation to the rotational constants in the excited state,

it is reasonable to assume that, as in other $\underline{n}\rightarrow\pi^*$ carbonyl transitions, the transition is primarily localised in the carbonyl group, and the main changes in geometry are in the carbonyl bond length and the out-of-plane angle θ_1 between the carbonyl bond and the C_6-C_1-C_2 plane. The geometry of the rest of the molecule was held constant at the values calculated from the infrared band analysis, Table 4.2.

The effect of changing both r(C=O) and θ_1 on the rotational constants A', B', C' for excited state are shown in Figs. 4.4, 4.5 and 4.6. These show the differences $\Delta A = A''-A'$ cm^{-1}, etc., and enable rough limits to be set on the change in rotational constants on excitation. The double potential minimum calculation indicates that θ_1 is around 30°,and the carbonyl bond length, by analogy with other carbonyl compounds, see Table 3.1, should increase by some 0.1 Å. With this in mind, the following preliminary limits were set: A' decreasing over the range 0.134 to 0.131 cm^{-1}, B' increasing over the range 0.084 to 0.087 cm^{-1} and C' increasing from 0.059 to 0.061.

A grid search was then carried out over this range of excited state rotational constants in successive incremental steps of 0.001 cm^{-1}. Type A, B, C band contours were calculated for each set of values. The results in summary are

Type A bands

The type A bands show a single head of about 4 cm^{-1} width. This profile was almost insensitive to the change in rotational constants.

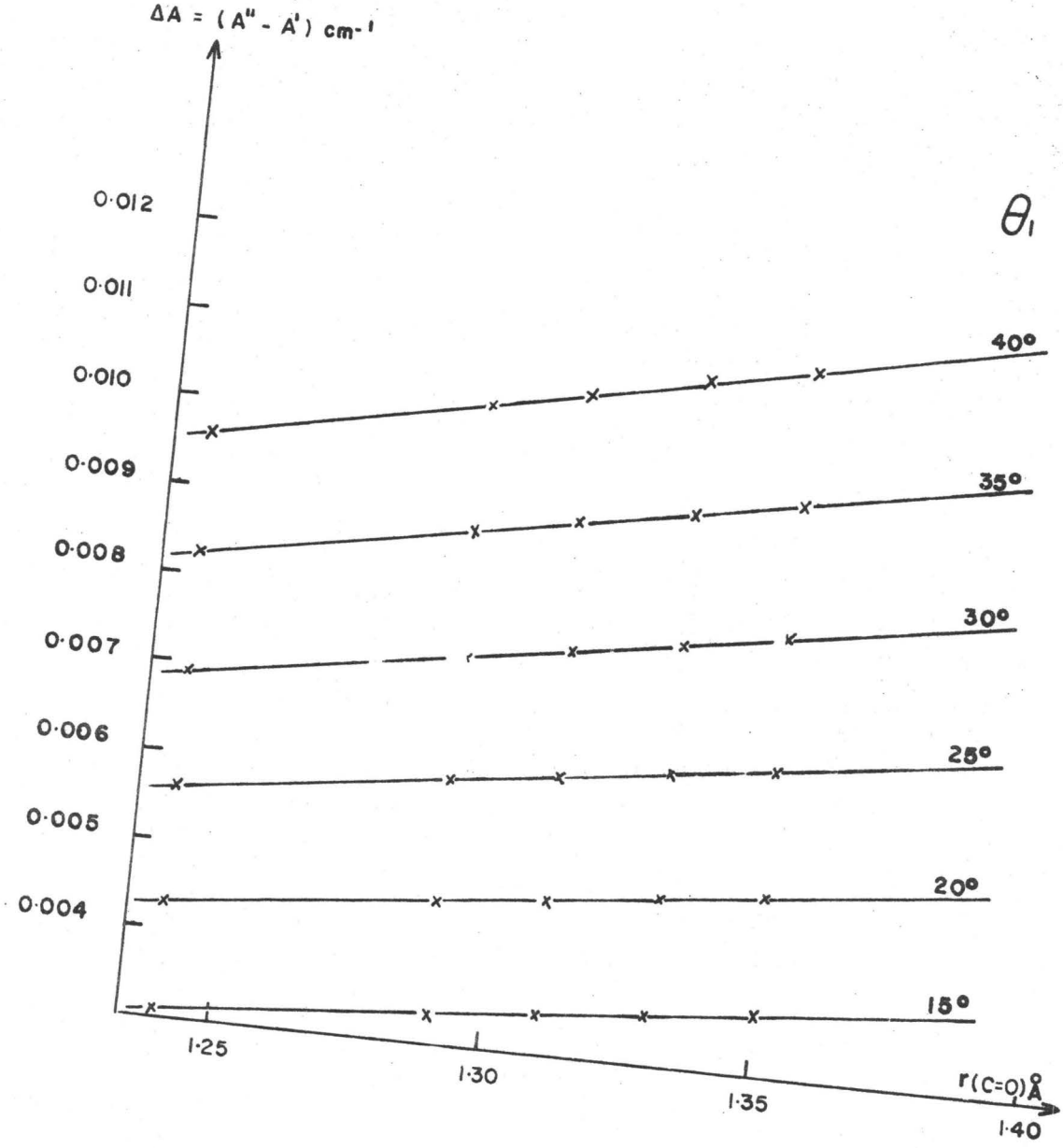

FIG (4·4) CHANGE IN ROTATIONAL CONSTANT A WHEN r (C=O) AND Θ_1 ARE VARIED. $A'' = 0{\cdot}140\ cm^{-1}$.

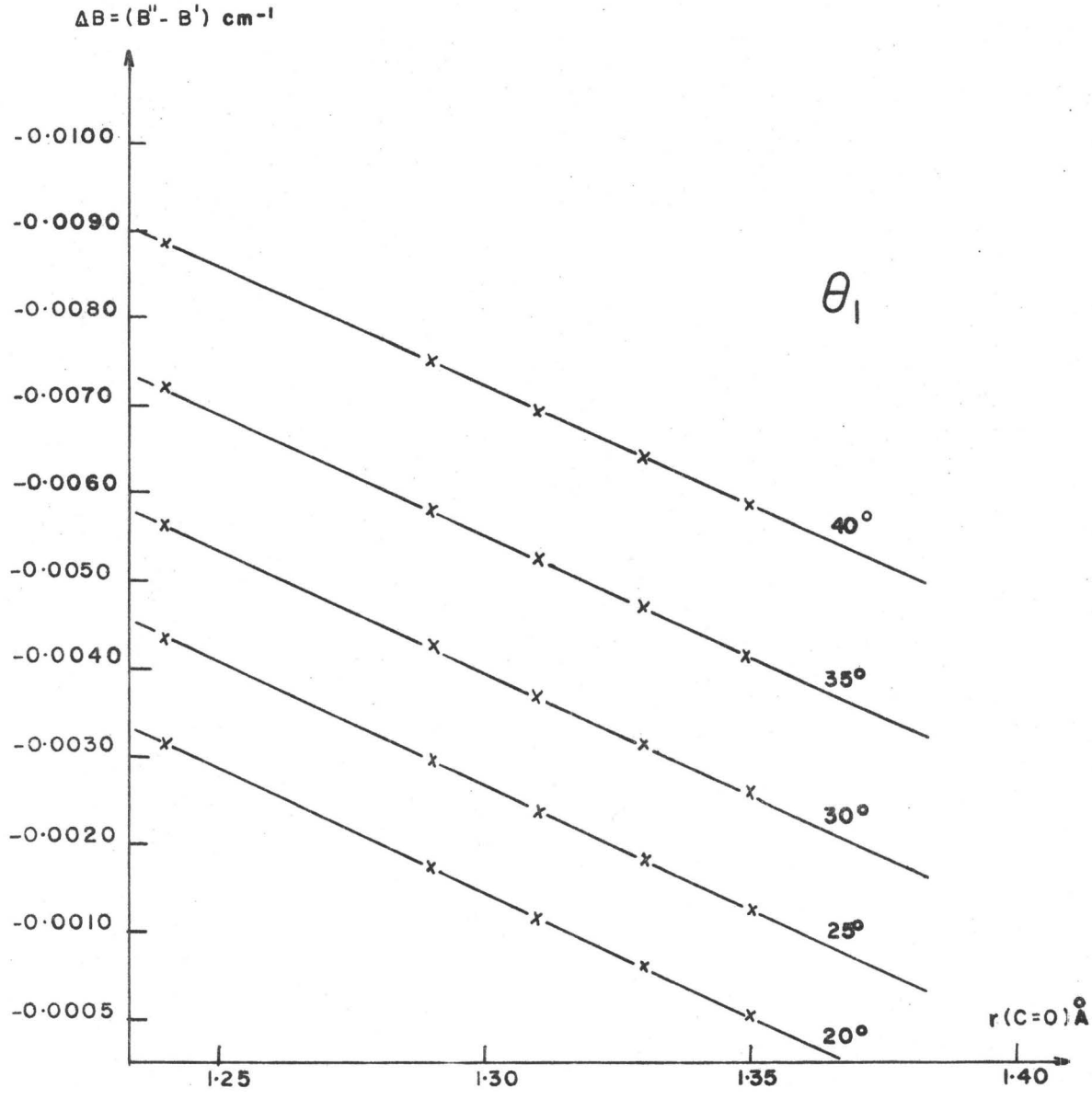

FIG(4·5) CHANGE IN THE ROTATIONAL CONSTANT B WHEN r(C=O) AND θ_1 ARE VARIED. $B'' = 0 \cdot 082\ cm^{-1}$.

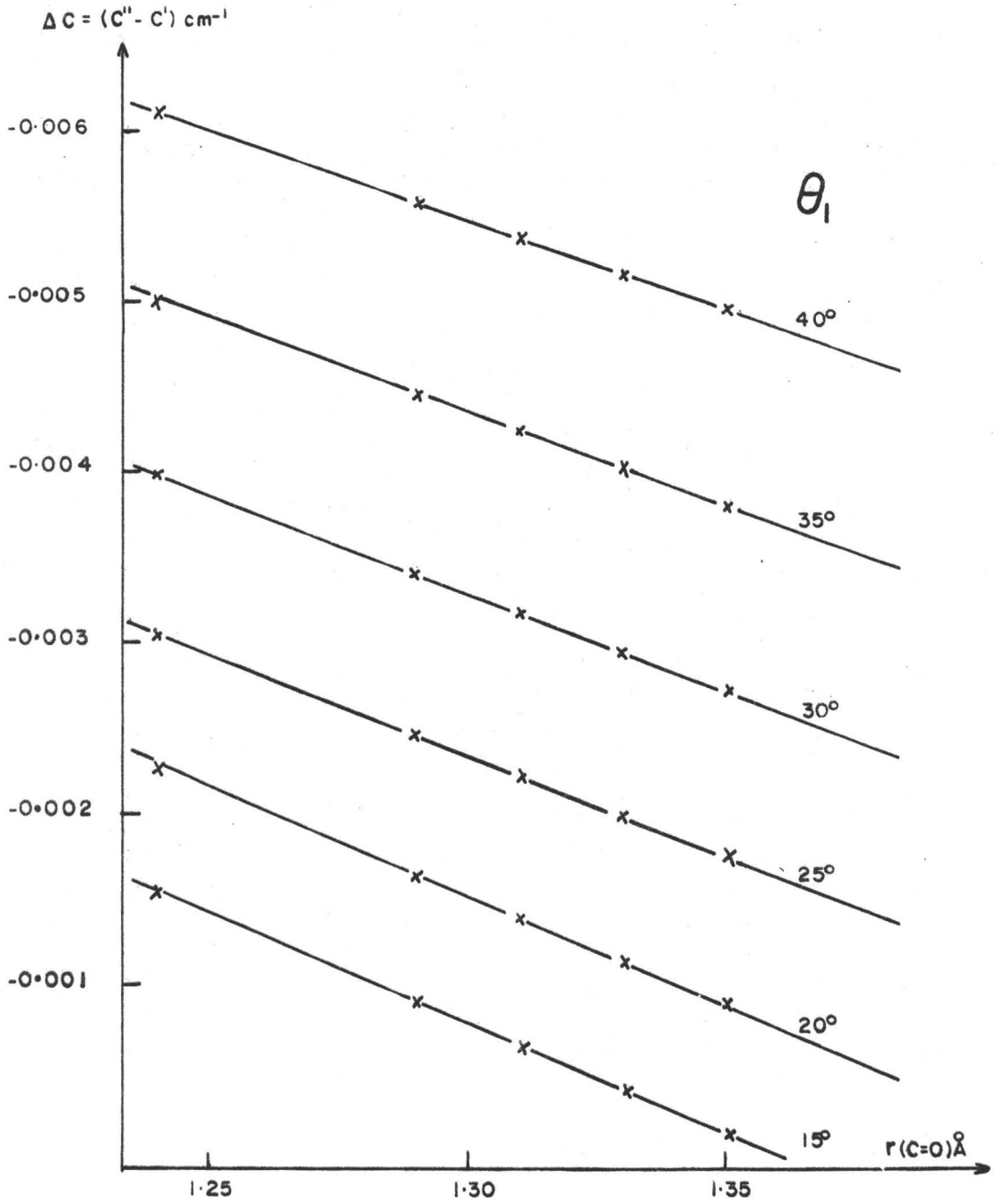

FIG(4·6) CHANGE IN THE ROTATIONAL CONSTANT C WHEN r(C=O) AND θ_1 ARE VARIED. $C'' = 0 \cdot 057\ cm^{-1}$.

Type B Bands

As B' was successively increased from 0.084 cm^{-1}, this band develops a sharp head at about -2 cm^{-1} from the origin, with a broad wing at about +4 cm^{-1}. When B' is increased above 0.085 cm^{-1}, this broad wing tends to disappear and only a sharp head, narrower than the A type head, remains at about -2 cm^{-1}. When A' = 0.134 cm^{-1}, the B type band is a broad featureless hump. As A' is progressively decreased, this starts to show some structure at -2 cm^{-1} + 4 cm^{-1} from the origin. The greatest amount of structure is obtained at about A' = 0.133 cm^{-1}. With A' decreased still further, this disappears to give a broad band with just three superimposed weak heads. As C' was increased the sharp head at -2 cm^{-1} from the origin decreases in intensity. Successively, three heads are prominent in the structure, and then these disappear, and the band becomes broad without any sharp feature.

Type C Bands

As A' was decreased, little change in profile occurred. The contours are not very sensitive to changes in this parameter. At B' = 0.084 cm^{-1}, the band shows two broad maxima $\sim$ 10 cm^{-1} apart. As B' increases an additional sharp head develops at -6 cm^{-1} from the origin, as well as a weaker one at about -2 cm^{-1}. The broad maximum to the blue becomes even broader. As C' was increased the head to the red end increases in intensity.

-Rotational Band Contour-

The best fit between calculated and observed profiles was obtained for the B type and A type bands that occur in the progressions of the CO out-of-plane mode ν_{21} shown in Fig. 3.11.

If the prediction of the origin band at 30132 cm^{-1} is correct, this band should be type A, with the type B 21_0^1 band having its origin at approximately 2.4 cm^{-1} to higher frequencies. The band at 1169 cm^{-1} ($7_0^1 21_0^1$) to the blue should also show approximately the same profile, and also consist of two overlapping components. Certainly the observed profiles are the same, each band showing three resolved maxima. They are both weak bands (see Fig. 4.7). The observed profile can be matched by superimposing computed type B and type A bands as shown in Fig. 4.8. As is shown in Figs. 4.7 and 4.8 the splitting between the origin of the B type band and the origin of the A type band in Fig. 4.8 is indeed 2.4 cm^{-1}. The splitting calculated from the double potential minimum function was 2.3 cm^{-1}, see Table 3.10 and Fig. 3.14.

In formaldehyde[27,28,68], both A and B type bands are active in the $^1A_2 \leftarrow {}^1A_1$ transition. Callomon and Innes[68] have shown that the A type bands are made possible by magnetic dipole radiation, for which vibronic A_2-A_1 transitions are allowed. But in the case of H_2CO, magnetic dipole transitions occur only as weak components in the electric dipole transition whose principal components, while forbidden, are much stronger

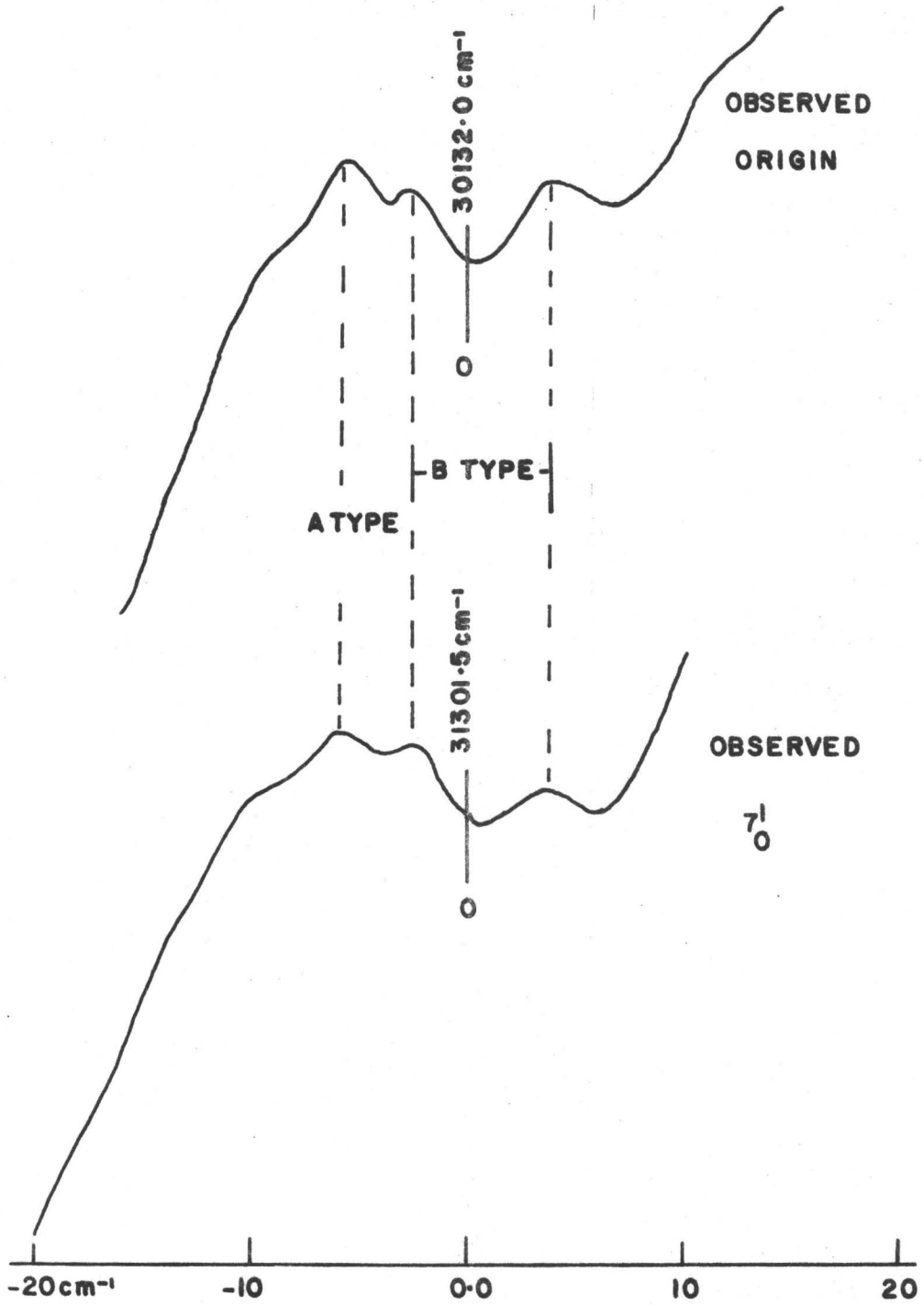

FIG(4·7) OBSERVED 0-0 AND 7^1_0 BANDS OF CH$_3$I

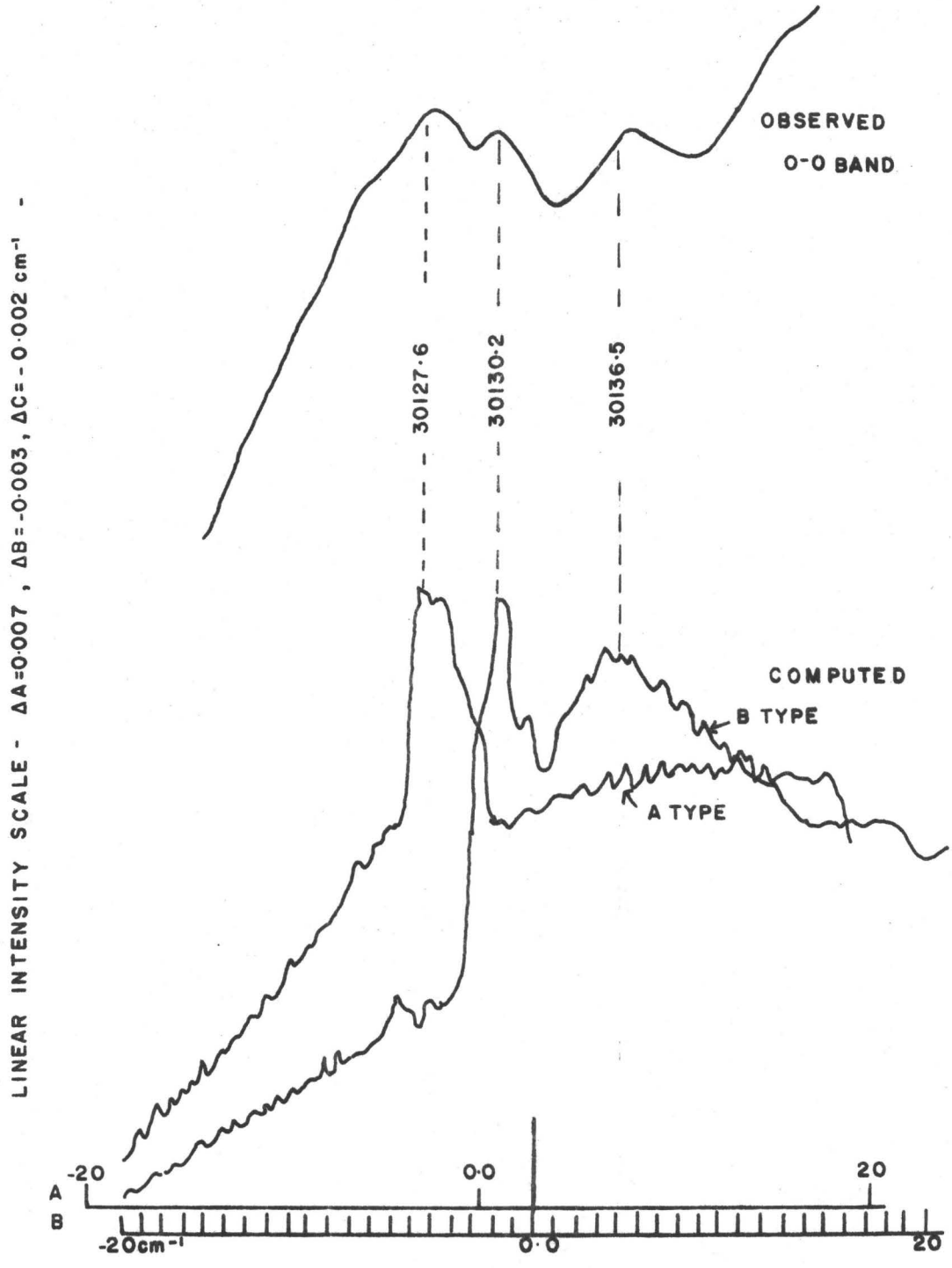

FIG(4·8) OBSERVED AND CALCULATED 0-0 BAND OF CHhIO

on account of vibronic interactions. In cyclohexanone the magnetic dipole transition which is the origin band is apparently as strong as the electric dipole transition. But the cyclohexanone electric dipole spectrum has very low intensity compared to that of H_2CO, which indicates that less intensity is borrowed through vibronic interaction. The intensity of the magnetic dipole transition is independent of the vibronic interaction which give intensity to the electric dipole component and so it is possible for the magnetic component to appear as strongly as the electric dipole transition. It must be mentioned that while the intensity of the electric dipole B_2-A_1 vibronic bands in the ν_{21} progressions increase in the spectrum, as more quanta of ν'_{21} are excited, the magnetic dipole transitions remain weak throughout.

If the assumption that the ring mode, ν_{45}, can be classified under the C_s point group is correct, then, all bands like $21_0^1 45_0^1$, $21_0^1 45_0^3$, as well as their combination with the ν_{21} mode, should be hybrid (A+C) type bands, the A and C components having the same origin. This is possible because the ν_{45}(a") mode involves a deformation of the ring which twists the CO bond out of the symmetry plane. The electric dipole transition can now have a component along the <u>a</u> and <u>c</u> axes. Some examples are given in Figs. 4.9, 4.10 and 4.11. In these three contours it can be seen that the A and C types of band have the same origin. Comparing Figs. 4.9, 4.10 and 4.11 one can see how a small change in the rotational constants

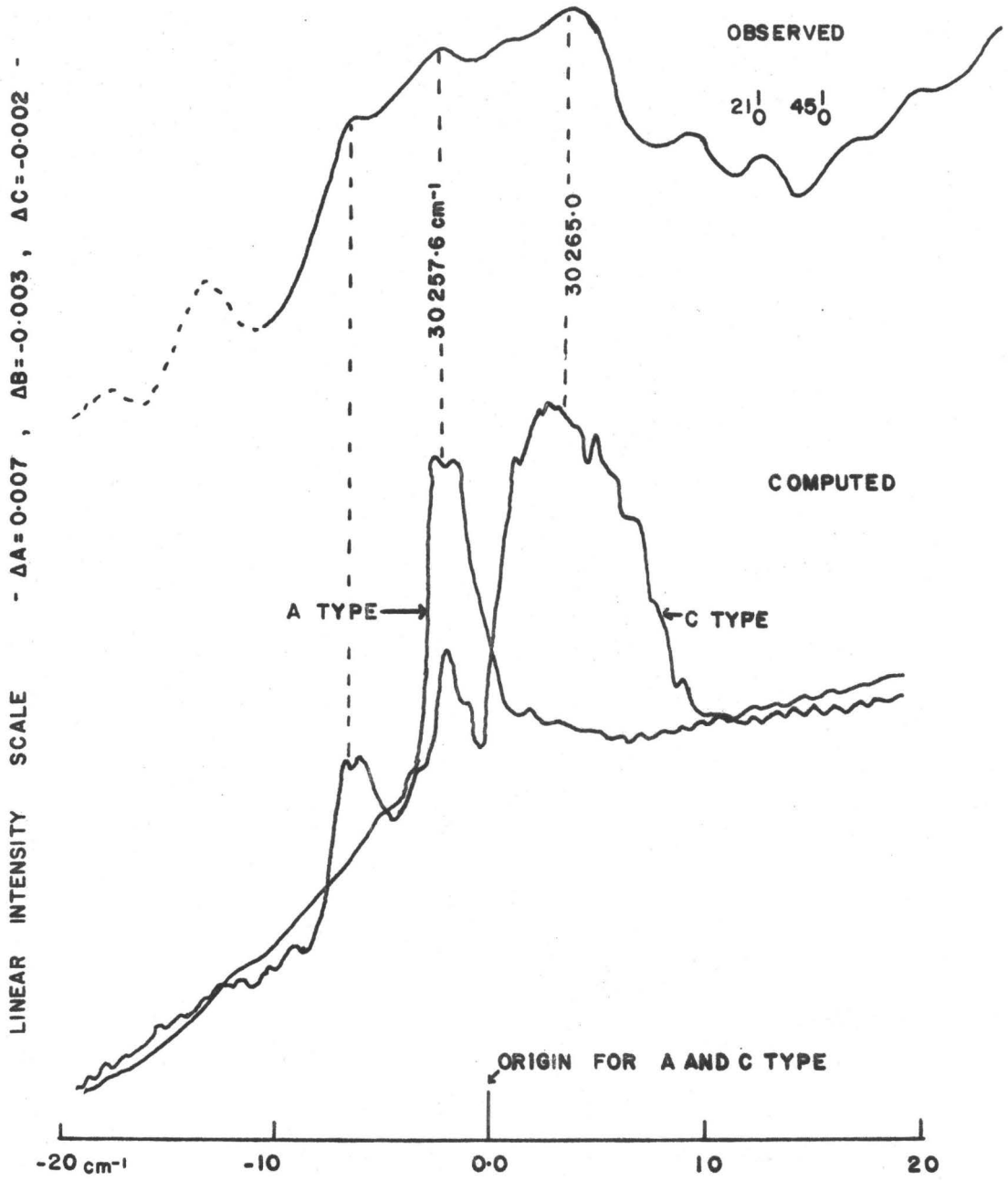

FIG(4·9) OBSERVED AND CALCULATED 21_0^1 45_0^1 BAND A+C TYPE

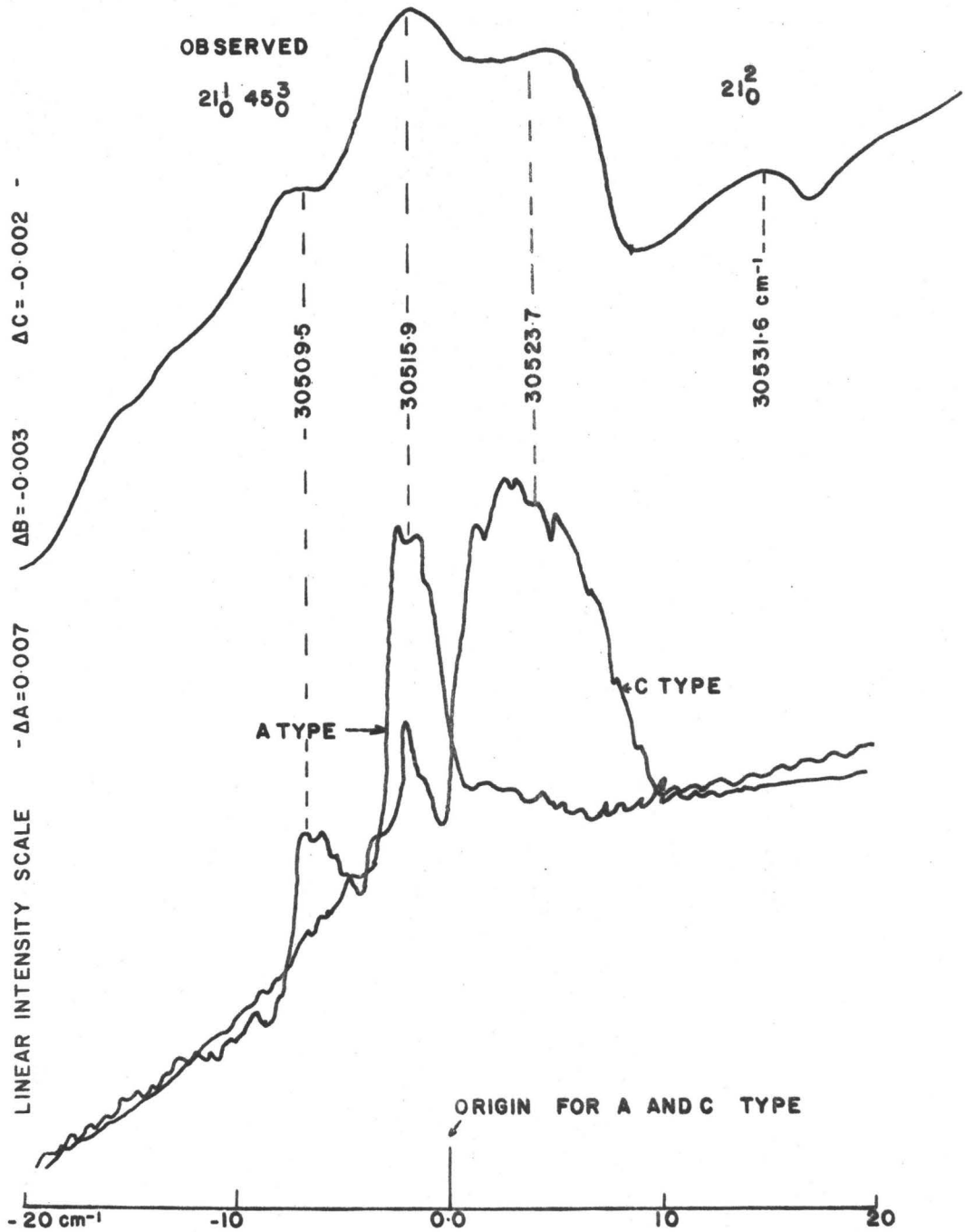

FIG(4·10) OBSERVED AND CALCULATED $21_0^1\ 45_0^3$ BAND A+C TYPE

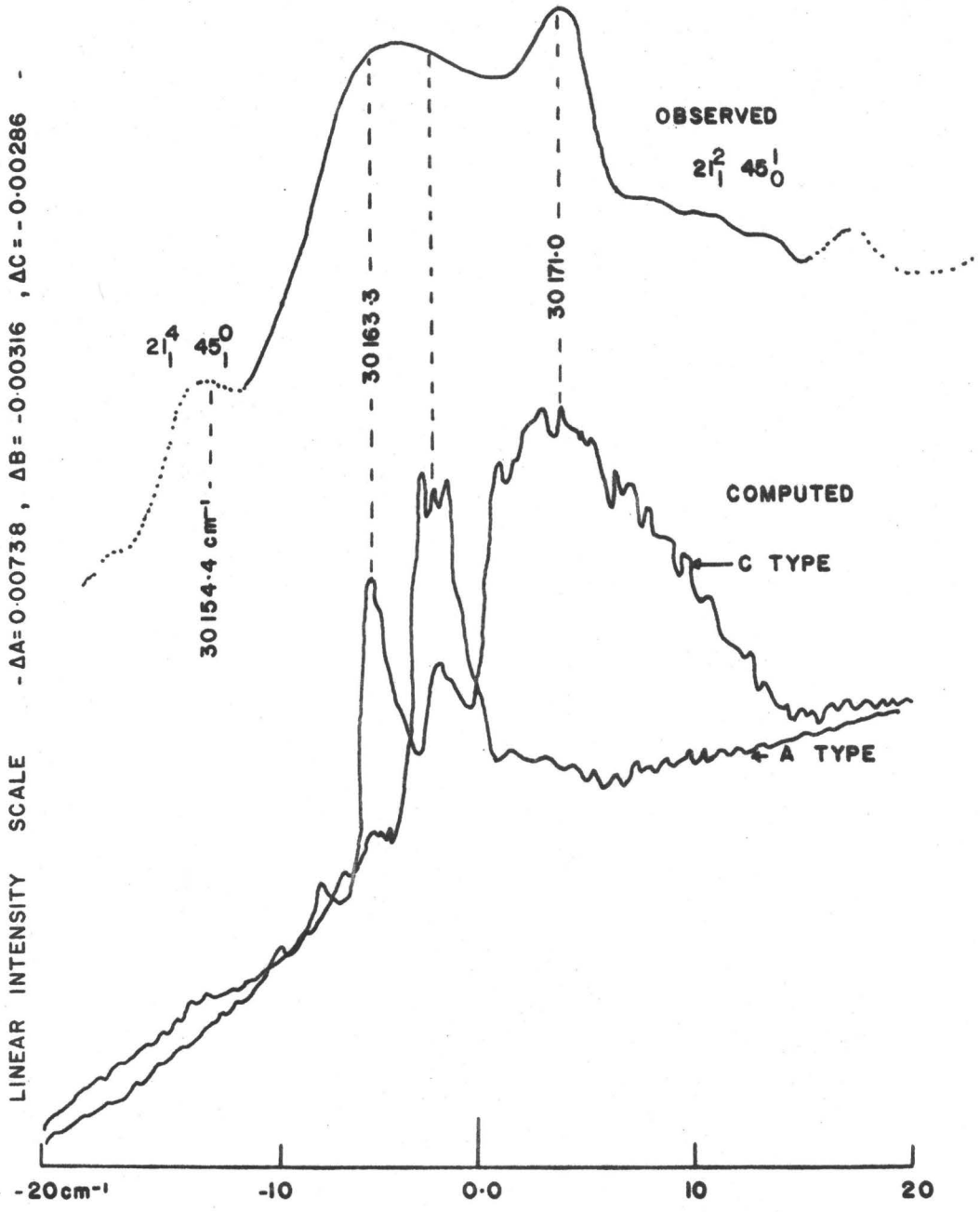

FIG(4·11) OBSERVED AND CALCULATED $21_1^2\ 45_0^1$ BAND A+C TYPE

A'B'C' can change the profile of the C type band. The fit in Fig. 4.11 is not as good as in Fig. 4.9 and 4.10. But as has been said previously, the geometry of CHh_{10} can be very much altered even when only one quantum is excited.

-Geometry of the Excited State-

The computed contours of Figs. 4.8, 4.9, 4.10 were obtained for $\Delta A_c^{(*)} = +0.007$, $\Delta B_c = -0.003$, $\Delta C_c = -0.002\ cm^{-1}$. These figures can now be used to refine the calculated geometry in the excited state. None of these changes in rotational constant correspond exactly to the constants obtained by varying only the carbonyl bond length and angle. So some of the other geometrical parameters of the molecule, θ_2 and R_2 (see Fig. 4.1) were also varied to get a better fit. The same process described previously for the ground state was used.

R_1 was varied from 1.31 to 1.34 Å in increments of 0.01 Å; θ_1 (the out-of-plane carbonyl angle) from 25° to 32° in increments of 1°, R_2 from 1.52 Å to 154 Å in increments of 0.01 Å and θ_2 was increased from 120° up to 122° in increments of 1°. To compare all the A', B', C' obtained by these calculations with those obtained by band contour analysis, a short program was written which calculated all the possible

---

* The subscript c indicates the value of ΔA etc... obtained by band contour analysis while the subscript t indicates the values obtained by moment of inertia calculations.

$\Delta A_t^{(*)}$, ΔB_t, ΔC_t, and then ΔA_t, ΔB_t, ΔC_t were compared with ΔA_c, ΔB_c, ΔC_c obtained from the band contour analysis,by means of the formula

$$R = \frac{(\Delta A_t - \Delta A_c)^2}{\Delta A_c} + \frac{(\Delta B_t - \Delta B_2)^2}{\Delta B_c} + \frac{(\Delta C_t - \Delta C_c)^2}{\Delta C_c}$$

The smallest value of R gives the closest possible geometry. The ten smallest values of R correspond to the geometrical ranges;

$$R_1 = 1.31 \pm 0.02 \text{ Å}$$

$$R_2 = 1.53 \pm 0.01 \text{ Å}$$

The out-of-plane $\theta_1 = 29° \pm 2°$

$\theta_2 = 121° \pm 2°$

All the other parameters of the ring were assumed to remain unchanged between the ground state and the excited state.

Hence, the band contour analysis suggests a small increase in the C_1-C_2-C_6 angle in the excited state, also an out of plane angle of about 29° ± 2° is obtained, while the double minimum potential calculation gives 30° ± 2°. These two results are in good agreement. The r(C=O) bond R_1 is increased to 1.31 ± 0.02 Å which is also in good agreement with results obtained for related molecules, see Table 3.1.

---

* The subscript t indicates the values of ΔA ... obtained by moment of inertia calculations.

CHAPTER 5

CONCLUSION

There is no doubt that the geometry of cyclohexanone changes between the ground state and the (π^*,n) excited state. As in related molecules, it is found that the carbonyl group in the (π^*,n) excited state is bent out-of-plane of the three adjacent carbons by about 30°. The carbon-oxygen bond length is increased between the ground state and the excited state by about 6%. The C-C-C angle adjacent to the carbonyl group is slightly increased by 2° from it ground state value.

The molecule interconverts from the two equivalent carbonyl bent configurations through an energy barrier of $\sim$ 800 cm^{-1}.

As in related molecules, the vibrations active in the n→π^* transition involve motion of the carbonyl group, namely, the carbonyl bond stretching motion and the carbonyl out of plane wag. It has been shown from the band contour analysis, that for these vibrations, the molecule can be classified under its localized C_{2v} symmetry, which gives vibronic transitions A_2-B_1, B_2-A_1 of type B. The type B character presumably borrowed intensity from the $^1B_2$(σ^*,n) closest electronic state, as is the case in formaldehyde[27,28,29].

An antisymmetric ring mode is strongly active in the

electronic spectrum. The latter gives hybrid transitions of A and C type. This is to be expected for an antisymmetric ring mode, because this vibration may have components along the three principal axes and can mix electronic states of different symmetry species with the $^1A_2$ state. This vibration involves motion of the molecular skeleton as a whole, and the localized symmetry is not applicable any more. The C_s point group becomes appropriate in the classification of the vibronic energy levels. On the other hand calculation of the principal axes of the molecule indicates that the principal axis a is the closest to the carbonyl direction, but does not coincide exactly with it in either electronic state. Thus hybrid bands of mixed polarisation can be expected in the spectrum.

The C type bands of the spectrum seem to originate in the same way as in cyclopentanone[30], through an admixture of $\nu_{45}(a'',a_2)$ and $\nu_{21}(b_1)$ vibrations, and can borrow intensity via a $^1B_1(\pi^*,\sigma)$ state. The A type bands probably borrow intensity via the (π,π^*) state by means of an (a_2,a'') vibration. there are more bands of A type character in cyclohexanone than in cyclopentanone.

The vacuum ultraviolet spectra of cyclic ketones[39] show that the intensities of the $\pi \rightarrow \pi^*$ electronic transition increase from cyclobutanone, cyclopentanone, cyclohexanone, and this could explain why the A character is stronger in cyclohexanone than in other cyclic ketones.

APPENDIX 1

In section 1.4, the frequency of the C=O stretching fundamental $\nu_7''(a')$ was briefly discussed. Most of the previous studies on its frequency were done using the liquid phase or in solution and only one in the vapour phase[5]. Also, the deuterated isomers have never been studied in this respect.

The spectroscopic information provided by the deuterated isotopes spectra are particularly important for the following reasons; on the assumption that the C=O stretch band really shows a double head a) Any Fermi resonance between the CO stretch energy level and one overtone of another vibration should disappear on deuteration, b) a double head for the band in all three isotopes would reinforce Batuev et al's[4] idea that cyclohexanone possesses two configurations with the oxygen either slightly above or below the plane of the three adjacent carbons in the ground state.

The infrared spectra of the three isomers $CHh_{10}/CHd_4/CHd_{10}$ in the vapour phase were recorded in the CO stretch region. The three isotopes were previously dried over molecular sieves #5A as follows; all the glass containers were dried in an oven for about two days. The molecular sieve was dried for 3 days, in an oven heated to 140°C, and cooled in a dessicator. The cyclohexanones were dried for four days in dried containers over molecular sieve. The containers were

kept in a dessicator. All the cells used for the experiments were previously evacuated. The sample was introduced into a side arm attached to the cell together with a small amount of molecular sieve. The compound was carefully degassed and the spectra were recorded immediately after this operation, at room temperature and vapour pressure.

An identical evacuated cell was kept on the reference beam and the spectrometer was continuously flushed during all the experiments with dry nitrogen. However it was not possible to remove completely the traces of water in the sample.

The spectrum of atmospheric water vapour was recorded on the same chart immediately afterwards. This spectrum was obtained by simply removing the sample sell from the cell compartment.

For the three isotopes the CO stretch band shows a maximum at about 1732±2 cm^{-1}. In the vapour phase, the shift on deuteration is extremely small. All the three isotopes show P, Q and R branches and the very weak shoulders at 1717.5 cm^{-1} and 1700 cm^{-1} can be identified as absorption by water vapour.

From the observation that only a single band is observed for the three isotopes, one can conclude that there is no Fermi resonance and that the oxygen is certainly in the C_1-C_2-C_6 plane.

The carbonyl bend absorption region (ν_{21} and ν_{43}) was also examined for the three isotopes. The bands in the three

cases are very borad and do not show any well-defined structure. CHh_{10} shows two maxima at 490 and 480 cm^{-1}, CHd_4 at 454 and 447 cm^{-1}, CHd_{10} at 460 and 450 cm^{-1}. The highest of these two values correspond to the value of the ground state frequency ν''_{21} observed in the ultraviolet spectra and can be assigned to the CO out-of-plane vibration. In most related ketones the carbonyl bend-in-plane ν_{43} is believed to be at a slightly higher frequency that the carbonyl out-of-plane. So either JNKM's assignments of the bands are wrong (see section 1.4 above), or else cyclohexanone behaves anomalously.

APPENDIX 2

BAND HEAD FREQUENCIES AND INTENSITIES FROM THE LOW RESOLUTION SPECTRUM OF CHh_{10}

	ν cm^{-1} vacuum	I		ν cm^{-1} vacuum	I		ν cm^{-1} vacuum	I		ν cm^{-1} vacuum	I
60 trs	28853	w		30298	m		31329	s		32377	s
	29064	m		30310	w		31394	w		32420	w
	29239	m		30342	m		31430	m		32464	w
	29327	m		30385	s		31468	m		32498	s
	29369	m		30438	w		31488	w		32560	w
	29457	s		30462	m		31504	w		32581	w
	29510	w		30478	w		31519	vw		32632	m
	29547	s		30508	ms	12 trs	31559	vw		32679	vw
	29597	w		30557	m		31587	wb		32735	ms
	29639	s		30630	s		31602	m		32818	m
40 trs	29684	m		30676	vs		31648	m		32853	m
	29728	w		30731	w		31690	m		32899	vw
	29770	sb		30754	w		31714	w		32935	m
	29819	w		30768	w		31731	m		32980	m
	29864	s		30784	w		31768	w		33020	m
	29900	w		30804	vsb		31790	w		33065	w
	29921	w		30857	s		31796	w	4 trs	33109	vw
	29954	m	16 trs	30886	w		31856	m		33138	m
	29997	s		30930	s		31898	m		33183	ms
	30040	s		30976	m		31945	w		33218	w
	30081	s		31037	vs+b		31978	s		33254	w
	30127	w		31094	w		32025	s		33299	ms
	30162	vs		31122	w	8 trs	32096	s		33365	m
	30214	m		31166	w		32139	vs		33413	ms
36 trs	30256	m		31212	vs		32210	s		33455	w
				31253	w		32260	s		33534	m
	30268	w		31295	m		32300	w		33577	w
							32332	w		33623	mw
										33648	m

APPENDIX 3

BAND HEAD FREQUENCIES FROM THE LOW RESOLUTION SPECTRUM OF CHd_4

	ν cm^{-1} vacuum	I		ν cm^{-1} vacuum	I		ν cm^{-1} vacuum	I
60 trs	29478	m		30320	ms		31039	w
	29489	vw		30346	ms		31045	w
	29505	vw		30367	s		31052	w
	29521	vw		30398	vsb		31063	w
	29566	m		30435	wb		31097	mw
	29589	w		30484	s		31106	m
	29657	m		30533	mb		31158	w
40 trs	29678	mw		30557	m		31167	
	29765	m		30604	w		31183	w
	29780	mb		30608	vw		31223	mw
	29820	w		30615	vw		31272	ms
	29852	m		30645	vs		31247	w
	29870	s		30674	mw		31255	w
	29904	mw		30693	w		31293	m
	29440	m		30702	w		31318	w
	29957	mb		30723	m		31332	s
	29991	ms		30729	s		31404	m
	30031	w		30761	s		31436	m
	30044	w		30771	w		31444	m
	30068	ms		30813	m		31505	wd
	30074	w		30819	m	12 trs	31524	wd
	30115	m	16 trs	30880	m		31684	md
	30127	vw		30890	m		31714	vwd
	30132	w		30929	w		31974	mwd
	30152	s		30943	m		32029	mwd
	30203	m		30992	m		32094	md
36 trs	30279	ms		31000	w		32100	
	30288	m		31008	w		32147	mwd

(continued next page)

ν cm^{-1} vacuum	I
32216	mbd
32265	mbd
32368	mbd
32454	mbd
32537	wbd

APPENDIX 4

BAND HEAD FREQUENCIES FROM THE LOW RESOLUTION SPECTRUM OF CHd_{10}

	ν cm^{-1} vacuum	I		ν cm^{-1} vacuum	I
60 trs	29467	w	32 trs	30226	ms
	29500	w		30270	m
	29508	m		30307	ms
	29533	m		30388	mw
	29552	m		30473	m
40 trs	29590	m		30565	m
	29633	ms		31051	mwd
	29674	ms		31106	mwd
	29715	ms		31139	mwd
	29760	s	20 trs	31159	wd
	29847	s		31165	wd
	29925	ms		31188	mwd
	29971	ms		31208	wd
	30014	s		31215	wd
	30050	mw		31244	msd
	30098	ms		31321	msd
	30135	m			
	30182	mw			
	30217	mb			

APPENDIX 5

BAND HEAD FREQUENCIES AND INTENSITIES OF HIGH RESOLUTION SPECTRUM OF CHh_{10}

	ν cm^{-1} vacuum	I	ν cm^{-1} vacuum	I		ν cm^{-1} vacuum	I
60 trs	29057	w	29812.9	w		30113.6	w
	29077	vw	29820.2			30127.6	
	29102	w	29853.3			30130.2	w
	29115	w	29859.4	m		30136.5	
	29152.4	mw	29863.1			30150.6	vw
	29173.1	vw	29866.7			30154.4	vw
	29203	w	29871.6	vw		30163.3	m
	29241	w	29887.8	vw		30171.0	
	29329	mw	29905.7	w		30217.2	w
	29368	w	29913.0	w	36 trs	30247.4	vw
	29452.4		29942.9			30257.5	m
	29458.5	m	29941.6	m		30265.0	
	29467.9		29951.6			30272.6	vw
	29510	w	29993.9	ms		30285	vw
	29544.8		29998.9			30297.9	mw
	29549.7	m	30013	vw		30302.9	
	29559.5		30022.7	vw		30308.1	w
	29568.0		30034.0			30314.4	
	29582.0	w	30037.8	ms		30332.2	
	29639.7	m	30042.9			30338.5	ms
	29642.0		30052.9	w		30348.7	
40 trs	29684.6	w	30059.2	vw		30355.1	
	29693.2		30063.0	vw		30379.4	
	29756.3		30071.8			30385.7	ms
	29762.5		30079.4	m		30389.6	
	29768.6	m	30090.8			30393.4	
	29772.3		30097.2	vw		30424.2	
	29774.8		20107.3	vw		30430.7	m
	29779.7					30440.9	

(continued next page)

ν cm^{-1} vacuum	I		ν cm^{-1} vacuum	I	ν cm^{-1} vacuum	I
30468.0			30844.6	vw	31516	w
30471.9	mw		30859.3			
30477.1			30965.9	s		
30509.5			30869.9			
30515.9	m	12 trs	30889.9	w		
30523.7			30928.8			
30531.6	vw		30934.2	s		
30564.2			30940.9			
30569.4	m		30982.0	sb		
30582.5			31028.3			
30628.7	vw		31040.4	m		
30635.0			31055.2			
30641.3	m		31096.2			
30648.9			31101.7	m		
30657.8	vw		31105.8			
30693.5	vs		31122.5	w		
30703.9	vw		31147.4	vw		
30725.9	vw		31169.1	mw		
30731.2	vw		31174.6			
30736.4	vw		31223.4	s		
30740.3	vw		31258.9	w		
30749.4	vw		31297.4	mw		
30752.0	vw		31299.5			
30755.0	vw		31338.6	s		
30761.2	vw		31396.7	w		
30773.0	vw		31405.0			
30782.3	vw		31429.9	w		
30789.9	vw		31439.7			
30808.9	vs		31474.4	w		
30816.9			31484.1			

BIBLIOGRAPHY

1. G. W. King, "Spectroscopy and Molecular Structure". New York, Holt, Rinehart and Winston, Inc. (1964).
2. G. Herzberg. Molecular Spectra and Molecular Structure. Vol. II, Infrared and Raman Spectra of Polyatomic Molecules, Inc. New York, 1956.
3. G. HErzberg, "Molecular Spectra and Molecular Structure", Vol. I. New Jersey, D. Van Nostrand Co., Inc. 1950.
4. H. I. Batuev, A. A. Akhrem, A. V. Kamernitskii, A. D. Matveeva. Dolk. Akad. Nauk. S.S.S.R., 53, 202 (1960).
5. J. Deprieux. Bull. Soc. Chim. belges 66, 218 (1957).
6. J. E. Katon, F. F. Bentley, Spectochimica Acta 19, 639-653 (1963).
7. M. T. Forel et J. Pétrissans. J. Chim. Phys. 63 4, 625, 34 (1966).
8. C. Romers, Rec. Trav. Chim. 75, 956 (1956).
9. F. R. Jensen, D. S. Nouce, C. H. Sederholm, and A. J. Berlin, J. Am. Chem. Soc. 84, 386 (1962).
10. W. S. Johnson, J. L. Margrave, V. J. Bauer, M. A. Fisch and all J. Am. Chem. Soc., 82, 1255 (1960).
11. F. R. Jenseon, B. H. Beck, J. Am. Chem. Soc. 90 1066 (1968).
12. C.W. Shoppee, J. Chem. Soc. 1138 (1946).
13. C. S. Beckett, K. S. Pitzer and Spitzer, J. Am. Chem. Soc. 69, 2488 (1947).

14. W. D. Chandler and L. Goodman, J. Mol. Spect. 35,232-243 (1970).

15. J. Sidman, Chem. Rev. 58, 689 (1958).

16. Yoh-Han Pao and D. P. Santry, J. Am. Chem. Soc. 88, 4158 (1966).

17. H. L. Murry, J. Chem. Phys. 9, 231 (1941).

18. A.B. F. Duncan, J. Chem. Phys. 8, 444 (1940).

19. R. S. Holdsworth and A. B. F. Duncan, Chem. Rev. 41, 311 (1947).

20. E. E. Barnes and W. T. Simpson, J. Chem. Phys. 39, 670 (1963).

21. P. Granger and M. M. Claudon, Bull. Soc. Chim. Fr.753-755,(1966).

22. R. G. Snyder and J. H. Schachtschneider. Spectro Chimica Acta 21, 169 (1965).

23. Takahashi, T. Shihahouchi, K. Fukushima and T. Miyazawa. J. Mol. Spec., 13, 43 (1964).

24. R. G. Snyder, J. Mol. Spec. 36, 204-221 (1970).

25. R. P. Bauman and E. Thomson, J. Opt. Soc. Am. 53, 1, 202 (1963).

26. R.N. Jones and H. H. Mantsh (Private Communication).

27. J.C.D. Brand. J. Chem. Soc., 858 (1956).

28. V. A. Job, V. Sethuraman, and K. K. Innes, J. Mol. Spec. 30, 365 (1969).

29. V. T. Jones and J. B. Coon, J. Mol. Spec. 31, 137-154 (1969).

30. H. E. Howard-Lock and G. W. King. J. Mol. Spec. 35, 396-412 (1970).

31. S. L. Altmann, Proc. Roy. Soc. (London) A298, 184 (1967).

32. S. L. Altmann, Rev. Mod. Phys. 35, 641 (1963).

33. S. L. Altmann, Phil. Trans. Roy. Soc. (London) A255, 216 (1963).

34. H. C. Longuet-Higgins, Mol. Phys. 6, 445 (1963).

35. A. W. Baker, Spectrochimica Acta, 21, 1603, 1611 (1965).

36. E. J. Hatwell, R. E. Richards, and H. W. Thompson. J. Chem. Soc. (1948) 1436.

37. D. C. Moule, Can. J. Phys. 47(11), 1235-6 (1969).

38. H. Howard-Lock. Ph.D. Thesis, McMaster University,(1968).

39. A. Udvarhazi and M. A. El. Sayed. J. Chem. Phys. 42, 3335 (1965).

40. L. K. Montgomery, A. O. Clousse, A. M. Crelier, L. E. Applegate, J. Am. Chem. Soc. 89(14), 3453-7 (1967).

41. J. U. White, J. Opt. Soc. Am. 32, 285 (1942).

42. N.R.C. Tables, donated by N.R.C., Ottawa, Ontario, Canada.

43. Bengt Edlen, J. Opt. Soc. Amer. 43, 339 (1953).

44. J. M. Foster and S. F. Boys. Rev. Mod. Phys. 32, 303 (1960).

45. G. W. Robinson and V. E. Digiorgio, Can. J. Chem. 36, 31 (1958).

46. L. E. Giddings and K. K. Innes, J. Mol. Spec., 6, 528 (1961).

47. K. K. Innes and L. E. Giddings, Jr. J. Mol. Spec. 7, 435 (1961).

48. J. M. Hollas, Spectrochim. Acta, 19, 1425 (1963).

49. A. V. K. Rao, J. Sci. Ind. Res. India, 21B, 446 (1962).

50. J. C. D. Brand, J. H. Callomon and J. K. Watson, Disc. Farad. Soc. 35, 175 (1963).

51. J. C. D. Brand and J. K. G. Watson, quoted in J. H. Collomon and K. K. Innes, J. Mol. Spec., 10, 166 (1963).

52. J. C. D. Brand, Trans. Farad. Soc., 50, 431 (1954).

53. G. W. King, J. Chem. Soc., 5054 (1957).

54. T. Anno and A. Sado, J. Chem. Phys., 32, 1602 (1960).

55. J. C. D. Brand, J. H. Callomon, D. C. Moule, J. Tyrrel and T. H. Goodwin. Trans. Farad. Soc. 61, 2365 (1965).

56. W. J. Balfour and G. W. King, Ibid., 26, 384 (1968).

57. J. B. Coon, N. W. Naugle and R. D. McKenzie, J. Mol. Spec., 20, 107-129 (1966).

58. E. B. Wilson, Jr., J. C. Decius and P. C. Cross, "Molecular Vibrations" . New York, McGraw-Hill Book Co. Inc., (1955).

59. P. Mirone, Spectrochimica Acta 20, 1646-1647 (1964).

60. G. Dellepiane and J. Overend, Spectrochimica Acta 22, 593-614 (1966).

61. K. L. Dorris, J. E. Boggs, A. Danti and L. L. Alpeter, J. Chem. Phys., 46, 1191 (1967).

62. D. Boone, C. Britt and J. Boggs, Ibid., 43, 1190 (1965).

63. K. Frei and H. H. Günthard, J. Mol. Spec., 5, 218 (1960).

64. M. T. Forel and M. Fouassier, Spectrochimica Acta, 23A, 1977-1980 (1967).

65. J. E. Parkin, J. Mol. Spec., 15, 483 (1965).

66. W. J. Balfour, Ph.D. Thesis, McMaster University (1967).

67. G. K. Kidd, Ph.D. Thesis, McMaster University (1971).

68. J. H. Callomon and K. K. Innes, J. Mol. Spec. 10, 166, (1963).

69. "Handbook of Chemistry and Physics". 49th Edition R. C. Weast.